UNIVERSITY OF OKLAHOMA

GRADUATE COLLEGE

BIOMARKER DISCOVERY FOR POINT-OF-CARE DIAGNOSTICS

A DISSERTATION

SUBMITTED TO THE GRADUATE FACULTY

in partial fulfillment of the requirements for the

Degree of

DOCTOR OF PHILOSOPHY

By REBECCA ULRICH VONBARGEN
Norman, Oklahoma
2026

Downloaded from SHAREOK. Persistent Handle URL: https://hdl.handle.net/11244/342916

BIOMARKER DISCOVERY FOR POINT-OF-CARE DIAGNOSTICS

A DISSERTATION APPROVED FOR THE
STEPHENSON SCHOOL OF BIOMEDICAL ENGINEERING

BY THE COMMITTEE CONSISTING OF

Dr. Matthias U. Nollert, Chair

Dr. Roger G. Harrison, Jr.

Dr. John Clegg

Dr. Keri Kornelson

©Copyright by REBECCA ULRICH VONBARGEN 2026
All Rights Reserved.

Abstract

Infectious diseases have caused billions of deaths in the last 200 years. Significant gaps persist in diagnosis, treatment, and eradication of nearly all infectious diseases. Identification of novel biomarkers addresses this gap by providing targets for diagnostics, treatments, disease monitoring, vaccines, and prognoses. Proteomics and metabolomics are two broad analytical approaches for biomarker discovery methodologies. In the following studies, varying methods are applied to two unique infectious diseases, tuberculosis and Chagas disease, for identification of novel biomarkers.

Chagas disease (CD), caused by *Trypanosoma cruzi* (*T. cruzi*) protozoa, is a complicated parasitic illness with inadequate medical measures for diagnosing infection and monitoring treatment success. To address this gap, we analyzed changes in the metabolome of *T. cruzi*-infected mice via liquid chromatography tandem mass spectrometry of two clinically accessible biofluids: urine and plasma. Metabolites perturbed by infection in urine include kynurenate, acylcarnitines, and threonylcarbamoyladenosine. Based on these results, we sought to implement urine as a tool for the assessment of CD treatment success. Strikingly, it was found that mice with parasite clearance following benznidazole (Bz) antiparasitic treatment had an overall urinary metabolome comparable to that of mice that failed to clear parasites. These results provide a complementary hypothesis to explain clinical trial data in which Bz treatment did not improve patient outcomes in late-stage disease, even in patients with successful parasite clearance. Overall, this study provides insights into new small-molecule-based CD diagnostic methods and a new approach to assess functional responses to treatment.

Tuberculosis (TB), caused by the bacillus *Mycobacterium tuberculosis* (*Mtb*), is a serious airborne disease that has claimed more than one billion lives. Serious gaps persist worldwide in rapid diagnosis and completion of treatment, despite treatments with high cure rates being available. Communities lacking appropriate economical and health resources often suffer the most, and rapid, point-of-care diagnostics are the first step in relieving the global TB disease burden. We utilized a novel rabbit model to analyze circulating antigens in serum and urine to identify six potential protein biomarker candidates. IgG antibody-producing hybridomas were developed to one of the identified targets for potential use in a point-of-care diagnostic assay format. Taken together, these studies support the utilization of multiple methodologies, such as proteomics and metabolomics, to gain valuable insights for development of point-of-care diagnostics for infectious diseases.

Acknowledgements

Work in Chapter 2 was conducted under the direction of Laura-Isobel McCall, Ph.D., in the Dodge Family College of Arts & Sciences Department of Chemistry & Biochemistry at the University of Oklahoma. It was supported by start-up funds from the University of Oklahoma, with partial support from NIH award number R21AI148886 and R21AI156669, and from the PhRMA foundation, award number 45188.

Work in Chapter 3 was conducted at Immuno-Mycologics, Inc. (IMMY) under the supervision of Brandon Neary and Beverly Crider, PhD. It was supported in part by NIH-STTR Phase I grant 5R41AI104377-02 and IMMY.

Dr. Matthias Nollert, who continues to believe in me more than I believe in myself. Thank you for taking me on as an undergraduate research volunteer fifteen years ago. Thank you for seeing me, supporting me, challenging me, guiding me, and mentoring me. Most importantly, thank you for never giving up on me.

Thank you to Dr. Handan Acar, Dr. Chris Lessard, Dr. Sanjay Bidichandani, and Dr. Laura-Isobel McCall for providing valuable contributions to my education, growth, and professional maturity. Thank you to all members of my committee, past and present, for your time, support, patience feedback, and guidance.

Many thanks to all members of Dr. McCall's former University of Oklahoma Lab, with special thanks given to Danya Dean, PhD, Zongyuan Liu, PhD, and Jarrod Laro (Roach), PhD.

Thanks to everyone at IMMY who contributed to my training and support: Beverly Crowder, PhD, Brandon Neary, and Sean Bauman, PhD. Thank you to Colorado State University researchers including Anita Amin, Kimberly Arnett, and Delph Chatterjee, PhD.

To my husband, Erich, thank you for patiently enduring this journey by my side. Thank you to my children, Cadence, Indira, and Otto, for motivating me, loving me, and cheering me on.

And to Dr. Sherri Irvin, thank you for providing countless hours of wise counsel through so many twists and turns along the way.

Contribution Statements, located at the beginning of Chapters 2 and 3, outline specific contributions made by individual authors and contributors.

Table of Contents

Abstract iv
Acknowledgements v
Table of Contents vi
List of Tables ix
List of Figures x
1 Introduction 1
1.1 Background and Significance 1
1.2 Biomarker Definitions, Classifications, and Current Setbacks 1
1.3 Biomarker Workflows and Experimental Approaches 3
2 Discovery of Small Molecule Metabolite Biomarkers-of-Cure for Chagas Disease 5
2.1 Publication Contribution Statement 5
2.2 Disease Overview and Pathology 6
2.3 Treatment Options 7
2.4 Chagas Disease Diagnostic Landscape 7
2.4.1 Diagnostics of Infection 7
2.4.2 Diagnostics of Cure 8
2.4.3 Treatments & Diagnostics in the Context of Disease Progression 8
2.5 Opportunities using Metabolomics 9
2.5.1 Metabolic adaptations to infection 9
2.6 Experimental Design 12
2.7 Methods 13
2.7.1 Ethics Statement 13
2.7.2 *In vitro* Parasite Cell Culture 13
2.7.3 *In vivo* Experimentation 14
2.7.4 Parasite Burden and Cardiac Fibrosis Quantification 15
2.7.5 qPCR 15
2.7.6 qRT-PCR 16
2.7.7 Determination of Persistent vs Cleared Parasites 17
2.7.8 Metabolite Extraction and LC-MS/MS Data Collection (Untargeted Analysis) 17
2.7.9 LC-MS/MS Data Processing in MZMine and Feature Table Generation 19

2.7.10 Data Analysis 19
2.7.11 Feature-Based Molecular Networking (FBMN) Using Global Natural Products Social Molecular Networking (GNPS) 22
2.8 Results 22
2.8.1 Serum Samples 22
2.8.2 Urine Samples 28
2.9 Discussion and Conclusion 32
2.10 Present Day Analysis and Future Opportunities 35
2.10.1 Chagas Disease Biomarkers 35
2.10.2 Low Metabolite Coverage 36
2.10.3 Molecular Networking in Infectious Diseases Metabolomics 37
3 Discovery of Novel Protein Biomarkers for Tuberculosis Point-of-Care Diagnostic Assay 37
3.1 Contributions Statement 38
3.2 Disease Overview and Pathology 38
3.2.1 Disease Pathology 39
3.3 Treatment Options at Time of Study (2014-2016) 39
3.4 Active Tuberculosis Diagnostic Landscape at Time of Study (2014-2016) 41
3.5 Opportunities Using Proteomics 42
3.6 Experimental Design 42
3.6.1 InMAD Method 42
3.7 Methods 44
3.7.1 Rabbit Model of Tuberculosis 44
3.7.2 Production of Urine and Serum from Infected Rabbits 45
3.7.3 Production of InMAD Immune Serum 45
3.7.4 Identification of *Mtb* Biomarkers 46
3.7.5 2-Dimensional Gel Electrophoresis 46
3.7.6 2-Dimensional Western Blot 47
3.7.7 MALDI-TOF 48
3.7.8 Immunization of Mice and Hybridoma Establishment 48
3.7.9 Indirect ELISA 49
3.8 Results 50
3.8.1 Identification of M. tuberculosis Antigens Secreted During Infection 50
3.9 Discussion and Conclusion 54

3.9.1 Identified Biomarker Targets 54
3.9.2 Testing and Validation in Human Samples 55
3.9.3 Composition of M. tuberculosis Culture Filtrate 55
3.10 Present-Day Analysis & Future Opportunities 56
3.10.1 Present-Day State of Global TB Burden 56
3.10.2 TB Diagnostic Landscape in 2026 57
3.10.3 Opportunities for Improved Experimental Design 60
4 Conclusions and Recommendations 60
4.1 Key Scientific and Engineering Contributions 60
4.2 Future Recommendations for Point-of-Care Diagnostics Research 61
4.2.1 Biological Layers and Integrative Biomarkers 61
4.2.2 Clever Point-of-Care Engineering Hacks 61
4.2.3 Ghosts and Dark Matters 62
5 References 64
6 Appendix A 84
7 Appendix B 85
8 Appendix C 87
9 Appendix D 88
10 Appendix E 89
11 Appendix F 90
12 Appendix G 91
13 Appendix H 92

List of Tables

Table 2-1. qPCR and qRT-PCR parameters. 16
Table 2-2. LC gradient. 18
Table 2-3. Serum Metabolite Features with BH-Significant Association with BZ Treatment Outcome and Confirmed Spectral Library Identity 28
Table 3-1. Protein Biomarker Targets Identified 51

List of Figures

Figure 2-1. Serum metabolomic profiles differ between treatment outcome groups throughout drug treatment. 26
Figure 2-2. Urine metabolome in mice that successfully cleared T. cruzi shows no significant difference from mice in which parasites failed to be cleared..... 29
Figure 2-3. Metabolite features identified as differing between infected and uninfected samples remain significantly perturned even after successful parasite clearance. 30
Figure 2-4. Extracted ion chromatograms (XICs) of internal standards and biomarkers. 31
Figure 3-1. InMAD strategy for identifying Mtb antigens secreted/shed in urine and/or blood during TB infection. 43
Figure 3-2. 2D-Gel Electrophoresis of *Mtb* Culture Filtrate Proteins..... 51
Figure 3-3. Anti-Ag85 IgG-Producing Hybridoma Development Screening. 53

1 Introduction

1.1 Background and Significance

Despite many advancements in the understanding, detection, and treatment of infectious diseases, they remain a major cause of death today.[1] Over 1 billion lost lives from tuberculosis have been recorded since its scientific discovery in 1882, more than any other infectious disease in history.[2] Other leading causes of infectious disease deaths include smallpox, plague, malaria, HIV/AIDS, cholera, and influenza. Very few infectious diseases, like smallpox, have managed to be eradicated through vaccines and/or cures; most have persisted for hundreds and sometimes thousands of years.[3]

Severity and distribution of disease outbreaks varies significantly, so there is a critical need for global health interventions, cooperations, and strategies.[4] Global health programs are facing unprecedented threats to funding in such a fragmented world.[3] Just this year, the United States pulled out of the World Health Organization (WHO), the United Nations agency responsible for connecting nations to promote health and serve the vulnerable.[5] And it is the most vulnerable and disenfranchised communities often bearing the brunt of infectious disease outbreaks.[6] Early diagnosis is a key factor in limiting outbreaks and preventing their spread.[7] Point-of-care diagnostics, which offer rapid results near the site of patient care, offer the most robust opportunities for global interventions.[8]

1.2 Biomarker Definitions, Classifications, and Current Setbacks

Accurate, predictive biomarkers are of utmost importance for effective decision-making in all diagnostics.[9]A biomarker is defined as a measurable, known characteristic of normal

biological processes, pathogenic processes, or responses to exposure or intervention.[10] Classification of biomarkers can become complicated, as many candidates fall into multiple, overlapping categories based on attributes such as biological origin and scale, physical structure, modality, evaluative characteristics, and clinical application. Regardless of its nature and intended use, an effective biomarker must be sensitive, specific, safe, reliable, reproducible, measurable, applicable, and modifiable with treatment.[11]

The first disease biomarker of record was discovered in 1847[12], and biomarker research in the decades that followed typically adopted targeted approaches driven by biological process hypotheses that resulted in single-analyte biomarker discoveries. Over the next 150 years, use of disease biomarkers in laboratories and clinics gradually became more objective and quantitative, while clinical studies and trials continued relying on clinical endpoint variables designed to capture how a patient feels, functions, or survives.[13]

Biomarker data does not always correlate with clinical state, and prioritizing the wrong data can lead to medical failures. An example of this is the Cardiac Arrhythmia Suppression Trial (CAST).[14] Arrhythmia was identified as a biomarker for patients suffering from heart attacks. Because heart attacks are strongly correlated to sudden cardiac death, it was hypothesized that drugs developed to normalize heart rhythms would prevent sudden cardiac deaths. The Federal Drug Administration (FDA) approved several of these drugs, but the CAST findings demonstrate the drugs significantly increase sudden death by triggering different, unseen, lethal cardiac malfunctions.

Concerns and discussions over what data are most useful in both clinical and biomedical research continued to escalate until a National Institutes of Health Biomarkers Definitions Working Group was formed in 1998 to resolve confusion, standardize definitions, and align

expectations.[15] This ultimately led to the development of a periodically-updated 'living' document known as the Biomarkers, EndpointS, and other Tools (BEST) Resource that continues to influence biomarker research agendas at all levels.[10,16]

Today, high translational failure rate, whereby the most promising discovery-phase biomarkers often fail late-stage clinical validation, persists as one of the biggest issues in all of biomarker research.[17] A recent review of the European Medicines Agency's biomarker qualification procedures and outcomes cited an 85% failure rate, with the most common issues of biomarker properties and assay validation indicating key gaps at early stage development.[18] Other identified key causes of failure include pre-analytical variability, replication failure, and lack of validation rigor at all stages.[19]

1.3 Biomarker Workflows and Experimental Approaches

At a glance, typical biomarker discovery workflows include sample collection, high-throughput screening, and targeted validation. Proteomics, metabolomics, genomics, and transcriptomics are biological modalities that define the scope of a biomarker workflow through use of specialized platforms like mass spectrometry, next-generation sequencing, and single-cell assays.

Biomarker study design can be divided into two major categories: targeted and untargeted. Targeted approaches are hypothesis-driven and require prerequisite knowledge and understanding of the disease of interest. The goal is typically to quantify known targets with low data coverage and high sensitivity. Conversely, the goal of untargeted approaches is to discover novel biomarkers. Untargeted experiments carry reduced bias, are hypothesis-generating, involve

high data coverage, but usually have lower sensitivity. Targeted approaches are often used to validate discoveries made during untargeted approaches.

After a list of biomarker candidates is identified through initial discovery, next steps in the development pipeline include qualification, verification, candidate prioritization, and validation. High sensitivity is the top priority during discovery and qualification, while focus begins to shift to specificity assessment during verification. Existing knowledge in disease pathophysiology and functional biology of candidate molecules drives effective candidate prioritization.

Proteomics in biomarker discovery is considered a reasonably established field within the core -omics technologies. The biggest plaguing issues current processes have yet to overcome are sample complexity, patient-to-patient variability, disease marker promiscuity, data analysis inefficiency, stability of analytical platforms, high cost, and the time it takes to bring a test to market.[20]

Metabolomics is still considered an immature field, and a number of notable gaps are currently stalling methodologies from producing meaningful disease knowledge and translational opportunities. MS/MS data interpretation, database content, isomer resolution, identification confidence, and False Discovery Rate (FDR) assessment metrics all require further development to allow for the successful biological analysis of metabolites.[21]

The following chapters follow several untargeted biomarker discovery projects in the context of two different diseases: tuberculosis and Chagas disease. The tuberculosis project centers around proteomics approaches, while the Chagas disease project focuses on small-molecule, metabolomics approaches. Both aim to discover novel biomarkers for diagnostic

purposes, but the end-use goals are different. While the tuberculosis project seeks antigenic biomarkers for initial disease diagnosis, the Chagas disease project hopes to yield novel biomarkers-of-cure to assess efficacy of drug treatment.

2 Discovery of Small Molecule Metabolite Biomarkers-of-Cure for Chagas Disease

2.1 Publication Contribution Statement

Some content from Chapter 2 stems from published manuscripts. To highlight the specific contributions of individual authors in Dean, et al., names have been added immediately below the captions for affiliated figures and at the top of methods subsections.

(1) Dean, D. A.; Roach, J.; Ulrich vonBargen, R.; Xiong, Y.; Kane, S. S.; Klechka, L.; Wheeler, K.; Jimenez Sandoval, M.; Lesani, M.; Hossain, E.; Katemauswa, M.; Schaefer, M.; Harris, M.; Barron, S.; Liu, Z.; Pan, C.; McCall, L.-I. Persistent Biofluid Small-Molecule Alterations Induced by Trypanosoma Cruzi Infection Are Not Restored by Parasite Elimination. ACS Infect. Dis. 2023, 9 (11), 2173–2189. https://doi.org/10.1021/acsinfecdis.3c00261.

Subsection 2.5.1, Metabolic Adaptations to Infections, contains key summarized content and direct excerpts from:

(2) Liu, Z.; vonBargen, R. U.; McCall, L.-I. Central Role of Metabolism in Trypanosoma Cruzi Tropism and Chagas Disease Pathogenesis. Curr Opin Microbiol 2021, 63, 204–209. https://doi.org/10.1016/j.mib.2021.07.015.

2.2 Disease Overview and Pathology

Chagas Disease (CD), caused by *Trypanosoma cruzi (T. cruzi)* protozoa, is a complicated parasitic illness with inadequate medical measures for diagnosing infection or monitoring treatment success. Globally, there are approximately 6-7 million CD cases with around 300,000 infections within the United States.[22] Transmission occurs through fecal matter from infected triatomine insects, congenital transmission, blood transfusion, organ transplantation, contaminated food, and laboratory exposure.[23]

The disease presents in three stages: acute, indeterminate, and chronic. The acute stage is initiated when metacyclic trypomastigotes penetrate a new host and differentiate into proliferative amastigotes. Intracellular replication is followed by differentiation back to the trypomastigote stage and trypomastigote release. Additional infection sites are then established.[24] Infected individuals experience non-specific symptoms such as nausea and fever but become asymptomatic within a few weeks. Left untreated, acute infection usually transitions into a long-term asymptomatic indeterminate stage.

Over decades of infection, approximately one-third of these indeterminate chronic *T. cruzi* infections progress to *symptomatic* chronic CD with life-threatening cardiovascular manifestations (cardiomegaly, apical aneurysms, arrhythmias, heart failure) and/or megacolon and megaoesophagus.[23] Up to two-thirds of patients exhibiting the symptomatic chronic form of the disease die due to cardiac arrest, one-quarter due to heart failure, and approximately 10% from a thromboembolic event.[25]

2.3 Treatment Options

Current treatments for CD include the antiparasitic drugs benznidazole (BZ) and nifurtimox (NFX). Unfortunately, these drugs have severe adverse effects, sometimes leading to treatment interruption. In addition, up to 20% of patients do not achieve full parasite clearance by these standard treatments.[26–30] Addressing treatment success is essential to prioritize follow-up treatment in these patient cohorts and to guide drug development.

2.4 Chagas Disease Diagnostic Landscape

Two important classes of CD diagnostics exist: diagnostics-of-infection (DOI) and diagnostics-of-cure (DOC). It is important to note that the DOI class refers to the patient's experience of initial diagnosis and is independent of the stage of the disease; most initial diagnoses occur during the final, chronic phase of CD. Because the disease is so complex, suitable methodologies and biomarkers for the multiple diagnostic classes of CD can be conflicting and strikingly different.

2.4.1 Diagnostics of Infection

Because symptoms are mild during the acute stage, infected individuals rarely seek medical treatment. For those who do, symptoms are often dismissed or incorrectly assessed as being affiliated with a common rotavirus. Correct diagnosis during the acute stage can occur via microscopy, but microscopy is only useful during the acute phase.

Most diagnostic focus is centered around the chronic disease form. Current chronic CD diagnostic methods include several serological tests: enzyme-linked immunosorbent assays, indirect hemagglutination, and indirect immunofluorescence assays.[31,32] These tests rely on the

presence of anti-*T. cruzi* antibodies for diagnosis and suffer from low reliability due to the rate of false positives (0.3 – 3.2%) and false negatives (0.7 – 3.7%). Clinical standards dictate there must be a minimum of two positive test results to conclusively diagnose CD.

In one study, approximately 50% of *T. cruzi*-positive blood was misdiagnosed in Venezuelan blood banks due to the low specificity and sensitivity of current diagnostic methods.[33,34] This is concerning not only due to the impact of lost treatment opportunities but also because misdiagnosed blood samples can be used for blood transfusions – ultimately leading to more *T. cruzi* infections.

2.4.2 Diagnostics of Cure

The traditional serological tests described above can take decades to become negative after parasite clearance, yielding false positive results even after parasite clearance. Instead, clinical trials exploring potential CD treatments often turn to PCR techniques as diagnostics-of-cure – techniques now being used to supplement initial diagnoses in suspected chronic cases as well.[26,35,36] PCR detection is unfortunately only 60-70% sensitive, as it is not consistently positive in infected individuals. PCR cannot indicate treatment success but only confirm parasitological treatment failure.[37–39]

2.4.3 Treatments & Diagnostics in the Context of Disease Progression

Importantly, all these diagnostic methods also lack the ability to monitor disease progression. In the BENEFIT clinical trial, while successful parasitological cure was achieved with benznidazole treatment, benznidazole-treated patients nevertheless went into cardiac failure or died at comparable rates to placebo controls, indicating that parasite burden alone cannot predict clinical outcomes.[35] While electrocardiograms may be useful for identifying heart

dysfunction, they cannot diagnose chronic stage CD but simply cardiac disease.[40] Furthermore, most patients in the chronic stage of CD have irreversible cardiac fibrosis, which highlights the importance of earlier diagnosis. Brain Natriuretic Peptide (BNP), a known biomarker of heart failure, is increased in patients with CD. It identifies cardiac disease but does not necessarily diagnose parasitic infection or predict progression to severe CD from the indeterminate stage.[41,42] Researchers have also tested magnetic resonance imaging (MRI) on CD patients to assess disease severity, but this was mainly effective in already-symptomatic patients.[43]

Every stage of CD maintains a strong need for novel diagnostic methods. In a survey of 155 CD experts around the world, 62 acknowledged early assessment of treatment response as a high need in research priorities in the CD community.[37]

2.5 Opportunities using Metabolomics

Metabolomics can help bridge this gap. Metabolomics is the integration of analytical and biochemical methods to study small molecules, broadly defined here as any molecule with a size of 1500 Da or less. These molecules are the products of metabolic pathways, critical signaling molecules, and the building blocks of biology, including amino acids, nucleotides and lipids. As such, they are direct markers of changes in biochemical processes.[44–46]

2.5.1 Metabolic adaptations to infection

Zongyuan Liu, Rebecca Ulrich vonBargen

T. cruzi undergoes significant metabolic adaptations during its shift from the extracellular insect-stage to a predominantly intracellular lifestyle within its mammalian host.[47,48] Many of the insect stage (epimastigote)-elevated transcripts are associated with metabolism or nutrient uptake.[48] *T. cruzi* is able to sense nutrient availability and adapt its proliferation accordingly.[49] *In*

vitro, at the mRNA level, amastigotes upregulate amino acid catabolism, fatty acid oxidation, oxidative phosphorylation, lipid and sterol biosynthesis, pyrimidine biosynthetic pathways, guanine salvage enzymes, and trypanothione antioxidant production compared to trypomastigotes or to timepoints early after host cell invasion.[48,50,51]

Amastigotes supplement their intrinsic metabolic activities by scavenging host metabolites. A prominent example is parasite reliance on host purines,[48] but amastigotes also scavenge host long chain fatty acids[52] and glucose.[53] However, these studies were performed during *in vitro* infection,[48,50,51] with no data on how *T. cruzi* adapts on a metabolic level to infect different organs *in vivo.*

Host metabolic adaptations may represent health-promoting or pathological compensation for parasite nutrient usage, immune response metabolic control, or adaptations to tissue damage. Via metabolic control of immune pathways, glucose and the pentose phosphate pathway support antiparasitic reactive oxygen and nitrogen species production by infected macrophages stimulated with IFNɣ.[54] Genes related to mitochondria function were downregulated in *in vitro*-infected cardiomyocytes,[55] and electron transport chain function was impaired.[56] Decreases in oxidative phosphorylation gene expression and electron transport chain function were also observed in mouse hearts[57–60] and in one human patient study,[60] though this contrasts with reports of increased mitochondrial respiration *in vitro* in fibroblasts[53] and macrophages,[61] and in other CD patient-derived samples.[62] These conflicting observations may reflect differences between *in vitro* and *in vivo* settings, between mRNA-based vs functional studies, and between timepoints and parasite strains. The increased oxidative metabolism in infected macrophages may help promote the production of antiparasitic nitric oxide.[61] Fatty acid synthesis was also decreased in acutely-infected mouse hearts.[63,64] Eliminating adipocytes

worsens acute and chronic experimental CD, supporting a causative role of fatty acid storage in CD progression.[65] In addition, these metabolic changes may be impacting antiparasitic immune responses: fatty acid synthesis is required for Th17 differentiation,[66] so that reduced fatty acid synthesis may impair parasite clearance and promote disease progression.[67,68]

In contrast, *T. cruzi* benefits from host fatty acid beta-oxidation and amino acid catabolism,[69] so that the observed reduction of fatty acid and amino acid catabolism at the mRNA level in acutely-infected[63] and chronically-infected[58] mouse hearts may slow parasite growth, though an increase in fatty acid catabolism gene expression was observed in one analysis of patient-derived samples.[62] On the other hand, *T. cruzi*-infected fibroblasts and myoblasts upregulate glucose uptake, but this favors *T. cruzi* proliferation.[53] Likewise, infected human foreskin fibroblasts upregulate tetrahydrobiopterin synthesis, lipid biosynthesis and mevalonate pathway gene expression. The latter has been postulated to be an adaptation to parasite sterol needs, or to mitigate reactive oxygen species produced in response to infection, while the former may help the parasite meet pterin needs.[48] Parasite reliance on host biopterin biosynthesis was confirmed via an RNAi screen, which also demonstrated reliance on host pyrimidine biosynthesis.[69]

In vivo studies further revealed complex interactions between organs during infection, with variable metabolic adaptations depending on the organ system. For example, glucose uptake, sorbitol pathway and phospholipid synthesis were increased in heart tissue but decreased in plasma during acute *T. cruzi* Y strain infection.[64] Likewise, PC(20:4) was increased by acute infection with *T. cruzi* strain CL Brener (luciferase-expressing) in the oesophagus and large intestine, but decreased in the small intestine.[70] Acute infection was also associated with increased acylcarnitines in the oesophagus and small intestine, which persisted in the oesophagus

during chronic infection, and elevated kynurenine in the large intestine at both disease stages.[70] Kynurenine is produced from tryptophan during inflammation and has immune-modulating properties. Kynurenine metabolites also directly inhibit *T. cruzi* growth and promote host survival *in vivo* during acute infection.[71] Cardiac glycerophosphocholines increased during mouse chronic infection with *T. cruzi* strains CL Brener and Sylvio X10/4, while infection depleted cardiac acylcarnitines.[72] This decrease in cardiac acylcarnitines may be an indicator of increased fatty acid beta oxidation flux, which may benefit *T. cruzi*.[69] The magnitude of cardiac phosphocholine perturbation was proportional to the levels of indicators of pro-fibrotic cytokines and to the magnitude of cardiac fibrosis and inflammation, in an independent chronic mouse infection model.[73] The representation of higher- vs lower-molecular-weight acylcarnitine and phosphatidylcholine family members also differed based on acute mouse *T. cruzi* infection severity.[74] Lastly, though *T. cruzi* is distal from sites of microbiota colonization,[75] altered microbiota composition and metabolism has been observed during acute and chronic experimental infection.[76,77]

2.6 Experimental Design

The development of an early test for CD treatment success is considered the top need in the field by a panel of sixty-two CD experts.[78] We hypothesized that liquid chromatography tandem mass spectrometry (LC-MS/MS)-based untargeted metabolomics could be used to discover novel small-molecule biomarkers of Chagas Disease treatment success versus failure in serum and/or urine. More specifically, we expected infection-induced circulating metabolic changes to be quickly reverted by Bz treatment in cured patients, while these metabolites will remain disturbed in patients that fail to respond to treatment.

We designed a mouse model that uses mice infected with luciferase-expressing strain CL Brener and treated with an intermediate benznidazole treatment dose in which some mice are expected to fully clear parasites and some mice are expected to remain infected (parasitological treatment failure)[79–81] to test our hypothesis. Serum and urine samples collected at timepoints before, during, and after CD treatment will be assessed for differentiated metabolites significant to treatment failure or treatment success groups.

2.7 Methods

2.7.1 Ethics Statement

All vertebrate animal studies were performed under protocol number R17-035 and R20-027, approved by the University of Oklahoma Institutional Animal Care and Use Committee.

2.7.2 *In vitro* Parasite Cell Culture

Shelley Kane

T. cruzi strain Sylvio X10/4 was obtained from ATCC (catalog number 50800) and placed in co-culture with C2C12 mouse myoblasts (ATCC catalog number CRL-1772). *T. cruzi* luciferase-expressing strain CL Brener was a kind gift of Dr. John Kelly, London School of Hygiene and Tropical Medicine,[79] and was likewise co-cultured with C2C12 cells. C2C12 cells were maintained in Dulbecco's Modified Eagle Medium (DMEM) supplemented with 5% iron-supplemented calf serum (Fisher catalog number SH3007203), 100 U/mL penicillin and 100 µg/mL streptomycin at 37˚C with 5% CO_2. Media was changed twice a week. Freshly-egresssed trypomastigotes were harvested from the culture media and added to fresh C2C12 culture flasks (for expansion) or counted using a hemacytometer, centrifuged at 2800 rpm for 5 min, resuspended in DMEM without serum, penicillin and streptomycin (for infections). All in vitro

culture time was kept to the minimum necessary to obtain sufficient parasite numbers for mouse infection cohorts.

2.7.3 *In vivo* Experimentation

Laura-Isobel McCall, Rebecca Ulrich vonBargen, Shelley Kane, Danya Dean

8-week-old male and female BALB/c mice (Jackson) were infected, uninfected, or injected with isoproterenol. Infected mice (n=90 [45f, 45m]) were injected intraperitoneally with 1,000 luciferase-expressing *T. cruzi* trypomastigotes of strain CL Brener parasites (TcVI DTU[82])[79]. Uninfected control mice (n=26 [13f, 13m]) were mock-infected using intraperitoneal injection of DMEM only. Isoproteronol mice (n=24 [12f, 12m]) were injected with a single dose (100mg/kg). 116-125 days post-infection (DPI), surviving infected mice were treated with 30 mg/kg benznidazole in solutol once daily via oral gavage. To assess antiparasitic treatment success vs failure, infected mice were then immunosuppressed beginning at 228 DPI (102 days post-treatment) with three rounds of cyclophosphamide, 200 mg/kg by intraperitoneal injection, every 4 days[81,83]. 4 days after the final immunosuppression, tail vein blood was collected for blood smear analysis and mice were euthanized and hearts collected to differentiate between successful vs failed parasite clearance by qPCR.

Serum samples were collected from the saphenous vein for metabolomics at four timepoints: pre-treatment, at treatment end, 4 weeks post-treatment, and immediately prior to the first cyclophosphamide dose. These timepoints correspond to 120 days-post-treatment (DPI), 130 DPI, 160 DPI, and 200 DPI. 161 DPI (35 days post-treatment), urine was collected from each surviving mouse by placing mice in a single cage until urination. The urine was pipetted into an

eppendorf. Prior to urine collection, cages were disinfected by spraying and wiping down with 70% ethanol to prevent cross-contamination. All samples were stored at -80℃ until extraction.

2.7.4 Parasite Burden and Cardiac Fibrosis Quantification

Laura-Isobel McCall, Shelley Kaine, Rebecca Ulrich vonBargen

DNA and RNA extraction of heart tissue from the heart base was performed using ZYMO research Quick-DNA/RNA Miniprep Plus Kit (ZD7003), per manufacturer's protocol. mRNA was reverse transcribed into cDNA using Invitrogen High-Capacity cDNA Reverse Transcription Kit with RNase Inhibitor. cDNA, DNA, and RNA were stored at -20℃ until analysis.

2.7.5 qPCR

Rebecca Ulrich vonBargen, Kate Wheeler

After extraction, DNA was quantified using nanodrop and 180 ng was used for qPCR analysis on a Roche Lightcycler 96 as in McCall *et al* 2017 [74] , using the conditions in **Table 2-1** and PowerUp SYBR Green master Mix (Fisher). $2x10^7$ *T. cruzi* trypomastigotes spiked into a known weight of uninfected tissue were used to extract DNA using the same procedure, and the resulting DNA used to generate standard curves. Primers used for analysis were ASTCGGCTGATCGTTTTCGA and AATTCCTCCAAGCAGCGGATA for parasite amplification[84] and TCCCTCTCATCAGTTCTATGGCCCA and CAGCAAGCATCTATGCACTTAGACCCC for normalization to mouse DNA.[85]

2.7.6 qRT-PCR

Rebecca Ulrich vonBargen

qRT-PCR analysis was conducted on a Roche Lightcycler 96. cDNA samples were diluted 1:100 in water and were mixed with PowerUp SYBR Green master Mix (Fisher). Brain natriuretic peptide (Forward: AAGTCCTAGCCAGTCTCCAGA, Reverse: GAGCTGTCTCTGGGCCATTTC) and *Gapdh* primers (Forward: GACTTCAACAGCAACTCCCAC, Reverse: TCCACCACCCTGTTGCTGTA were used for analysis and were added in 0.25 µM concentration[86,87]. qRT-PCR parameters are as in **Table 2-1.**

Table 2-1. qPCR and qRT-PCR parameters.

Program	**Description**	**Acquisition mode**
Preincubation	1 cycle	
	95°C for 600s	none
3 Step Amplification	40 cycles	
	95°C for 30s	none
	58°C for 60s	none
	72°C for 60s	single
Melting	1 cycle	
	95°C for 60s	none
	55°C for 30s	none
	95°C for 1s	continuous

2.7.7 Determination of Persistent vs Cleared Parasites

Rebecca Ulrich vonBargen, Laura-Isobel McCall

At the end of the study, hearts were collected to differentiate between successful vs failed parasite clearance. Extracted DNA was analyzed using qPCR, as described in **Section 2.7.5,** with care being taken to normalize to mouse DNA. For comparison of parasite clearance vs parasite persistence, a parasite burden cut off post-immunosuppression of uninfected group value + 3 standard deviations was used (20 parasite equivalents). By this definition, in the female cohort, 17 mice were deemed to have successfully cleared parasites, and 25 were deemed parasitological treatment failures.

2.7.8 Metabolite Extraction and LC-MS/MS Data Collection (Untargeted Analysis)

Rebecca Ulrich vonBargen, Jarrod Roach, Sayre Barro, Zongyuan Liu (LC-MS/MS only)

Samples were extracted according to Dunn et al., 2011.[88] Briefly, all samples were extracted with 100% HPLC-grade methanol with internal control (0.5 µM sulfachloropyridazine) to a final concentration of 74% methanol. Samples were then vortexed and centrifuged at 16,000xg for 15 min. The supernatant was then dried overnight in a Speedvac and stored at -80 °C until LC-MS/MS analysis. For LC-MS/MS analysis, samples were resuspended in 150 µL HPLC-grade water + 0.5 µM sulfadimethoxine, sonicated for 5 min and centrifuged at 16,000xg for 15 min. The supernatant was then transferred to a run plate. Pooled quality controls (QC) were made using 1 µL per well per sample type, and blanks made of resuspension solvent. Samples were analyzed in randomized order per sample type and 25 µL was injected for analysis, with the injection volume determined empirically based on peak shape, magnitude of the overall

signal intensity, and proportional increase of the overall signal intensity, peak height of internal standards and peak height for molecules of known interest, compared to the increase in injection volumes. LC analysis was performed using a Thermo Scientific Vanquish UHPLC. A Phenomenex 1.6 µm 100 Å Luna Omega Polar C18 column (50 × 2.1 mm) was used for separation. The LC column temperature was set to 40 °C and analysis was done using mobile phase A (water + 0.1% formic acid) and mobile phase B (acetonitrile + 0.1% formic acid) with a 0.5 mL/min flow rate (12.5 min gradient, details shown below in **Table 2-2**). Instrumental drift was monitored using a solution of 6 known molecules at the beginning of analysis, between each sample type, and at the end of analysis. Instrument calibration was done using Pierce LTQ Velos ESI positive ion calibration solution immediately prior to analysis. A Q Exactive Plus (Thermo Scientific) high resolution mass spectrometer was used for MS/MS detection (**Appendix A**) and ions were generated for MS/MS analysis in positive mode.

Table 2-2. LC gradient.

Time(min)	**Flow (ml/min)**	**%B**	**Curve**
0.000	Run		
0.000	0.500	5.0	5
1.000	0.500	5.0	5
9.000	0.500	100.0	5
11.000	0.500	100.0	5
11.500	0.500	2.0	5
12.500	0.500	2.0	5
12.500	Stop Run		

2.7.9 LC-MS/MS Data Processing in MZMine and Feature Table Generation

Rebecca Ulrich vonBargen (serum, urine), Monica Ness (serum), Jarrod Roach (urine), Sayre Barron (urine)

Data was obtained from LC-MS/MS analysis and converted to mzXML files using MSConvert.[89] A feature table containing all metabolites for further analysis was developed using MZmine version 2.53 [90], with data processing parameters optimized for each dataset individually, by manually inspecting built chromatograms in MZmine and based on detection of internal standards in all samples. See **Appendix B** for parameter details. Three-fold blank removal was performed and total ion current (TIC) normalization performed in Jupyter notebooks in R. We elected not to normalize to creatinine because of evidence that it can be affected by infection status in multiple infection systems (*e.g.*[91]).

2.7.10 Data Analysis

Rebecca Ulrich vonBargen, Jarrod Roach, Sayre Barron

TIC normalization

Because minor differences exist in sample volume, detector sensitivity, matrix effects, column retention, and more, technical variations exist that complicate feature comparison between sample points. The TIC normalization we employed divides an individual feature peak (intensity) by the total sum of all ion intensities within that sample run to resize the relative range, which ultimately standardizes the range across all samples.

Principal Coordinate Analysis (PCoA)

Principal coordinate analysis (PCoA) was performed on Bray-Curtis dissimilarity matrices calculated from TIC-normalized feature intensities using a classical multidimensional scaling approach (double-centering of the squared distance matrix followed by eigendecomposition). Analyses were implemented in Python (version 3.10.12) using SciPy (v1.15.3) for distance calculations and NumPy (v2.2.6) for eigendecomposition. Figures were generated using Matplotlib (v3.10.9). Group separation between treatment outcomes was assessed at each timepoint using permutational multivariate analysis of variance (PERMANOVA; 999 permutations) with pseudo-F statistics calculated following Anderson (2001).[92]

Hartigan's Dip Test

The dip statistic was calculated on PCo1 coordinate values using the diptest Python package (v0.1.4), which implements Hartigan and Hartigan's 1985 algorithm. The p-value was estimated by comparison to a simulated null distribution.

Bimodality Coefficient (BC)

Skewness and excess kurtosis of PCo1 coordinates were computed using scipy.stats (SciPy v1.15.3). The bimodality coefficient was calculated with the finite-sample correction. A threshold of 0.555 was applied as the criterion for bimodality.[93] More details provided in cited reference.

Gaussian Mixture Model (GMM) with BIC Comparison

Gaussian mixture models with 1 and 2 components were fit to PCo1 coordinate values using sklearn.mixture.GaussianMixture (scikit-learn v1.7.2) with full covariance and random state set to 42 for reproducibility. Model fit was compared using the Bayesian Information Criterion (BIC); a positive ΔBIC ($BIC_1 - BIC_2$) indicates the 2-component model fits better.[94]

Feature-By-Feature Logistic Regression

To identify individual serum metabolite features associated with benznidazole (BZ) treatment outcome, a feature-by-feature univariate logistic regression approach was applied. Analysis was restricted to the BZ treatment group (n = 74 animals per timepoint). Treatment outcome was defined as a binary variable: success (≤20 parasite equivalents; ≤ mean + 3 SD of the DMEM vehicle control group) versus failure (>20 parasite equivalents). Features were analyzed separately at each of the four collection timepoints (TP1–TP4). At each timepoint, a separate logistic regression model was fit for each metabolite feature independently using scikit-learn (v1.x, LogisticRegression, lbfgs solver, max_iter=1000). Prior to model fitting, each feature was standardized to zero mean and unit variance (z-score normalization) using StandardScaler to place coefficients on a comparable scale across features. Statistical significance was evaluated using a likelihood ratio test: the log-likelihood of the fitted model was compared to that of a null (intercept-only) model, and the resulting test statistic was evaluated against a chi-squared distribution with one degree of freedom. Within each timepoint, p-values were corrected for multiple comparisons across all features using the Benjamini-Hochberg (BH) false discovery rate procedure (adjusted $p < 0.05$ threshold). The sign of the standardized regression coefficient was used to assign direction of association: a positive coefficient indicates higher feature abundance associated with treatment success; a negative coefficient indicates higher abundance in treatment

failure. To identify features with reproducible signal across the treatment time course, two convergent-evidence metrics were computed for each feature: (1) the number of timepoints at which the feature reached nominal significance (raw $p < 0.05$), and (2) the number of timepoints at which it was BH-significant (adjusted $p < 0.05$). A direction-consistency score was defined as the number of timepoints at which the coefficient sign agreed with the majority direction across all four timepoints. Features were considered high-priority candidates if they were BH-significant at one or more timepoints and maintained direction consistency across at least two timepoints.

2.7.11 Feature-Based Molecular Networking (FBMN) Using Global Natural Products Social Molecular Networking (GNPS)

Rebecca Ulrich vonBargen (serum, urine), Monica Ness (serum), Jarrod Roach (urine)

Feature-based molecular networking (FBMN) was performed using global natural products social molecular networking (GNPS)[95,96] based on the parameters in **Appendix C**. Annotations were generated from the GNPS data using an in-house script (https://github.com/camilgosmanov/GNPS[97]). This provides level 2/3 metabolite annotations based on the Metabolomics Standards Initiative rankings.[98] All resulting annotations were manually inspected for good mirror plot matching and biological plausibility, as recommended by Theodoridis et al.[99]

2.8 Results

2.8.1 Serum Samples

A comprehensive serum metabolite feature table was constructed from the LC-MS/MS data, as described in **2.7.9**, containing 2,594 total features. Principal coordinate analysis (PCoA),

described in **Data Analysis**, was used to transform the data variables into a table of pair-by-pair differences called a distance matrix. Bray-Curtis method was then used to measure dissimilarities, reported between 0 (minimum dissimilarity) and 1(maximum dissimilarity), shown as a percentage, and visualized by plotting the largest source of variation along the x-axis and second-largest variation source along the y-axis. PERMANOVA (permutational multivariate analysis of variance) tested whether the centroids of groups varied in multivariate space. For example, did a cluster of treatment success samples occupy a different metabolome space than a cluster of treatment failure samples? A pseudo-F statistic calculated actual difference between group centroids, then randomly shuffled and recalculated 999 times before reporting a final p-value showing what proportion of the shuffled pseudo-F values was equal to or greater than the observed one. It's important to note that PERMANOVA considers dispersion in addition to location, so significance can persist in certain cases of similar centroids.

Looking below at **Figure 2-1**, differences in treatment outcome groups across all four timepoints in serum samples are visualized. A pattern consistent to all four panels can be noticed. At each timepoint, there appears to be two groups of samples in parallel distribution with a central gap. To investigate what might be causing this gap, we began assessing different metadata categories. One thought was gender. We quickly noticed that in the timepoint 1 (TP1) panel of **Figure 2-1**, the females (circles) trend toward the bottom right while the males (triangles) trend toward the upper left. There is even a clear visual midpoint separating the gender groups, and these trends are consistent on both sides of the central gap. This means the central gap is likely caused by something else, but gender is creating a secondary gradient in TP1. Looking further into gender, we calculated that 67% of the success group across all four timepoints is female, while the failure group is 41% female. Looking closely at other timepoints, this is visually

apparent, and gender should be acknowledged as a covariate. Biological sex differences in CD expression and immune control are well-documented in human patients, but drug treatment outcome is typically not strongly correlated to gender.[100]

Next, we hypothesized plate batch effects might be causing the central gap in the data distribution. While not the root cause, we did uncover something notable between plates and genders. The lab workflow we designed to process samples efficiently and reduce batch effects during metabolite extractions resulted in processing all the female samples first, followed by all the male samples. Though we did randomize sample order within each gendered set of extractions, out of the six total sample plates for the run, three contained exclusively female samples and three were exclusively male. As a downstream consequence, gender effects and plate batch effects cannot be separated in the data analysis stage.

To test whether the gap is real or an artifact of the distance calculation, we decided to look at the raw data from TP1 in a scatter plot (not shown). There was a small valley on the Pco1 histogram, so we chose three different statistical tests (additional details in methods) to run on the raw data to assess significance:

1. Hartigan's dip test was used to check for bimodality, essentially determining how much the data departs from unimodal distribution.[101] A p-value < 0.05 indicates data is significantly non-unimodal. Pco1 results gave $D = 0.041$ ($p = 0.316$, not significant).
2. Bimodality Coefficient (BC) was used to assess whether the Pco1 data distribution departed from unimodality by skewness (asymmetry) and excess kurtosis (flat-top). Bimodal distributions typically exhibit high skewness or low kurtosis. BC of 0.555 shows perfectly unimodal normal distribution, and values above 0.555 suggest bimodality. Pco1 results calculated $BC = 0.44$ (below threshold).

3. A Gaussian mixture model (GMM) assumes the observed data were generated by a mixture of k Gaussian (normal) distributions. We performed a GMM mixture model comparison (1 vs 2components). Fitting the 1-component tests normal distribution while fitting a 2-component tests whether two overlapping normal distributions fit better. The Bayesian Information Criterion (BIC) penalizes model complexity. More complex model (k=2) is only preferred if it fits substantially better than the simpler one (k=1). Change in BIC is calculated by subtracting BIC-2 from BIC-1, so a positive value for BIC indicates the 2-component model is a better fit. A BIC change > 10 is conventionally considered strong evidence in favor of the more complex model. Change in BIC < 6 is considered weak evidence. TP1 results = 3.87 mean 2-component is slightly better but not meaningful.

Since all three statistical tests were in agreement, the valley is not statistically significant, and we hypothesized the central gap is an artifact. When PCoAs were re-run with Aitchison distance, the artifact disappears (**Appendix D**), and samples are mostly distributed in a cloud across all timepoints. This supports the central gap and parallel distribution being a geometric artifact of Bray-Curtis in PCoA space, not a real biological dichotomy in the data.

However, Aitchison finds only TP3 significant (F=1.86, p=0.037), and the effect sizes (F-statistics around 1.2) are weak across all timepoints. By comparison, TP1, TP2, and TP3 were significant in the Bray-Curtis method. The Bray-Curtis method is sensitive to the dominant features, or high-abundance metabolites. CLR/Aitchison log-transforms relative to the geometric mean to treat features more equally, but it also dilutes signal from the metabolites that are the most different.

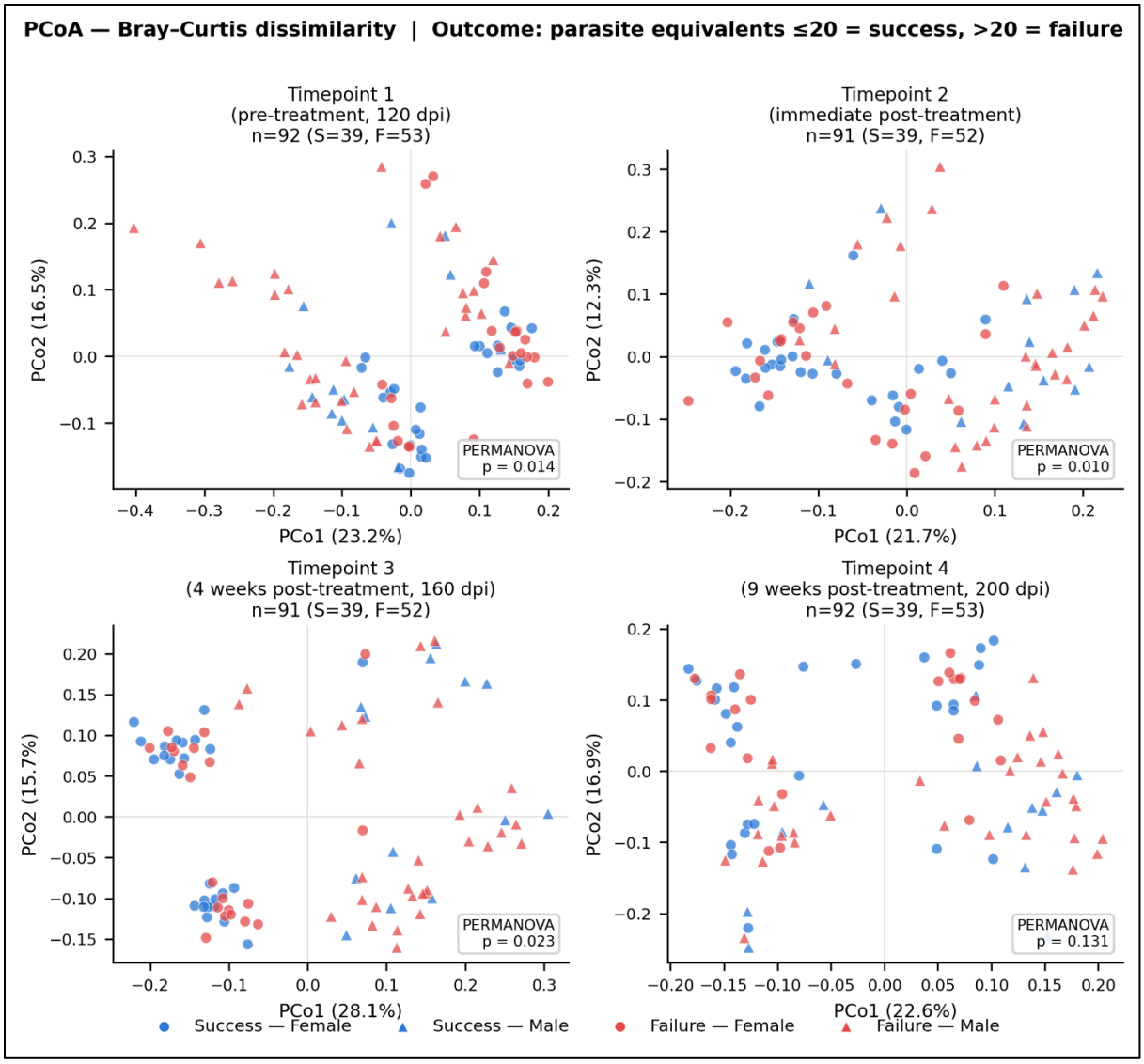


Figure 2-1. Serum metabolomic profiles differ between treatment outcome groups throughout drug treatment. Principal coordinate analysis (PCoA) of Bray–Curtis dissimilarity calculated for Bz treatment group only. Each point represents one mouse serum sample, colored by treatment outcome, shaped by sex (circle = female, triangle = male). Outcome defined as failure at or above 20 parasite equivalents threshold (mean+3SD of DMEM control group). Panels show four collection timepoints: pre-treatment (120 dpi), immediate post-treatment (130 dpi), 4 weeks post-treatment (160 dpi), and 9 weeks post-treatment (200 dpi). Group separation was assessed by permutational multivariate analysis of variance (PERMANOVA; 999 permutations). Metabolomic profiles were significantly separated between outcome groups at TP1 ($p = 0.014$), TP2 ($p = 0.010$), and TP3 ($p = 0.023$), indicating presence of metabolic differences between eventual successes and failures before, during, and 4 weeks after treatment. Separation was not significant at 9 weeks post-treatment (TP4, $p = 0.131$), suggesting metabolic convergence between groups at the study endpoint. Axes represent the first and second principal coordinates, capturing the largest and second largest sources of variation in pairwise metabolomic dissimilarity, labeled by percentage of total variance. Dpi = days post infection.

Feature-By-Feature Logistic Regression Analysis

A feature-by-feature logistic regression (LR) was prepared to examine the biomarkers present at each timepoint and their ability to predict treatment outcome. Samples with outcome of treatment success and treatment failure were filtered out from the full dataset, separate regressions to compare treatment success vs failure were run for each timepoint, and a Benjamini-Hochberg FDR correction (BH) was applied to each run. We also factored in the positive or negative value of the coefficient at each timepoint because a positive coefficient represents higher probability of success while a negative coefficient represents higher probability of failure. We are looking for features where the relationship to outcome is stable in direction across timepoints. A direction consistency score was calculated by summing the absolute value of the sign of each coefficient (4 = all timepoints agree in direction).

Table 2-1 shows the five features that reached Benjamini-Hochberg FDR-corrected significance (BH-significance) and were confirmed by GNPS Feature-Based Molecular Network spectral library match. 30 additional features were BH-significant but could not be confirmed. These unannotated features are listed in **Appendix E**. N-Acetyl tryptophan was discussed earlier in this chapter for its connection to the kynurenine pathway. Interestingly, inosine is a critical life support molecule for *T. cruzi*, so its metabolic pathway is actually a major target for drug discovery.[102] the strongest directionally consistent *downregulated* candidate – consistently goes down in failures relative to controls/successes. Both parasite and host use these pathways in regulation and progression to chronic infection.

Table 2-3. Serum Metabolite Features with BH-Significant Association with BZ Treatment Outcome and Confirmed Spectral Library Identity. Five serum metabolite features identified by feature-by-feature logistic regression as BH-significant (adjusted q < 0.05) at one or more timepoints in the BZ treatment group, with confirmed spectral library identity via GNPS FBMN (MQ Score > 0.7). All four directionally consistent features were elevated in mice achieving treatment success (≤20 parasite equivalents), consistent with metabolic recovery following effective BZ treatment. sn-Glycero-3-phosphocholine showed mixed directionality across timepoints and is included for completeness. RT, retention time (min); MQ Score, mirror quality score reflecting spectral match fidelity to the GNPS library (range 0–1); BH-sig TPs, number of timepoints reaching Benjamini–Hochberg-corrected q < 0.05; Raw-sig TPs, number of timepoints with nominal p < 0.05

Precursor m/z	RT (min)	Compound	MQ Score	Adduct	BH-sig TPs	Raw-sig TPs	Direction
269.0878	0.55	**Inosine**	0.987	M+H	1	1	Higher in success
247.1076	3.53	**N-Acetyl-tryptophan**	0.982	M+H	1	3	Higher in success
182.0813	0.51	**Tyrosine**	0.980	M+H	1	2	Higher in success
136.0758	0.52	**Octopamine**	0.863	M+H−H_2O	1	2	Higher in success
258.1098	0.54	**sn-Glycero-3-phosphocholine**	0.780	M+H	1	1	Mixed

MQ Score: mirror quality score from GNPS spectral library match (range 0–1).
BH-sig TPs: number of timepoints reaching Benjamini–Hochberg-corrected q < 0.05.
Raw-sig TPs: number of timepoints with nominal p < 0.05.

2.8.2 Urine Samples

Female mice with parasite clearance following benznidazole antiparasitic treatment had comparable overall urine metabolome to mice that failed to clear parasites.

There was a clear and significant difference in the overall urine metabolome between the uninfected controls and the infected mice by principal coordinate analysis (whether treatment cleared parasites or not, PERMANOVA $p<0.05$, $R^2 = 0.08$, Figure **2-2B**). Note that these samples were collected prior to immunosuppression, to avoid confounding effects from the cyclophosphamide treatment. In contrast, there was no significant difference between the mice that successfully cleared parasites and mice that failed to do so, at 35 days post-treatment

(PERMANOVA p>0.05, **Figure 2-2C**). Likewise, no proportional correlation to post-immunosuppression parasite burden was observed (**Figure 2-2D**).

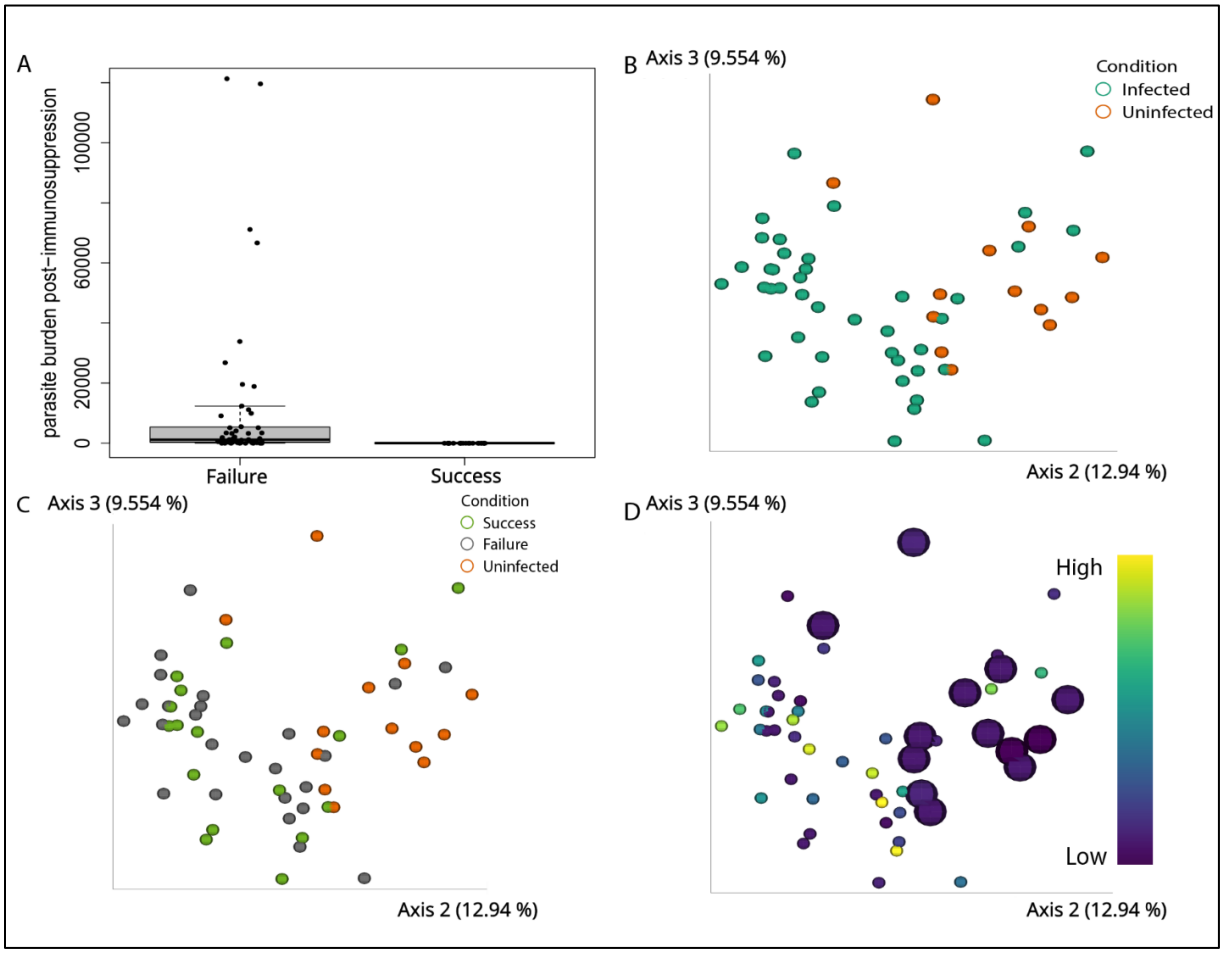


Figure 2-2. Urine metabolome in mice that successfully cleared T. cruzi shows no significant difference from mice in which parasites failed to be cleared. **(A)** Cardiac parasite burden post-infection, treatment and immunosuppression in mice in which parasites persisted (parasitological treatment failures) versus those where parasites were successfully cleared (success), as defined by our cutoff compared to qPCR background in uninfected samples (cutoff = 20 parasite equivalents). **(B)** Urine sample principal coordinate analysis for mice that were infected and then treated (irrespective of successful or failed parasite clearance) versus uninfected control mice. Samples collected prior to immunosuppression. PERMANOVA $p < 0.05$ for treated mice versus uninfected mice, $R^2 = 0.08$. **(C)** Same PCoA analysis as in **(B)**, re-colored to compare successfully-treated mice, mice where treatment failed to clear parasites, and uninfected control mice. PERMANOVA $p > 0.05$ for successful parasite clearance versus failed parasite clearance, $R^2 = 0.03$. **(D)** Same PCoA analysis as in **(B)**, re-colored to display normalized cardiac parasite burden post-immunosuppression, $R^2 = 0.02$. No segregation by parasite burden was observed. Uninfected controls enlarged for contrast.
Rebecca Ulrich vonBargen, Jarrod Roach

More specifically, four features significantly differed between infected and uninfected female samples but did not show any restoration even following sterile cure by benznidazole, shown in **Figure 2-3.**

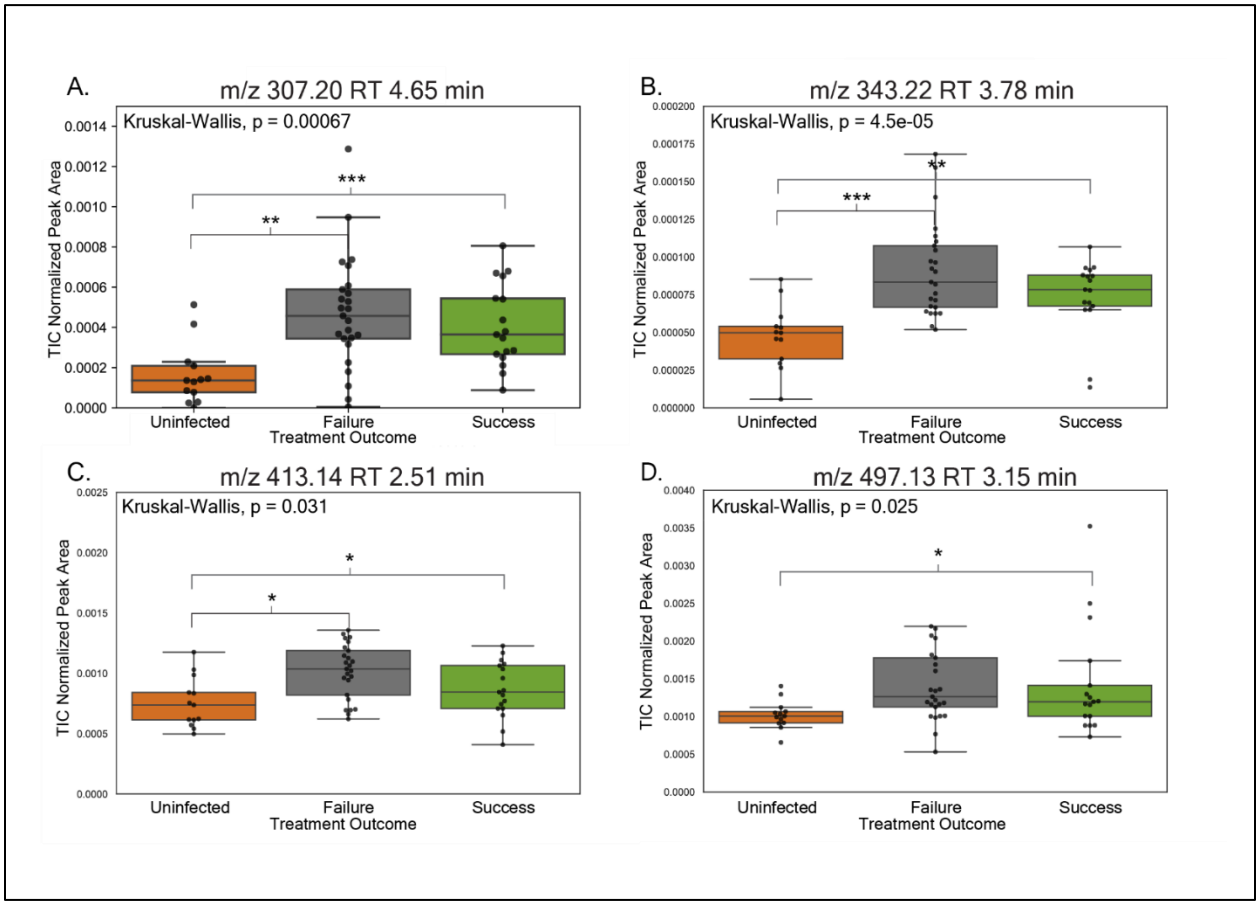


Figure 2-3. Metabolite features identified as differing between infected and uninfected samples remain significantly perturned even after successful parasite clearance.
Significance was established using p-values determined by a Kruskal-Wallis test. P-values were corrected using a Dunn Test with Benjamini-Hochberg adjustment to control the false discovery rate; FDR-corrected $p < 0.05$ = *, FDR-corrected $p < 0.01$ = **, FDR-corrected $p < 0.001$ = ***.
Rebecca Ulrich vonBargen, Jarrod Roach

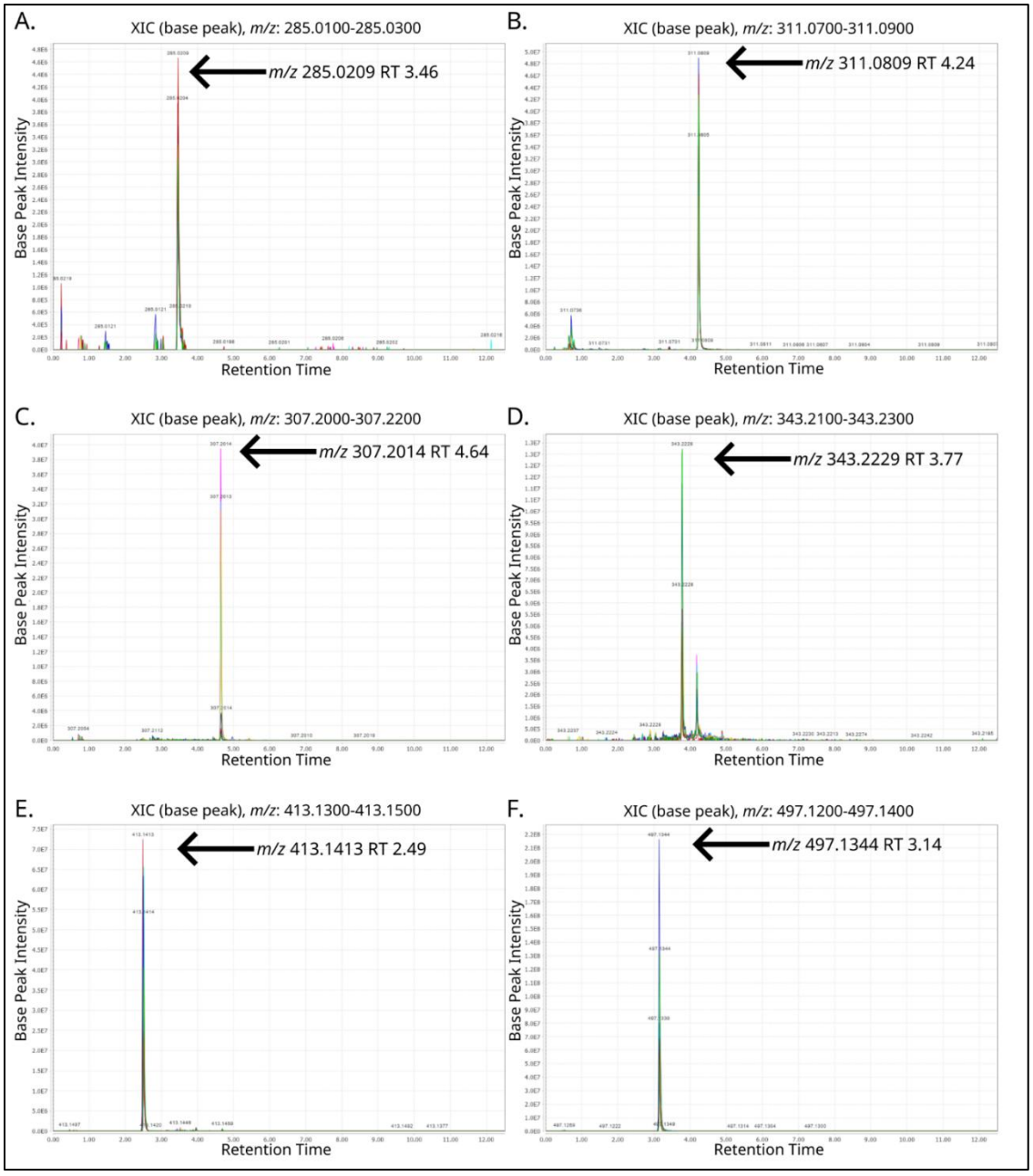


Figure 2-4. Extracted ion chromatograms (XICs) of internal standards and biomarkers. Chromatograms correspond to metabolite features from Figure 2-2 and two internal standards. Each color is a representative mouse (n = 9); differential peak areas and peak heights are to be expected due to animal-to-animal and group-to-group variability, but retention time alignment is good. **(A)** XIC for *m/z* range covering internal standard 1, sulfachloropyridazine (*m/z* 285.0209, RT 3.46 min). **(B)** XIC for *m/z* range covering internal standard 2, sulfadimethoxine (*m/z* 311.0809, RT 4.24 min). **(C)** XIC for range covering *m/z* 307.20, RT 4.65 min. **(D)** XIC for range covering *m/z* 343.22, RT 3.78 min **(E)** XIC for range covering *m/z* 413.14, RT 2.51 min. **(F)** XIC for range covering *m/z* 497.13, RT 3.15 min.
Jarrod Roach, Danya Dean, Rebecca Ulrich vonBargen

2.9 Discussion and Conclusion

We sought to use both the urine and serum metabolomes to assess treatment success vs failure, using a mouse model with post-treatment immunosuppression as the gold standard of antiparasitic treatment assessment. Urinary sample set allowed only for assessment of females at a single timepoint (35 days post-treatment) for discovering differentiated metabolites between and among treatment successes, treatment failures, and uninfected controls. Serum samples were collected at four timepoints corresponding to pre-treatment (120 days post-infection, DPI), immediately post-treatment (130 DPI), ~4 weeks post-treatment (160 DPI), and ~9 weeks post-treatment (200 DPI).

Interestingly, during chronic CD, while benznidazole treatment did indeed clear parasites in a subset of mice, as expected (**Figure 2-2A**), there was no difference in the overall urine metabolome between mice that achieved parasitological cure and those that did not, so that the metabolome of successfully treated infected mice was not reset by antiparasitic treatment (**Figure 2-2C**). This contrasts with acute-stage benznidazole treatment, which restored the plasma and heart metabolome.[77] This could be due to the use of different mouse and parasite strains,[103] but may also reflect the lack of improvements of functional and survival outcomes in late-stage patient treatment,[26] even in cases of parasitological cure, and the disconnect between parasite burden and symptomatic vs asymptomatic chronic infection.[104] Importantly, our urine results concur with analysis of cardiac tissue in an independent infection model, which likewise showed only minor and incomplete metabolic restoration and functional restoration 56 days post-benznidazole treatment, even with successful parasite elimination.[105]

Only one of the four identified differentiated female urine metabolite features was successfully annotated, and 25% falls well within the expected range of untargeted metabolomics experiments.[106–108] While an annotation can provide insight into the biological processes occurring within a disease condition, it is not required to be useful for developing detection models.[109,110]

Acylcarnitine metabolism has been causally linked to cardiac metabolism and disease severity in acute *T. cruzi* infection in mouse models.[77] Interestingly, acylcarnitines were decreased by chronic CD in heart tissue in C3H/HeJ mice but increased in acute stage infection in the gastrointestinal tract[72,77] and in chronic stage in the heart of BALB/c mice.[105] Lizardo *et al* also identified these classes of molecules as perturbed in the serum by chronic *T. cruzi* infection in mouse models.[103] Other molecules identified by Lizardo *et al* as potential biomarkers were citrulline, glutamine, spermidine and several sphingolipids.[103] These metabolites were not identified in our urine study and may be due to differences in sample type, sample preparation and data acquisition methods, and limits of detection, or had no statistical difference based on the selected analysis.

Interestingly, a proof of concept diagnostic test using urine called the Chunap test has been used to determine parasite presence in congenital CD and in *T. cruzi*/HIV co-infected patients.[111,112] Both of these studies showed increased specificity and sensitivity when compared to current blood-based PCR, microscopy and ELISA methods. *T. cruzi* parasite antigens and DNA have been previously detected in the urine of patients with acute, chronic, and congenital CD.[113–115] In guinea pigs, parasite antigens and DNA in urine were not associated with kidney injury or parasites in kidney but were rather an effect of heart and cardiovascular system damage.[116] Lemos *et al.* identified changes in the kidney in mice infected with high dose

(30,000) *T. cruzi* trypomastigotes during the acute stage of the disease.[117] However, alterations in kidney function were due to cardiac alterations of CD, and the kidneys remained functional.[117] While kidney damage is seen in CD patients, there is little research assessing how this damage occurs. Heart failure could be contributing to kidney damage in CD, as is known in other cardiovascular diseases.[118] These studies signify that our results are not just an artifact of the mouse model, and that the role of the kidney in CD pathogenesis warrants further investigation.

Given the relationship between immunity and metabolism (*e.g.*[119]), and prior work demonstrating persistent immunological dysfunction after benznidazole treatment, in association with perturbed cardiac metabolism that is improved by an immunomodulating therapeutic,[105] some of these biomarkers may be a reflection of immune signaling. It will be important to assess their specificity to CD as part of their continued development. Biomarkers that are not unique to *T. cruzi* could still be useful to predict progression of CD, in the context of an infection diagnosed by existing methods such as PCR or serology.

One limitation is that we only assessed urinary metabolic restoration at 35 days post-treatment. It is possible that metabolism gradually improves over time, though incomplete metabolic restoration was also observed in heart tissue 56 days post-treatment.[105] A study of CD patients treated with the other antiparasitic nifurtimox showed restoration of many but not all metabolic perturbations up to three years after treatment.[120] In contrast, the BENEFIT trial that followed patients 7 years post-treatment did not observe improved clinical outcomes in benznidazole-treated patients,[26] indicating that longer follow up may not show improvements and that our urine metabolome analysis could be well reflective of clinical outcomes. Further testing in clinical human populations will be necessary to determine whether the biomarkers identified in this study reliably reproduce in human CD patients.

2.10 Present Day Analysis and Future Opportunities

2.10.1 Chagas Disease Biomarkers

A 2024 cross-sectional study analyzed human sera from 120 patients, grouped by healthy volunteers, those with indeterminate CD (ICD), those with chronic chagasic cardiomyopathy (CCC), and those with other cardiomyopathies, using untargeted metabolomics for biomarker identification.[121] Phenylacetylglutamine and fibrinopeptide B (1–13) were identified as potential biomarkers with an increasing trend from health to ICD to CCC. Reduced levels of bilirubin and biliverdin alongside elevated urobilin correlated with disease progression. And, cystathionine, phenol glucuronide, and vanillactate were increased in CCC compared to ICD and controls. Perhaps the most important finding of the study is that CD patients exhibit CD stage-dependent distinct metabolic profiling. The most significantly altered metabolites in the study were dipeptides, which decreased during ICD, increased in CCC, and eventually returned to control levels. Our study assumed, but did not verify, established chronic disease stage in our model or subsequent analyses. Furthermore, we selected for consistent directionality during post-treatment bleed analysis without considering other directionality signatures. It would likely be worth (1) retesting our model with disease-stage validation and/or expanded timecourse considerations and (2) reassessing our acquired data with available insights on both disease stage-specific metabolic profiles and different direction-over-time signatures.

2.10.2 Low Metabolite Coverage

No single, analytical method currently exists to cover the entire metabolome.[122] Because metabolites are found in extensive ranges of concentration, polarity, stability, and more, any given method can only detect and analyze a small subset of metabolites at a time. Reverse-phase LC-MS/MS can detect non-polar features while Hydrophilic Liquid Interaction Chromatography MS/MS can detect polar features. Positive and negative ion modes can or must be combined for adequate coverage of metabolites in certain use-cases. Integrating these datasets introduces inherent risk in analysis, so creative development of more seamless and comprehensive methods could improve data acquisition efforts.

Unsurprisingly, analytical methods of choice can significantly bias metabolite detection and subsequent pathway analysis. One study simulated metabolite misidentification and found that rates as low as 4% resulted in loss of truly significant pathways as well as gain of false-positive pathways across all datasets.[123] These issues persist despite existence of a widely adopted over-representation analysis (ORA) approach to pathway analysis, indicating the need for stricter reporting guidelines and improved standardization.

Even within the studies described in this text, hundreds of in-the-moment decisions had to be made during data processing and analysis, including disease and spectral cutoff values, feature filtering thresholds, peak-picking tolerances, retention time alignment, signal-to-noise thresholds, relative standard deviation-based feature removal, reference library selection, mass error tolerance, and more.[124–126] Every one of these decisions impacted the resulting biomarker candidate lists. Accounting for all of them is unreasonable, but identifying and ranking the pipeline choices most significantly impacting results variation would indicate where standardization efforts would have the biggest impact.

2.10.3 Molecular Networking in Infectious Diseases Metabolomics

Infectious disease pathogens are under-studied in the field of metabolomics, especially parasitic infections, so reference metabolites are often missing from existing databases.[127] When they are present, comparative analysis remains difficult because the same metabolite species may be reported under many different names across databases.[128–130] This makes pathogen-derived metabolite discovery projects particularly difficult at the analysis stage.

A National Metabolomics Data Repository (NMDR) was built and subsequently leveraged to curate an analytical-chemistry-centric database in 2020 for metabolite structures and isobaric species known as the Reference Set of Metabolite Names, or RefNet.[128] Backed by the NIH, the hope is improved capacity for analysis, annotations, molecular network connections, and the generation of new knowledge and disease understanding.

Unlike most of the other omics, metabolomics lacks sequences that can be matched against each other or any other comparable characteristic to be used in similar fashion. This is part of what makes the bioinformatics of metabolomics so difficult and likely is a big factor impeding better pathway analysis scaffolding. Given the current state the field of metabolomics seems to be in, perhaps focusing efforts on the organization, standardization, interconnectedness, and confidence of preexisting untargeted datasets would provide better gains than continuously adding to the massive piles of uncharacterized, dark matter.

3 Discovery of Novel Protein Biomarkers for Tuberculosis Point-of-Care Diagnostic Assay

3.1 Contributions Statement

In this chapter, the rabbit model, production of infected urine and serum samples, and production of InMAD immune serum were all contributions by co-investigators from Colorado State University. MALDI-TOF was performed through the Mass Spectrometry Core Lab of the University of Texas Medical Branch in Galveston, Texas.

3.2 Disease Overview and Pathology

Tuberculosis (TB), caused by the bacillus *Mycobacterium tuberculosis* (*Mtb*), is a serious airborne disease that claims the lives of more than 1 million people every year.[131] Despite being preventable and typically curable, TB remains the world's leading cause of death from a single infectious agent. Transmission occurs when aerosolized droplets from an actively infected individual are inhaled through the large and/or small airways.[132] Exposure yields a 10-50% infection rate that is largely dependent on closeness and duration of contact as well as infectiousness of the source patient.[133,134]

Approximately one quarter of the world's population is latently infected with TB, but only 10% of those infections develop into active disease.[135] Of the 10% progressing to active disease, half will do so within the first 2 years post-infection, and the remaining half will develop an active infection later.[136] Major risk factors contributing to the development of active disease include human immunodeficiency virus (HIV), malnutrition, and young age.[137] Indoor pollution, alcohol consumption, diabetes, use of immunosuppressive drugs, and tobacco smoke are also significant contributing factors.[137,138]

3.2.1 Disease Pathology

Mtb are slow-growing, nonmotile, non-spore-forming, aerobic bacilli. Generation time is roughly 20 hours, and growth on solid media does not become visible for up to eight weeks. *Mtb*'s slow, linear growth profile provides a critical evolutionary advantage because the gradual, subtle infection evades triggering an acute immune response in the infected host.[132,139]

Infection primarily begins in alveolar macrophages, where detection of the bacilli triggers phagocytosis. After a macrophage engulfs the pathogen within a phagosome, *Mtb* counters by inhibiting both phagolysosome fusion and phagosome acidification, thereby preventing its own degradation.[140–142] Latent infection (LTBI) is successfully established as pathogen replication proceeds from within the host macrophage, followed by a metabolic transition into dormancy.[140] Host-pathogen interactions actively continue during LTBI, as organized clusters of immune cells form localized granulomas in the connective tissue surrounding infection site(s).

Active TB is established when the center of a granuloma liquefies into a nutrient-dense growth medium, and previously arrested *Mtb* begin to rapidly multiply. Bacilli disseminate extracellularly throughout the lungs in pulmonary TB and can also travel through the lymphatic system or blood to other tissues in extrapulmonary TB.[141,143] Common extrapulmonary manifestations include TB lymphadenitis, TB meningitis, skeletal TB (Pott's Disease), and Miliary TB.[144]

3.3 Treatment Options at Time of Study (2014-2016)

NOTE: The series of experiments discussed in this chapter were conducted from 2014 to 2016. The upcoming sections provide a point-of-view consistent with the experimental timeline. At the

close of this chapter, an updated analysis section ties the results obtained into the present-day TB landscape.

Without treatment, the death rate of TB is close to 50%.[145] The global treatment success rate is 88% for drug-susceptible TB (DS-TB), 71% for drug-resistant TB (DR-TB), and only 44% for extensively drug-resistant TB (XDR-TB).[146–148] Standard treatment recommendation in cases of DS-TB is a 4- to 6-month injection therapy regimen involving the administration of four drugs: isoniazid, rifampin, pyrazinamide, and ethambutol.[149] This course of treatment boasts high efficacy in yielding cure rates of up to 95%.[150] DR-TB cases require personalized treatment plans that must factor in comorbidities, current medications, and drug-susceptibility test results to be effective.[151]

A major factor contributing to the discrepancies between the higher treatment-specific cure rates and the overall lower global treatment success rates is the duration of standard treatment regimens.[152] A multitude of health and socioeconomic factors often prevent TB patients from completing treatment regimens.[153]

In the last several decades, despite having special regulatory pathways in place to expedite approvals for therapies of life-threatening infections that disproportionately impact marginalized populations, far fewer drugs have been successfully brought to market for TB compared to drugs for human immunodeficiency virus (HIV), and hepatitis C virus (HCV).[154] Bedaquiline (2012), delamanid (2014), and pretomanid (2019) are the only three novel, first-in-class anti-TB drugs to gain approval in recent years.[155] Importantly, nearly 20 years passed from the time pretomanid was first documented as having strong antitubercular activity to its FDA approval. Though the FDA required only eight months to review the new drug application, pretomanid spent six years in the discovery and pre-clinical phase followed by 13 years in the

clinical testing phase.[154] Bedaquiline required eight total years for FDA approval. As points of comparison, two recently approved new human immunodeficiency virus (HIV) drugs required 2.6 and 4.7 total years for approval, and two new hepatitis C virus drugs required 3.2 and 1.6 years.[154]

Regardless of root cause, in order to meet the WHO's call to action to reduce TB incidence by 80% and TB deaths by 90% by 2030, impediments to TB treatment advancements must be resolved.[156] The most significant opportunities for swiftly improving TB treatment outcomes are (1) shorter drug regimens, (2) safer drug regimens, (3) digital health integrations, (4) community support, and (5) addressing social determinants.[157–160]

3.4 Active Tuberculosis Diagnostic Landscape at Time of Study (2014-2016)

After advising against mass TB screening programs for nearly 40 years, the WHO reversed course by developing and publishing guidelines on screening for active TB in 2013.[161] The WHO's first set of formal TB diagnostic guidelines, released in 2015, recommended microscopy, culture, drug-susceptibility testing (DST), molecular testing (line-probe assays and Xpert MTB/RIF assay), and LTBI testing.[162] The Xpert MTB/RIF assay was in the process of being approved for use and rolled out in countries around the world.

At the same time, an unprecedented warning was published by the WHO to strongly discourage the use of commercial serodiagnostic tests, both antibody- and antigen-detecting, for diagnosis of TB disease.[163] The warning was based largely on a 2011 meta-analysis evaluation of 19 commercially available antibody-detection rapid diagnostic tests showing high variability in both sensitivity and specificity, high rates of false-positives, high rates of false-negatives, no evidence supporting improved patient outcomes, and overall adverse impacts on patient

safety.[164,165] A number of other studies at the time, however, report significant benefits to incorporating serodiagnostic strategies in TB diagnostics.[166–168]

Though research in protein biomarkers for TB seemed uncertain, TB proteomics research was advancing in other ways. A reference map and resource of assays to the complete proteome of Mtb (H37Rv) had recently been published.[169] 'The Mtb Proteome Library' was shifting scientific interest toward functional proteomics research in targeted drug discovery, vaccine development, host-pathogen interaction mapping, biomarker identification, and understanding the mechanisms of dormancy.[170–177] Building on proteomics techniques and methods for biomarker discovery, a novel target identification strategy for determination of immunogenic bacterial antigens was built.[178]

3.5 Opportunities Using Proteomics

3.6 Experimental Design

3.6.1 InMAD Method

The in vivo Microbial Antigen Discovery (InMAD) method is an unbiased technique used to identify circulating microbial antigens shed within a host's biofluids during infection.[178,179] Using the InMAD method, a host animal is infected with the pathogen of interest. Serum and/or urine is collected from the infected animal and filtered to yield only soluble, circulating antigens. The filtered product is subsequently injected into a second group of genetically identical (naïve) animals, and this triggers an immune response specific to the injected antigens. Serum samples harvested from the second animal group contain antibodies highly specific to the antigens that were shed during initial infection. This InMAD immune serum is used to probe blots of *Mtb* lysates, culture filtrate proteins, or proteome microarrays.

Antigens that are reactive with the InMAD immune serum are identified as the target antigens, suitable for development into a diagnostic immunoassay.

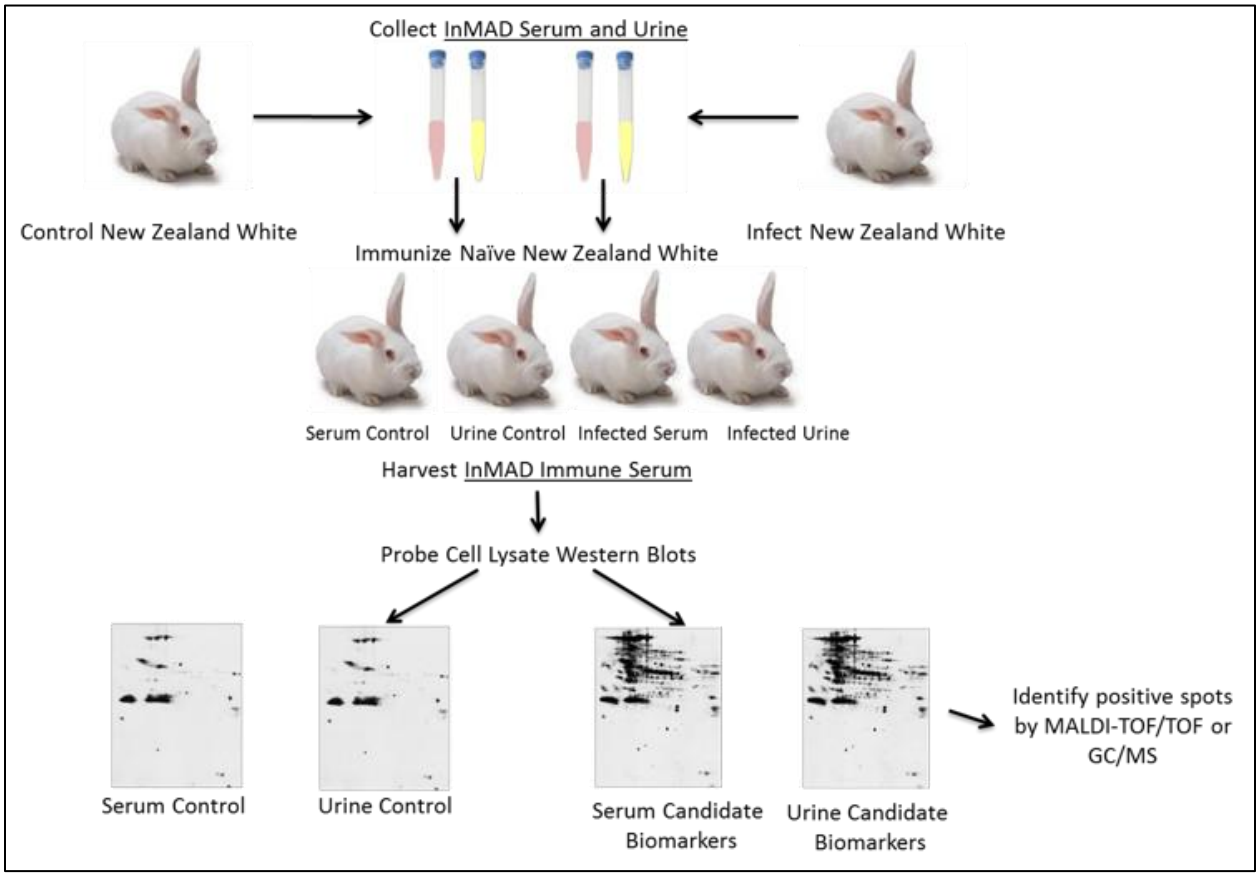


Figure 3-1. InMAD strategy for identifying Mtb antigens secreted/shed in urine and/or blood during TB infection. NZW rabbits were infected with Mtb, and InMAD serum and urine samples were collected. InMAD samples were combined with adjuvant and used to immunize syngeneic rabbits. InMAD immune sera was collected from immunized animals and used to probe whole cell lysates and culture filtrates by Western Blot.

While the InMAD strategy was originally developed using mice, we sought to utilize it with a rabbit model and highly virulent strain of TB. Various animal models are available to study *Mtb* infections, including the mouse, guinea pig, rabbit, and non-human primate, and each model has its own advantages and disadvantages.[180] Like humans, rabbits are innately resistant to

TB. However, when an infection does occur, the disease bears close resemblance to human TB with analogous lung pathologies and the ability to develop caseation and lung cavities.[181–183] We hypothesized that utilization of the InMAD technique using a rabbit model, depicted in **Figure 3-1**, will enable the discovery of TB biomarkers well-suited for use within a lateral flow assay format.

Based on clinical evidence of it being a high-transmission strain and its successful integration into animal models, we hypothesized the W-Beijing strain 14149 from the RD207 sublineage will be well-suited for biomarker validation.[184,185] This strain represents a typical outbreak strain that can transmit and infect large proportions of the population and should be ideal for identifying appropriate biomarkers.

Our initial strategy yields six potential protein biomarker targets validated against culture filtrate proteins of *Mtb*. Attempts to further validate these biomarkers against InMAD-immune serums were inconclusive. However, one biomarker target, Ag85, was chosen for continued development of hybridoma antibodies against the chosen antigen. The monoclonal antibodies generated were then used to validate reactivity against infected serum and infected urine in ELISA format.

3.7 Methods

3.7.1 Rabbit Model of Tuberculosis

Performed by co-investigators at Colorado State University

Fifteen New Zealand white (NZW) rabbits were divided into 3 categories: non-infected, 30-day infection (acute), and 60-day infection (chronic). Infected animals received a dose of 3.2 log 10 of clinical W-Beijing strain TN14149 [(HN878) Lot 9/22/2006 Box 131] bacilli using a

nose-only aerosol exposure system (CH technologies Inc, West-wood, NJ). We determined the bacterial load versus time in the lung and spleen in rabbits euthanized on days 30 and 60. For CFU's, 1 lung lobe, ¼ spleen, ¼ liver in 9.0 ml sterile saline; Plated 1:10 dilution, 0-7 on 7H11 agar. 2 lung lobes, ¼ spleen, 1 liver lobe were added to 5 mLs RNA later, stored at 4 degrees C for 24 hours, then ground into 5 mLs Trizol for qRT-PCR analysis and stored at -80 degrees C. 1 lung lobe, ¼ spleen, 1 liver lobe were added to 4% paraformaldehyde for histology. All homogenate was stored in cold room at 4ºC.

3.7.2 Production of Urine and Serum from Infected Rabbits

Performed by co-investigators at Colorado State University

Urine was obtained by bladder massage method and serum from blood by cardiac puncture. After collection, the urine samples were flash frozen and serum samples frozen and disinfected by gamma irradiation (6000 Ci ^{137}Cs for 1200 mins) over a frozen ice pack. An aliquot was pre-screened with all the available CSU antibodies to examine the integrity of dominant, secreted antigens. Although, this method of disinfection is not optimal (causes warming up of the samples), other alternatives such as filtration through 0.2 micron membranes and heating is known to cause significant loss in immunopotency.

3.7.3 Production of InMAD Immune Serum

Performed by co-investigators at Colorado State University

InMAD serum and urine from non-infected and infected rabbits was used to immunize naive NZW rabbits. Prior to immunization, serum was processed using a commercially available serum depletion kit to remove abundant proteins unrelated to *Mtb.* Urine was concentrated to increase the antigen levels present. Rabbits were immunized subcutaneously (SC) with Day 60

InMAD serum or InMAD urine (two animals per sample) using TiterMax® adjuvant. According to the manufacturer, one injection using TiterMax® is largely superior to Freund's adjuvant and boosts. However, to ensure acceptable immune response, a typical immunization schedule was followed: the rabbits were boosted SC with adjuvant on Day 14 and Day 35 followed by IV injections on Day 56. After 30, 45, and 60 days, serum ("InMAD immune serum") was collected from all rabbits and screened for reactivity to WCL and/or CFP via EIA. Once acceptable reactivity, as measured by titers to *Mtb* WCL and/or CFP, is observed, we proceeded to identification of biomarkers using the InMAD immune serum collected for screening that showed greatest reactivity in the EIA. Serum from 60 days post-immunization was more immunogenic than that collected at 30 and 45 days.

3.7.4 Identification of *Mtb* Biomarkers

Rebecca Ulrich vonBargen

InMAD immune sera from animals, containing antibodies to antigens shed in serum and urine during a *Mtb* infection, as well as control sera, was used to probe two-dimensional immunoblots of *Mtb* whole cell lysates and culture filtrates. Spots present in blots were probed with the test sera and urine, but not with the control sera and urine, and were analyzed using Matrix-Assisted Laser Desorption/Ionization Time-of-Flight (MALDI-TOF) mass spectrometry for protein identification.

3.7.5 2-Dimensional Gel Electrophoresis

Rebecca Ulrich vonBargen

200 µl of sample (CFP or WCL) was loaded onto a pH 3-10 11 cm IPG strip by overnight passive rehydration. Isoelectric focusing was performed on a Bio-Rad Protean IEF cell as

follows: 250 V, linear ramp for 20 min; 8000 V, linear ramp for 2.5 h; and 8000 V for a total of 20,000 Vhr (all steps with a maximum current of 50 µA per gel). The strips were stored at –80°C, then thawed and incubated twice for 10 min each in 8 M urea, 2% SDS, 0.05 M TrisHCl, pH 8.8, 20% glycerol. The first incubation contained 2% DTT, and the second contained 2.5% iodoacetamide. The strips were then layered on 8-16% Criterion Tris HCl gradient gels, and protein ladder MW markers were loaded. Electrophoresis was done at a constant voltage of 200 V until the dye front ran to the bottom of the gel. Gels were stained overnight with Bio-Safe Coomassie Blue then rinsed thoroughly three times with water (soaking 5 minutes each on orbital-shaker).

3.7.6 2-Dimensional Western Blot

Rebecca Ulrich vonBargen

Gels were transferred onto PVDF membranes (membrane briefly soaked in pure methanol for ~3 minutes prior to transfer) using BioRad Trans-Blot Turbo System and affiliated protocols. Membranes were blocked for 1 hour by soaking in blocking buffer (fish gelatin in PBS + 0.1% Tween; 0.45um filtered) followed by washing 3x in PBST. Membranes probed with ~1:30 dilution of pooled InMAD immune serum (diluted in blocking buffer, soak for 1 hour, wash x3). Mouse anti-rabbit-HRP antibody used as secondary detect antibody (diluted in blocking buffer, soak for 1 hour, wash x3), followed by development with BioRad Clarity Western ECL Substrate used according to protocol. Imaged using Bio-Rad Chemidoc XRS+ System and Bio-Rad Image Lab Software. Exposure = 3.4s unless otherwise stated.

3.7.7 MALDI-TOF

Protein digestion and mass spectrometry were performed by the Mass Spectrometry Core Lab of the University of Texas Medical Branch in Galveston, Texas. MALDI TOF/TOF 5800 (AB Sciex) was used with protocols comparable to those described by Nuti et al., in 2011.[186] Resulting files were searched by Mascot on NCBI and/or UniProt databases.

3.7.8 Immunization of Mice and Hybridoma Establishment

Rebecca Ulrich vonBargen

Native purified Ag85 complex was acquired from BEI Resources and used for immunizations. Five balb/C mice (female, 6-weeks) were acquired from Jackson Laboratories. Initial immunogen was prepared by emulsifying equal volumetric parts purified Ag85 and Freund's Complete Adjuvant. Total injection volumes containing 50-100ug of purified Ag85 were administered intraperitoneally. Booster immunogens, using Freund's Incomplete Adjuvant, were prepared and injected in the same manner every two weeks following initial injection for a 10-week period. Indirect ELISA method was used to screen serum for reactivity to Ag85 beginning on Day 16 after initial injection and repeated every 2 weeks until the titer goal, described in the Indirect Elisa section, was reached. Tail bleeds were used for blood collection, followed by centrifugation for serum separation. On Day 63, all five mice surpassed titer goal. A final booster injection of Ag85 in PBS was administered intraperitoneally three days prior to fusion. Mouse Splenocytes were harvested and fused with X63-Ag8.653 mouse myeloma cell line using polyethylene glycol classic hybridoma generation methods. Resulting clones were cultured in HAT-medium, and cell lines were separated using a minimum of two rounds of

cloning by limiting dilution. Isotyping performed using Pierce Rapid Antibody Isotyping Kit - Mouse.

3.7.9 Indirect ELISA

Rebecca Ulrich vonBargen

Serum and hybridoma samples were screened for antibody reactivity against Ag85 (or other sample of interest) using indirect ELISA method. Costar EIA strip 96-well flat-bottom plates were coated with 2ug/mL purified Ag85 at 100uL/well and left to incubate for 2 hours at 37 degrees C -OR- overnight at 4 degrees C. Plates were then washed three times with PBS-Tween 0.02% (PBST) and blocked with either casein blocking buffer or blocking buffer containing 2% bovine serum albumin in PBS at 37 degrees C for 2 hours before being washed three times with PBST. Primary antibody (mouse serum or hybridoma culture supernatant) dilutions were prepared in PBS and added to wells at 50uL/well. Covered plates were incubated for 1 hour at 37 degrees C before being washed with PBST. Goat anti-mouse IgG1-HRP antibody (Santa Cruz Biotechnology) was used as the secondary detect antibody by diluting 1:10,000 in PBS, adding to wells, and incubating for 1 hour at 37 degrees C. Wells were then washed three times with PBST. TMB substrate was added, and wells were left undisturbed at room temperature for 10 minutes. Stop solution was added, and all plates were assessed at $A_{450/630}$ within 10 minutes of adding stop solution using Agilent Biotek microplate readers.

Rabbit serum and urine samples coated onto ELISA plates at 1:10 dilution.

3.8 Results

3.8.1 Identification of M. tuberculosis Antigens Secreted During Infection

Many potential targets were identified by probing both the urine-immunized serum and serum-immunized serum against culture filtrate proteins (CFPs) and comparing the results to probes from naïve rabbit samples. Eight potential spots, demonstrating reactivity in both urine and serum, were excised for additional proteomic analysis, shown in **Figure 3-2**. This resulted in the identification of six targets, shown in **Table 3-1.** Protein Biomarker Targets Identified., as two of the original eight submissions gave redundant results. Three of the targets are considered novel and unnamed, and three are previously identified but not thoroughly studied for use in TB diagnostics. The six targets mapped back to the urine-immunized serum blot and the serum-immunized serum blot are shown in **Appendix F**and **Appendix G**, respectively. Results from naïve serum visualized in **Appendix** H**.** Exposure time was set to 3.4 seconds for all western blots.

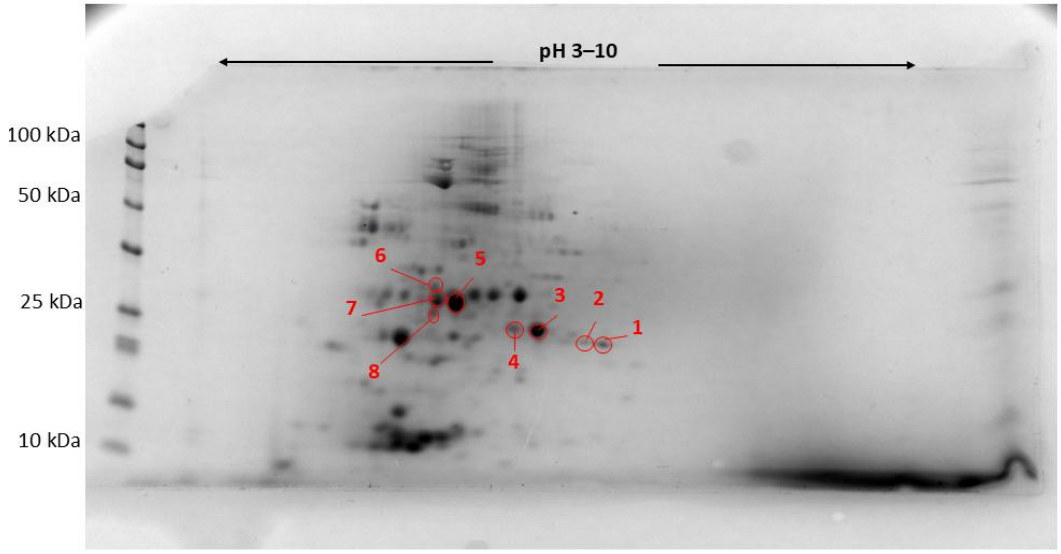


Figure 3-2. 2D-Gel Electrophoresis of *Mtb* Culture Filtrate Proteins. Two-dimensional gel electrophoresis of Mycobacterium tuberculosis culture filtrate proteins, resolved by isoelectric point (pH 3–10) and molecular weight (10–100 kDa). Stained with Bio-Safe Coommassie Stain. Numbered spots (1–8) were excised and submitted for protein identification by MALDI-TOF/TOF mass spectrometry.

Table 3-1. Protein Biomarker Targets Identified. Successfully identified protein targets from candidate list in Figure 3-2.

Biomarker ID	Protein Accession	Molecular Weight (kD)	Novel and Unnamed	MALDI E-score
PT-1	gi|15610982	23	No	3.97164E-15
PT-2	gi|490005446	27.1	Yes	7.92447E-33
PT-3	gi|490004226	27	Yes	2.50594E-07
PT-4	gi|157874756	30.7	No	2.50594E-48
PT-5	gi|392387600	28.3	Yes	3.97164E-61
PT-6	gi|15839702	32.1	No	5E-31

Urine and serum specimens from infected rabbits were pre-treated and analyzed on a 2-dimensional protein gel. pH 4-7 range was used instead of ph 3-10, as all proteins of interest are found within the narrower range. Western blots were then prepared by transferring these gels and using the same urine-immunized serum and serum-immunized serum, shown in used in the previous Western blot series.

Over 40 proteins of interest were identified; none of these spots were confirmed by way of MALDI or LC/MS-MS, as none of the expectation scores were of acceptable value. It is possible the pre-treatments of the specimens prior to use in the 2-dimensional gel format depleted the biomarkers from the samples. It is also possible that native rabbit proteins and molecules were simply too abundant and consequently masked detectable reactivity to the biomarkers of interest. These concerns do not discredit the results obtained using the CFPs though. Therefore, the decision was made to move forward with developing monoclonal antibodies.

PT-4, selected for its ease of acquisition and purification, was selected for monoclonal IgG antibody development. Following a strong serum reactivity response to Ag85 at day 63 of the immunization schedule, shown below in **Figure 3-3A**, hybridoma cell lines were produced, and 24 resultant clones showed adequate production of IgG antibody against PT-4 (data not shown). Supernatant from the top five producing subclones containing IgG antibody was tested across six sample types: lipoarabinomannan (LAM), naïve rabbit urine, infected rabbit urine, naïve rabbit serum, infected rabbit serum, and PBS using indirect ELISA method, described in methods. Results from this test, shown below in **Figure 3-3B**, show clone 5D5 produces a signal above the positivity threshold for both infected urine and infected serum, but not in naïve urine and serum, LAM, or PBS. Clone 4D5 shows the highest clearance of the positive threshold

against infected urine. These results help support validation of both the antigen and the clones, though it's important to note that extreme volume limitations during early-stage hybridoma screening allow only for single-replicate testing. Follow-up runs will need to confirm and expand on the results shown.

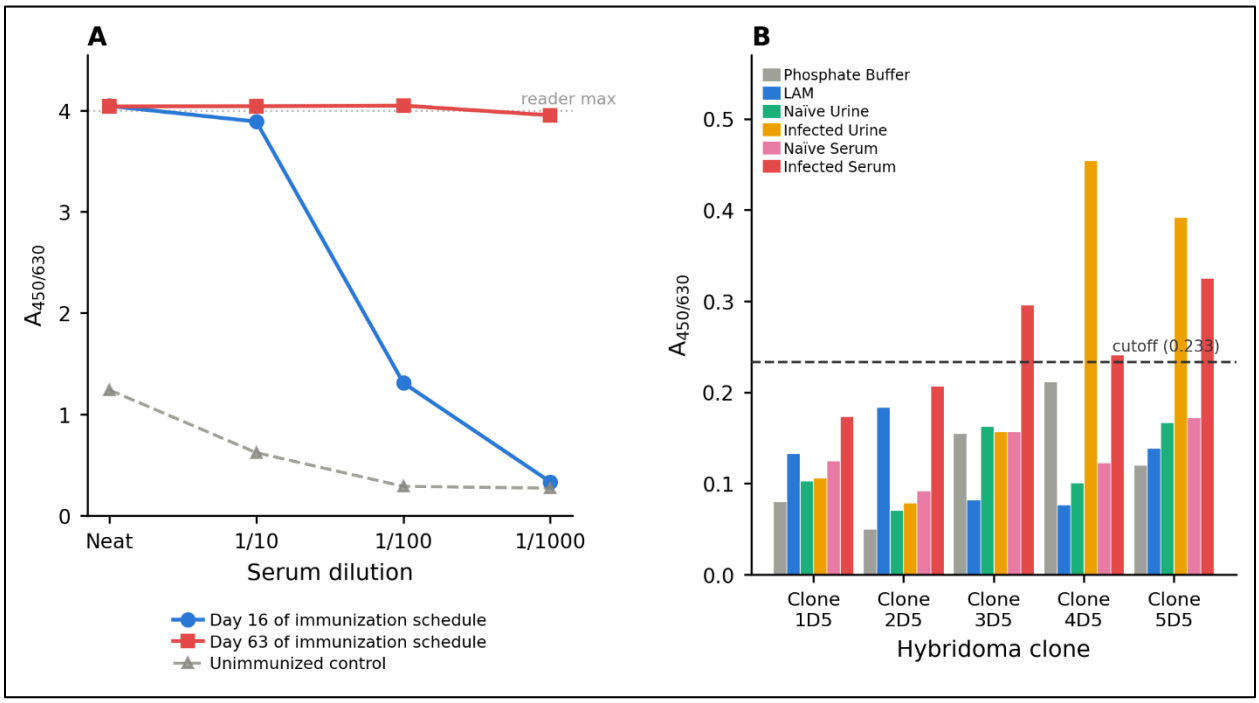


Figure 3-3. Anti-Ag85 IgG-Producing Hybridoma Development Screening. ELISA values are background-corrected absorbance at 450/630nm (A450/630). **(A) Serum titration of immunized vs. control mouse**. Serial dilution screening of mouse serum at Day 16 and Day 63 of immunization schedule compared to non-immunized control serum. Wells contain immobilized, purified Ag85 protein. Day 63 response saturates plate reader at all dilutions tested, indicating immune schedule and subsequent hybridoma generation were well-timed. Of note, control serum at neat demonstrates unexpectedly elevated relative value compared to 1:10, perhaps due to viscosity of serum. **(B) Hybridoma Clone Screening.** Post-fusion screen of five IgG-producing hybridoma subclones generated against Ag85. Supernatant tested at neat across six sample conditions. Dashed line indicates positivity cutoff (mean + 3 SD of negative controls). Data shown is single replicate because insufficient volume during early stages of hybridoma growth precludes replicate runs. A450/630 is net absorbance where A450 = signal wavelength and A630 = reference wavelength. Calculation is A450 – A630.

3.9 Discussion and Conclusion

3.9.1 Identified Biomarker Targets

Although original results indicated 3 novel and unnamed proteins, updated analysis reveals the identity of all six target proteins and provides insight into each target's potential use as a diagnostic biomarker for active TB disease.

PT-1/Superoxide dismutase [FE] SodA: Superoxide dismutase A is an iron-cofactored enzyme and key virulence factor that neutralizes oxidative bursts and allows bacteria to evade host immune defenses.[187] It has been identified in other independent studies as a potential biomarker present in both serum and granulomas, though using it poses concerns of cross-reactivity with other diseases.[188,189]

PT-2 & PT-3/Hypothetical Proteins → MPT51: Results from 2016 labeled the 27kD protein, located on the 2DE map near the Ag85 antigen family protein spots, as a hypothetical protein. An updated inquiry matches this spot to MPT51/FbpC1, a well-characterized T-cell antigen.[190–193] MPT51 exhibits strong cross-reactivity with all three components of the Ag85 complex and exhibits >60% sequence homology to them in its N-terminal region. MPT51 has been explored extensively as a potential TB biomarker in an MPT51-detection (antigen) ELISA for diagnosis of extrapulmonary TB from urine samples[194], in an anti-MPT51 (antibody) ELISA for latent TB infection in asymptomatic HIV-positive individuals[195], and most recently in a novel magnetic nanoparticle antibody-conjugate and aptamer-based assay for diagnosing pleural TB.[196]

PT-4/Ag85b, Chain A: The Antigen 85 complex, containing protein components A, B, and C, is a major, well-characterized antigenic component known to be found on the *Mtb* cell wall and to circulate in the blood of patients with active TB disease. Detection has been documented in

blood, urine, sputum, and cerebrospinal fluid of TB patients, making it one of the most popular antigenic targets to date for both diagnostics and vaccines. Different iterations of its use in diagnostics regularly report sensitivities >90% and specificities >85%.[168,197]

PT-5/Unnamed Protein Product → Aldo/keto reductase: The 28.3kD oxidoreductase helps shield the bacteria from oxidative stress. It is an intracellular and membrane-associated protein and was considered at one time for potential vaccines.[198,199] Because it is normally located in the cytosolic fractions, rather than extracellular culture filtrate, it would not be considered a classic target for diagnostics. Its identification in this study may be worth exploring further.

PT-6/Beta-Glucanase: This is shown to be a pseudo-enzyme, as changes to its active site render it incapable of binding beta-glucans.[200] It is likely not a good candidate for a diagnostic biomarker, but there is some potential for its involvement in improved efficacy of vaccines.

3.9.2 Testing and Validation in Human Samples

One study combined 16 human serum samples from patients with confirmed active TB and screened the pool against 2D-GE-separated CFPs. Reactive spots were processed, identified, and compared for relative quantitation. Based on relative antibody quantities, antibodies against all three homologous components of the Ag85 complex were the most abundant in the pool. MPT51was also identified in the study[201]

3.9.3 Composition of M. tuberculosis Culture Filtrate

The composition of proteins released by bacilli into culture supernatant is significantly impacted by culture incubation time. Previous studies have shown that CFPs can be divided into three main groups based on early, gradual, or late release into filtrate, and these groups correspond to protein function.[202] Additionally, proteomic variation exists among different *Mtb*

strains.[203,204] These factors need to be taken into account when using culture filtrate maps to identify potential antigen targets.

This study provides multiple antigen biomarker candidates suitable for expanded validation studies. for potential development of a rapid, POC TB diagnostic suitable for use in both urine and serum samples. Follow-up studies will need to corroborate or expand on the preliminary results obtained in this project.

While there is still some potential for singular protein biomarkers used in a TB diagnostic, TB diagnostic needs have grown beyond mere initial confirmation of active TB disease. Risk of disease development, monitoring treatment response, and diagnosing TB cure are all identified as areas of greatest opportunity for reducing the burden of TB disease.[205] Future outlooks indicate tests involving biomarker panels, combined biomarker stratification across multiple biological layers of data, or new technologies may be better suited for the reliability requirements of TB diagnostics.

3.10 Present-Day Analysis & Future Opportunities

The experiments in this chapter were conducted just over a decade ago, from 2014-6, and quite a bit has changed in the infectious diseases landscape since that time. The final section of this chapter provides an updated perspective on TB diagnostics and integrates the results obtained in these studies with present-day opportunities.

3.10.1 Present-Day State of Global TB Burden

In 2024, over half (55%) of the global total of new TB cases occurred in five countries: India (25%), Indonesia (10%), the Philippines (6.8%), China (6.8%), and Pakistan (6.3%). However, the highest *incidence* rates tended to be in the WHO Africa region.[131] Over 80% of

global cases remain concentrated in low-income and lower-middle-income communities, as economic disadvantages like crowded living conditions, malnutrition, and limited access to adequate healthcare increase TB risk factors .[206,207]

According to the WHO's 2035 plan for the effective elimination of TB, updated milestone targets include (1) improved coverage of TB diagnostic, treatment, and preventative interventions, (2) increased understanding on new infection determinants or risk of developing the disease once infected, and (3) technological breakthroughs such as a new TB vaccine.[131]

The FDA fully approved a new drug called pretomanid in 2019 for the treatment of multi-drug-resistant TB. Pretomanid is most often used in a combination therapy known as BPaLM with three other drugs (bedaquiline, linezolid, and moxifloxacin) to provide a 6-month, all-oral therapy option for DR-TB and XDR-TB with demonstrated treatment success rates of 90% or higher.[208–211]

BPaLM halved what used to be a much longer and highly variable expected treatment timeline for DR-TB, but there is still significant room for improvement. Major obstacles in the development of new or improved TB drugs include lack of biomarkers and surrogate endpoints, complexities of combination therapies, slow growth and dormancy of the bacteria impacting duration of clinical trials, lack of validated biomarkers-of-cure, and weaker commercial incentives of treating primarily resource-limited populations.[154,212–214]

3.10.2 TB Diagnostic Landscape in 2026

No single TB test satisfies all these criteria for all patient populations, so multi-test or parallel testing strategy is often utilized or recommended.[215,216]

Even pared down to its simplest form, the WHO's 2025 guidance for diagnosing TB provides a set of 21 different circumstance-dependent recommendations. TB infection versus TB disease, drug resistance, age of patient, and comorbidities of patients are all complicating factors requiring differentiated testing combinations to achieve an effective TB diagnosis.[217]

Confirmed diagnosis of TB disease requires microbiological detection through one of four WHO-approved testing options: sputum smear microscopy, culture, WHO-recommended molecular tests, and lateral flow urine lipoarabinomannan (LF-LAM) assays.[131] Approximately 63% of new cases of pulmonary TB are diagnosed through bacteriological confirmation each year, and that percentage has remained largely consistent for the last 15 years.[218] The remaining cases receive diagnoses through clinical (empirical) evaluations.

Historically, microscopy and culture methods were predominantly used for diagnosing TB disease, especially in resource-limited settings. For the past 15 years though, rapid molecular assays have been steadily transforming the diagnostic landscape. In 2023, the United Nations high-level meeting on TB called for 100% use of WHO-recommended rapid diagnostic tests (WRDs) during initial TB diagnosis by the year 2027. In short, this initiative formally recommended use of molecular and/or biomarker rapid diagnostics over microscopy and culture-based methods. By 2024, a WRD was used for 54% of the 8.3 million people newly diagnosed with TB – up from 38% in 2021 and 48% in 2022.[131]

Two main classes of diagnostics are represented in the WHO's recommendations for testing guidelines: nucleic acid amplification tests (NAATs) and biomarker-based detection tests. NAATs are further classified based on their level of complexity. Most NAATs offer the significant advantage of providing drug-resistance detection alongside disease diagnosis. The current list of recommended NAATs also boast significantly higher sensitivity and specificity

scores compared to the biomarker-based testing option, though that is not an inherent limitation of lateral flow assays. Lateral flow assays, on the other hand, offer the significant advantage of being truly point-of-care. They require no equipment, no trained expertise, and no electricity to run or interpret. Some of the low-complexity NAAT options offer manual processing using only basic lab equipment, but these simplified options do not offer drug-resistance detection.

While the low-complexity NAATs for TB are praised as being "near-POC," studies on Xpert MTB/RIF roll-outs in multiple countries cite concerns in affordability, user-friendliness, equipment failures, and deliverability.[219,220] Xpert MTB/RIF was predicted to reduce TB mortality up to 20%-35% by facilitating earlier treatment initiation. However, multiple studies show no mortality benefit.[221–224]

Alere/Abbott's Determine™ TB LAM Ag product, available for antigen detection of lipoarabinomannan in urine samples, has suboptimal sensitivity and specificity, so it is not recommended for all populations. It does possess improved sensitivity among individuals coinfected with HIV, so it is recommended for use in tandem with a low -complexity nucleic acid test (LC-NAAT).[217]

Sensitivity and specificity in LFAs are significantly impacted by choice of target antigen. Lipoarabinomannan (LAM) is one option for a highly immunogenic antigen used as a target antigen in TB diagnostics. However, the only LAM-based diagnostic test is recommended only for use in a subset of potential cases in tandem with a molecular test.[217] Consequently, it is necessary to continue efforts to identify alternative TB biomarkers that can be used to develop more sensitive diagnostic assays.

3.10.3 Opportunities for Improved Experimental Design

Monoclonal Antibody Development: The classic hybridoma approach to antibody discovery remains respected and relevant to this day, as it is cited as being the most successful and efficient method for isolation, generation, and production of monoclonal antibodies.[225] As used and described in this chapter, the original methods do inherently possess several inefficiencies that have greatly benefited from recent advancements. Most notably, the B cell fusion efficiency of the PEG-mediated cell fusion method is 1 in 100,000.[226] Of the 0.001% because the hybridomas providing the highest yield of Mabs tend to be the slowest-growing cells, the best candidates within the initial post-fusion colony are easily overtaken by low-yielding but fast-multiplying competitor cells. Next, it is difficult for a slow-growing cell line to survive multiple rounds of cloning by limiting dilution, whereby a single cell must overcome apoptosis-inducing damage and stress signals in an environment that is inherently high-risk for contamination. Many advancements in the field, such as electrofusion of antibody-secreting cells (ASCs) and fluorescence-activated cell sorting (FACS), serve as supporting technologies to improve fusion efficiency and functional yield.

4 Conclusions and Recommendations

4.1 Key Scientific and Engineering Contributions

One of the key contributions in this thesis is validation of the InMAD model in rabbits. Another contribution is the demonstration in a rabbit model that TB-specific antigens are abundant enough in both urine and serum of infected individuals to be diagnostically relevant, as was demonstrated by utilizing infected samples as effective immunogens. A key Chagas Disease finding is the insight that successful clearance of parasite burden through Bz treatment does not

restore the metabolome. I think this is a key insight for infectious disease research and in the clinic, and I hope it inspires other to rethink their understanding of infections. In both project sets, returning to the results and data five and ten years later, provided identification of previously unnamed or missed biomarker candidates, and I hope it inspires others to reengage with their older research.

4.2 Future Recommendations for Point-of-Care Diagnostics Research

4.2.1 Biological Layers and Integrative Biomarkers

As many single-omics approaches stall out in biomarker discovery research, popularity is growing around the apparent need for improved resolution of interconnected biological and disease layers through multi-omics integration. Mass spectrometry (MS) is cited as a central analytical strategy incorporating assessment of proteins, metabolites, lipids, and spatial omics.[227] Most attempts to connect data from different layers rely on computational integration. While this is certainly a good start, retrofitting independently-processed data sets can be challenging and leave gaps in understanding. True breakthrough will likely be achieved with advancements in MS instrumentation, spatial multi-omics, creative experimental design, and improved interdisciplinary efforts between life scientists and bioinformatitions.[228]

4.2.2 Clever Point-of-Care Engineering Hacks

Chip electrophoresis titration biosensors, suitable for both proteins and metabolites, combine chemical reactions with moving reaction boundary distance-based measurements for quantitative detection.[229] A group researching electrochemical labels for bioassays recently discovered that changing the shape of silver nanoparticles from a sphere to a cube significantly lowered the limit

of detection and may allow for a lower limit of 0.1 pM, an order of magnitude lower than the spherical labels.[230]

4.2.3 Ghosts and Dark Matters

The dark metabolome and dark proteome represent the unmatched spectra from shotgun proteomics and untargeted metabolomics studies, much like the ones discussed in this dissertation. Some estimates predict up to 98% of the metabolome and 50% of the proteome remain in the dark, though expanded discussions insist much of the data is fragment ions and not real molecules.[231–233] A few years ago, a research team developed a freely available software package called BioTransformer to reveal the dark metabolome and improve understanding.[234] A reasoning engine has been incorporated for reaction site and chemical product prediction, which could be leveraged for biomarker discovery.

For decades, scientists ignored the non-coding portion of the genome as junk, but the last 15 years have unearthed countless biochemical functions from the 'dark matter.' In the last five years, literature has formally recognized the ghost proteome (GP), which umbrellas noncanonical translational products like 5′/3′ UTRs, alternative reading frames of mRNAs, pseudogenes, or long noncoding RNAs.[235] There is great potential for infectious disease biomarker discovery within the GP, as pathogens are known to interface with alternative proteins (AltProts), and off-the-grid peptides, termed dark antigens, provide new mapping territory that traditional databases have missed.[236]

Seeing so few biomarkers make it all the way to clinical use has forced a lot of rethinking of fundamental approaches to biomarker discovery. It is unlikely the major methods utilized in the studies of this text will yield improved rates of discovery on their own. Coordinating their

utilization for integrative biomarker POC technologies would likely be a better investment. Integrating the physics of multiple biological layers onto a single POC platform is a challenge, but it can be overcome with better interdisciplinary collaborations on projects that combine the best of clever engineering and strategic molecular design.

5 References

(1) Standing up to Infectious Disease. *Nat Microbiol* **2019**, *4* (1), 1. https://doi.org/10.1038/s41564-018-0331-3.

(2) Kim, P. S.; Swaminathan, S. Ending TB: The World's Oldest Pandemic. *J Int AIDS Soc* **2021**, *24* (3), e25698. https://doi.org/10.1002/jia2.25698.

(3) Combating Infectious Diseases in a Fragmented World. *Nat Med* **2026**, *32* (5), 1559–1559. https://doi.org/10.1038/s41591-026-04443-1.

(4) Liu, Q.; Liu, M.; Liang, W.; Li, X.; Jing, W.; Chen, Z.; Liu, J. Global Distribution and Health Impact of Infectious Disease Outbreaks, 1996–2023: A Worldwide Retrospective Analysis of World Health Organization Emergency Event Reports. *J Glob Health 15*, 04151. https://doi.org/10.7189/jogh.15.04151.

(5) *About WHO*. https://www.who.int/about (accessed 2026-07-14).

(6) Tosam, M. J.; Ambe, J. R.; Chi, P. C. Global Emerging Pathogens, Poverty and Vulnerability: An Ethical Analysis. *Socio-cultural Dimensions of Emerging Infectious Diseases in Africa* **2019**, 243–253. https://doi.org/10.1007/978-3-030-17474-3_18.

(7) *Early Warning Diagnostics for Emerging Infectious Diseases in Developing into Late-Stage Pandemics | Accounts of Chemical Research*. https://pubs.acs.org/doi/10.1021/acs.accounts.1c00383 (accessed 2026-07-14).

(8) Larkins, M. C.; Zubair, M.; Thombare, A. Point-of-Care Testing. In *StatPearls*; StatPearls Publishing: Treasure Island (FL), 2026.

(9) Hayden, O.; Luppa, P. B.; Min, J. Point-of-Care Testing—New Horizons for Cross-Sectional Technologies and Decentralized Application Strategies. *Anal Bioanal Chem* **2022**, *414* (10), 3161–3163. https://doi.org/10.1007/s00216-022-03987-8.

(10) FDA-NIH Biomarker Working Group. *BEST (Biomarkers, EndpointS, and Other Tools) Resource*; Food and Drug Administration (US): Silver Spring (MD), 2016.

(11) Califf, R. M. Biomarker Definitions and Their Applications. *Exp Biol Med (Maywood)* **2018**, *243* (3), 213–221. https://doi.org/10.1177/1535370217750088.

(12) Jones, H. B. III. On a New Substance Occurring in the Urine of a Patient with Mollities Ossium. *Phil. Trans. R. Soc.* **1848**, No. 138, 55–62. https://doi.org/10.1098/rstl.1848.0003.

(13) Strimbu, K.; Tavel, J. A. What Are Biomarkers? *Curr Opin HIV AIDS* **2010**, *5* (6), 463–466. https://doi.org/10.1097/COH.0b013e32833ed177.

(14) null, null. Preliminary Report: Effect of Encainide and Flecainide on Mortality in a Randomized Trial of Arrhythmia Suppression after Myocardial Infarction. *New England Journal of Medicine* **1989**, *321* (6), 406–412. https://doi.org/10.1056/NEJM198908103210629.

(15) Califf, R. M. Biomarker Definitions and Their Applications. *Exp Biol Med (Maywood)* **2018**, *243* (3), 213–221. https://doi.org/10.1177/1535370217750088.

(16) Califf, R. M. Biomarker Definitions and Their Applications. *Exp Biol Med (Maywood)* **2018**, *243* (3), 213–221. https://doi.org/10.1177/1535370217750088.

(17) Frangogiannis, N. G. BIOMARKERS: HOPES AND CHALLENGES IN THE PATH FROM DISCOVERY TO CLINICAL PRACTICE. *Transl Res* **2012**, *159* (4), 197–204. https://doi.org/10.1016/j.trsl.2012.01.023.

(18) Bakker, E.; Hendrikse, N. M.; Ehmann, F.; van der Meer, D. S.; Llinares Garcia, J.; Vetter, T.; Starokozhko, V.; Mol, P. G. M. Biomarker Qualification at the European Medicines

Agency: A Review of Biomarker Qualification Procedures From 2008 to 2020. *Clin Pharmacol Ther* **2022**, *112* (1), 69–80. https://doi.org/10.1002/cpt.2554.
(19) Kim, K.-H.; Yoo, M.; Choi, M. Y.; Yoo, B. C. A Practical Roadmap for Clinical Translation of Metabolic Biomarkers: A Review. *Int J Mol Sci* **2026**, *27* (4), 2030. https://doi.org/10.3390/ijms27042030.
(20) Thomas, S.; Hao, L.; Ricke, W. A.; Li, L. Biomarker Discovery in Mass Spectrometry-Based Urinary Proteomics. *Proteomics Clin Appl* **2016**, *10* (4), 358–370. https://doi.org/10.1002/prca.201500102.
(21) Schrimpe-Rutledge, A. C.; Codreanu, S. G.; Sherrod, S. D.; McLean, J. A. Untargeted Metabolomics Strategies – Challenges and Emerging Directions. *J Am Soc Mass Spectrom* **2016**, *27* (12), 1897–1905. https://doi.org/10.1007/s13361-016-1469-y.
(22) Rassi, A.; Rassi, A.; Marin-Neto, J. A. Chagas Disease. *The Lancet* **2010**, 1388–1402. https://doi.org/10.1016/s0140-6736(10)60061-x.
(23) Nunes, M. C. P.; Beaton, A.; Acquatella, H.; Bern, C.; Bolger, A. F.; Echeverría, L. E.; Dutra, W. O.; Gascon, J.; Morillo, C. A.; Oliveira-Filho, J. : : Chagas Cardiomyopathy: An Update of Current Clinical Knowledge and Management: A Scientific Statement From the American Heart Association. *Circulation* **2018**, 138 169-209.
(24) Lewis, M. D.; Kelly, J. M. Putting Infection Dynamics at the Heart of Chagas Disease. *Trends Parasitol* **2016**, *32* (899–911).
(25) Hidron, A.; Vogenthaler, N.; Santos-Preciado, J. I.; Rodriguez-Morales, A. J.; Franco-Paredes, C.; Rassi, A., Jr. Cardiac Involvement with Parasitic Infections. *Clin. Microbiol. Rev* **2010**, *23* (2), 324–349.
(26) Morillo, C. A.; Marin-Neto, J. A.; Avezum, A.; Sosa-Estani, S.; Rassi, A., Jr; Rosas, F.; Villena, E.; Quiroz, R.; Bonilla, R.; Britto, C.; Guhl, F.; Velazquez, E.; Bonilla, L.; Meeks, B.; Rao-Melacini, P.; Pogue, J.; Mattos, A.; Lazdins, J.; Rassi, A.; Connolly, S. J.; Yusuf, S. BENEFIT Investigators. *Randomized Trial of Benznidazole for Chronic Chagas' Cardiomyopathy. N. Engl. J. Med* **2015**, *373* (14), 1295–1306.
(27) Fabbro, D. L.; Streiger, M. L.; Arias, E. D.; Bizai, M. L.; Barco, M.; Amicone, N. A. Trypanocide Treatment among Adults with Chronic Chagas Disease Living in Santa Fe City (Argentina), over a Mean Follow-up of 21 Years: Parasitological, Serological and Clinical Evolution. *Rev. Soc. Bras. Med. Trop* **2007**, *40* (1), 1–10.
(28) Antunes, A. P.; Ribeiro, A. L. P.; Sabino, E. C.; Silveira, M. F.; Lorenzo Oliveira, C.; Carvalho Botelho, A. C. Benznidazole Therapy for Chagas Disease in Asymptomatic Trypanosoma Cruzi -Seropositive Former Blood Donors: Evaluation of the Efficacy of Different Treatment Regimens. *Revista da Sociedade Brasileira de Medicina Tropical* **2016**, 713–720. https://doi.org/10.1590/0037-8682-0165-2016.
(29) Britto, C.; Cardoso, M. A.; Vanni, C. M.; Hasslocher-Moreno, A.; Xavier, S. S.; Oelemann, W.; Santoro, A.; Pirmez, C.; Morel, C. M.; Wincker, P. Polymerase Chain Reaction Detection of Trypanosoma Cruzi in Human Blood Samples as a Tool for Diagnosis and Treatment Evaluation. *Parasitology* **1995**, *110* (Pt 3), 241–247.
(30) Lana, M. de; Lopes, L. A.; Martins, H. R.; Bahia, M. T.; Machado-de-Assis, G. F.; Wendling, A. P.; Martins-Filho, O. A.; Montoya, R. A.; Dias, J. C. P.; Albajar-Viñas, P.; Coura, J. R. Clinical and Laboratory Status of Patients with Chronic Chagas Disease Living in a Vector-Controlled Area in Minas Gerais, Brazil, before and Nine Years after Aetiological Treatment. *Mem. Inst. Oswaldo Cruz* **2009**, *104* (8), 1139–1147.

(31) Keating, S. M.; Deng, X.; Fernandes, F.; Cunha-Neto, E.; Ribeiro, A. L.; Adesina, B.; Beyer, A. I.; Contestable, P.; Custer, B.; Busch, M. P.; Sabino, E. C. NHLBI Retrovirus Epidemiology Donor Study-II (REDS-II. *International Component. Inflammatory and Cardiac Biomarkers Are Differentially Expressed in Clinical Stages of Chagas Disease. Int. J. Cardiol* **2015**, *199*, 451–459.
(32) Vieira, J. L.; Távora, F. R. F.; Sobral, M. G. V.; Vasconcelos, G. G.; Almeida, G. P. L.; Fernandes, J. R.; Escóssia Marinho, L. L.; Mendonça Trompieri, D. F.; Souza Neto, J. D.; Mejia. *J. A. C. Chagas Cardiomyopathy in Latin America Review. Current Cardiology Reports* **2019**. https://doi.org/10.1007/s11886-019-1095-y.
(33) Ndao, M.; Spithill, T. W.; Caffrey, R.; Li, H.; Podust, V. N.; Perichon, R.; Santamaria, C.; Ache, A.; Duncan, M.; Powell, M. R.; Ward, B. J. Identification of Novel Diagnostic Serum Biomarkers for Chagas' Disease in Asymptomatic Subjects by Mass Spectrometric Profiling. *J. Clin. Microbiol* **2010**, *48* (4), 1139–1149.
(34) Berrizbeitia, M.; Ndao, M.; Bubis, J.; Gottschalk, M.; Aché, A.; Lacouture, S.; Medina, M.; Ward, B. J. Field Evaluation of Four Novel Enzyme Immunoassays for Chagas' Disease in Venezuela Blood Banks: Comparison of Assays Using Fixed-Epimastigotes, Fixed-Trypomastigotes or Trypomastigote Excreted-Secreted Antigens from Two Trypanosoma Cruzi Strains. *Transfus. Med* **2006**, *16* (6), 419–431.
(35) Molina, I.; Prat, J.; Salvador, F.; Treviño, B.; Sulleiro, E.; Serre, N.; Pou, D.; Roure, S.; Cabezos, J.; Valerio, L.; Blanco-Grau, A.; Sánchez-Montalvá, A.; Vidal, X.; Pahissa, A. Randomized Trial of Posaconazole and Benznidazole for Chronic Chagas' Disease. *N. Engl. J. Med* **2014**, *370* (20), 1899–1908.
(36) Torrico, F.; Gascón, J.; Barreira, F.; Blum, B.; Almeida, I. C.; Alonso-Vega, C.; Barboza, T.; Bilbe, G.; Correia, E.; Garcia, W.; Ortiz, L.; Parrado, R.; Ramirez, J. C.; Ribeiro, I.; Strub-Wourgaft, N.; Vaillant, M.; Sosa-Estani, S.; group, B. E. N. D. I. T. A. New Regimens of Benznidazole Monotherapy and in Combination with Fosravuconazole for Treatment of Chagas Disease (BENDITA): A Phase 2, Double-Blind, Randomised Trial. *Lancet Infect. Dis* **2021**, *21* (8), 1129–1140.
(37) Picado, A.; Angheben, A.; Marchiol, A.; Noya, B.; Flevaud, L.; Pinazo, M. J.; Gállego, M.; Meymandi, S.; Moriana, S. Development of Diagnostics for Chagas Disease: Where Should We Put Our Limited Resources? PLoS Negl. *Trop. Dis* **2017**, *11* (1), 0005148.
(38) Murcia, L.; Carrilero, B.; Muñoz, M. J.; Iborra, M. A.; Segovia, M. Usefulness of PCR for Monitoring Benznidazole Response in Patients with Chronic Chagas' Disease: A Prospective Study in a Non-Disease-Endemic Country. *J. Antimicrob. Chemother* **2010**, *65* (8), 1759–1764.
(39) Pérez-Ayala, A.; Pérez-Molina, J. A.; Norman, F.; Navarro, M.; Monge-Maillo, B.; Díaz-Menéndez, M.; Peris-García, J.; Flores, M.; Cañavate, C.; López-Vélez, R. Chagas Disease in Latin American Migrants: A Spanish Challenge. *Clin. Microbiol. Infect* **2011**, *17* (7), 1108–1113.
(40) Sánchez-Montalvá, A.; Salvador, F.; Rodríguez-Palomares, J.; Sulleiro, E.; Sao-Avilés, A.; Roure, S.; Valerio, L.; Evangelista, A.; Molina, I. Chagas Cardiomyopathy: Usefulness of EKG and Echocardiogram in a Non-Endemic Country. *PLOS ONE* **2016**, 0157597. https://doi.org/10.1371/journal.pone.0157597.
(41) Lima-Costa, M. F.; Cesar, C. C.; Peixoto, S. V.; Ribeiro, A. L. P. Plasma B-Type Natriuretic Peptide as a Predictor of Mortality in Community-Dwelling Older Adults with

Chagas Disease: 10-Year Follow-up of the Bambui Cohort Study of Aging. *Am. J. Epidemiol* **2010**, *172* (2), 190–196.
(42) Okamoto, E. E.; Sherbuk, J. E.; Clark, E. H.; Marks, M. A.; Gandarilla, O.; Galdos-Cardenas, G.; Vasquez-Villar, A.; Choi, J.; Crawford, T. C.; Do, R. Q.; Fernandez, A. B.; Colanzi, R.; Flores-Franco, J. L.; Gilman, R. H.; Bern, C. Chagas Disease Working Group in Bolivia and Peru. *Biomarkers in Trypanosoma Cruzi-Infected and Uninfected Individuals with Varying Severity of Cardiomyopathy in Santa Cruz, Bolivia. PLoS Negl. Trop. Dis* **2014**, *8* (10), 3227.
(43) Rochitte, C. E.; Oliveira, P. F.; Andrade, J. M.; Ianni, B. M.; Parga, J. R.; Avila, L. F.; Kalil-Filho, R.; Mady, C.; Meneghetti, J. C.; Lima, J. A. C.; Ramires, J. A. F. Myocardial Delayed Enhancement by Magnetic Resonance Imaging in Patients with Chagas' Disease: A Marker of Disease Severity. *J. Am. Coll. Cardiol* **2005**, *46* (8), 1553–1558.
(44) Johnson, C. H.; Ivanisevic, J.; Siuzdak, G. Metabolomics: Beyond Biomarkers and towards Mechanisms. *Nat. Rev. Mol. Cell Biol* **2016**, *17* (7), 451–459.
(45) Wishart, D. S.; Guo, A.; Oler, E.; Wang, F.; Anjum, A.; Peters, H.; Dizon, R.; Sayeeda, Z.; Tian, S.; Lee, B. L.; Berjanskii, M.; Mah, R.; Yamamoto, M.; Jovel, J.; Torres-Calzada, C.; Hiebert-Giesbrecht, M.; Lui, V. W.; Varshavi, D.; Varshavi, D.; Allen, D.; Arndt, D.; Khetarpal, N.; Sivakumaran, A.; Harford, K.; Sanford, S.; Yee, K.; Cao, X.; Budinski, Z.; Liigand, J.; Zhang, L.; Zheng, J.; Mandal, R.; Karu, N.; Dambrova, M.; Schiöth, H. B.; Greiner, R.; Gautam, V. HMDB 5.0: The Human Metabolome Database for 2022. *Nucleic Acids Res* **2022**, *50* (D1), 622–631.
(46) Wishart, D. S.; Tzur, D.; Knox, C.; Eisner, R.; Guo, A. C.; Young, N.; Cheng, D.; Jewell, K.; Arndt, D.; Sawhney, S.; Fung, C.; Nikolai, L.; Lewis, M.; Coutouly, M.-A.; Forsythe, I.; Tang, P.; Shrivastava, S.; Jeroncic, K.; Stothard, P.; Amegbey, G.; Block, D.; Hau, D. D.; Wagner, J.; Miniaci, J.; Clements, M.; Gebremedhin, M.; Guo, N.; Zhang, Y.; Duggan, G. E.; Macinnis, G. D.; Weljie, A. M.; Dowlatabadi, R.; Bamforth, F.; Clive, D.; Greiner, R.; Li, L.; Marrie, T.; Sykes, B. D.; Vogel, H. J.; Querengesser, L. HMDB: The Human Metabolome Database. *Nucleic Acids Res* **2007**.
(47) The Steady-State Transcriptome of the Four Major Life-Cycle Stages of Trypanosoma Cruzi. *BMC Genomics* **2009**, *10* (370).
(48) Li, Y.; Shah-Simpson, S.; Okrah, K.; Belew, A. T.; Choi, J.; Caradonna, K. L.; Padmanabhan, P.; Ndegwa, D. M.; Temanni, M. R.; Corrada Bravo, H. : : Transcriptome Remodeling in Trypanosoma Cruzi and Human Cells during Intracellular Infection. *PLoS Pathog* **2016**, 12 1005511.
(49) Dumoulin, P. C.; Burleigh, B. A. Stress-Induced Proliferation and Cell Cycle Plasticity of Intracellular Amastigotes. *MBio* **2018**, 9.
(50) Houston-Ludlam, G. A.; Trey Belew, A.; El-Sayed, N. M. Comparative Transcriptome Profiling of Human Foreskin Fibroblasts Infected with the Sylvio and Y Strains of Trypanosoma Cruzi. *PLOS ONE* **2016**, 11 0159197.
(51) Belew, A. T.; Junqueira, C.; Rodrigues-Luiz, G. F.; Valente, B. M.; Oliveira, A. E. R.; Polidoro, R. B.; Zuccherato, L. W.; Bartholomeu, D. C.; Schenkman, S.; Gazzinelli, R. T. : : Comparative Transcriptome Profiling of Virulent and Non-Virulent Trypanosoma Cruzi Underlines the Role of Surface Proteins during Infection. *PLoS Pathog* **2017**, 13 1006767.
(52) Gazos-Lopes, F.; Martin, J. L.; Dumoulin, P. C.; Burleigh, B. A. Host Triacylglycerols Shape the Lipidome of Intracellular Trypanosomes and Modulate Their Growth. *PLoS Pathog* **2017**, 13 1006800.

(53) Shah-Simpson, S.; Lentini, G.; Dumoulin, P. C.; Burleigh, B. A. Modulation of Host Central Carbon Metabolism and in Situ Glucose Uptake by Intracellular Trypanosoma Cruzi Amastigotes. *PLoS Pathog* **2017**, 13 1006747.
(54) Koo, S.-J.; Szczesny, B.; Wan, X.; Putluri, N.; Garg, N. J. Pentose Phosphate Shunt Modulates Reactive Oxygen Species and Nitric Oxide Production Controlling in Macrophages. *Front Immunol* **2018**, *9* (202).
(55) Manque, P. A.; Probst, C. M.; Pereira, M. C. S.; Rampazzo, R. C. P.; Ozaki, L. S.; Pavoni, D. P.; Silva Neto, D. T.; Ruth Carvalho, M.; Xu, P.; Serrano, M. G. : : Trypanosoma Cruzi Infection Induces a Global Host Cell Response in Cardiomyocytes. *Infection and Immunity* **2011**, *79*, 3471–3471.
(56) Gupta, S.; Bhatia, V.; Wen, J.-J.; Wu, Y.; Huang, M.-H.; Garg, N. J. Trypanosoma Cruzi Infection Disturbs Mitochondrial Membrane Potential and ROS Production Rate in Cardiomyocytes. *Free Radic Biol Med* **2009**, *47* (1414–1421).
(57) Garg, N.; Popov, V. L.; Papaconstantinou, J. Profiling Gene Transcription Reveals a Deficiency of Mitochondrial Oxidative Phosphorylation in Trypanosoma Cruzi-Infected Murine Hearts: Implications in Chagasic Myocarditis Development. *Biochim Biophys Acta* **2003**, *1638* (106–120).
(58) Soares, M. B. P.; Lima, R. S.; Rocha, L. L.; Vasconcelos, J. F.; Rogatto, dos S., SR; RR, I.; S, G.; RC, I.; DA, T.; H.B. : : Gene Expression Changes Associated with Myocarditis and Fibrosis in Hearts of Mice with Chronic Chagasic Cardiomyopathy. *J Infect Dis* **2010**, *202* (416–426).
(59) Wen, J.-J.; Garg, N. J. Mitochondrial Complex III Defects Contribute to Inefficient Respiration and ATP Synthesis in the Myocardium of Trypanosoma Cruzi-Infected Mice. *Antioxid Redox Signal* **2010**, *12* (27–37).
(60) Wen, J.-J.; Yachelini, P. C.; Sembaj, A.; Manzur, R. E.; Garg, N. J. Increased Oxidative Stress Is Correlated with Mitochondrial Dysfunction in Chagasic Patients. *Free Radic Biol Med* **2006**, *41* (270–276).
(61) Koo, S.-J.; Chowdhury, I. H.; Szczesny, B.; Wan, X.; Garg, N. J. Macrophages Promote Oxidative Metabolism To Drive Nitric Oxide Generation in Response to Trypanosoma Cruzi. *Infect Immun* **2016**, *84* (3527–3541).
(62) Cunha-Neto, E.; Dzau, V. J.; Allen, P. D.; Stamatiou, D.; Benvenutti, L.; Higuchi, M. L.; Koyama, N. S.; Silva, J. S.; Kalil, J.; Liew, C.-C. Cardiac gene expression profiling provides evidence for cytokinopathy as a molecular mechanism in Chagas' disease cardiomyopathy. *Am J Pathol* **2005**, *167*, 305–313.
(63) Ferreira, L. R. P.; Ferreira, F. M.; Laugier, L.; Cabantous, S.; Navarro, I. C.; Silva Cândido, D.; Rigaud, V. C.; Real, J. M.; Pereira, G. V.; Pereira, I. R. : : Integration of miRNA and Gene Expression Profiles Suggest a Role for miRNAs in the Pathobiological Processes of Acute Trypanosoma Cruzi Infection. *Sci Rep* **2017**, *7* (17990).
(64) Gironès, N.; Carbajosa, S.; Guerrero, N. A.; Poveda, C.; Chillón-Marinas, C.; Fresno, M. Global Metabolomic Profiling of Acute Myocarditis Caused by Trypanosoma Cruzi Infection. *PLoS Negl. Trop. Dis* **2014**, *8* (11), 3337.
(65) Lizardo, K.; Ayyappan, J. P.; Oswal, N.; Weiss, L. M.; Scherer, P. E.; Nagajyothi, J. F. Fat Tissue Regulates the Pathogenesis and Severity of Cardiomyopathy in Murine Chagas Disease. *PLoS Negl Trop Dis* **2021**, *15*, 0008964.

(66) Berod, L.; Friedrich, C.; Nandan, A.; Freitag, J.; Hagemann, S.; Harmrolfs, K.; Sandouk, A.; Hesse, C.; Castro, C. N.; Bähre, H. : : De novo fatty acid synthesis controls the fate between regulatory T and T helper 17 cells. *Nature Medicine* **2014**, *20*, 1327–1333.
(67) Magalhães, L. M. D.; Villani, F. N. A.; CP, N. M.; Gollob, K. J.; Rocha, M. O. C.; Dutra, W. O. High Interleukin 17 Expression Is Correlated with Better Cardiac Function in Human Chagas Disease. *J Infect Dis* **2013**, *207* (661–665).
(68) M, G. P. M.; PM, M. G.; FRS, G.; FL, M.; CM, M.; GK, S.; WR, P.; JS, S. IL-17 Produced during Trypanosoma Cruzi Infection Plays a Central Role in Regulating Parasite-Induced Myocarditis. *PLoS Neglected Tropical Diseases* **2010**, 4 604.
(69) Caradonna, K. L.; Engel, J. C.; Jacobi, D.; Lee, C.-H.; Burleigh, B. A. Host Metabolism Regulates Intracellular Growth of Trypanosoma Cruzi. *Cell Host Microbe* **2013**, *13* (108–117).
(70) Hossain, E.; Khanam, S.; Dean, D. A.; Wu, C.; Lostracco-Johnson, S.; Thomas, D.; Kane, S. S.; Parab, A. R.; Flores, K.; Katemauswa, M.; Gosmanov, C.; Hayes, S. E.; Zhang, Y.; Li, D.; Woelfel-Monsivais, C.; Sankaranarayanan, K.; McCall, L.-I. Mapping of Host-Parasite-Microbiome Interactions Reveals Metabolic Determinants of Tropism and Tolerance in Chagas Disease.
(71) Knubel, C. P.; Martínez, F. F.; Fretes, R. E.; Díaz Lujan, C.; Theumer, M. G.; Cervi, L.; Motrán, C. C. Indoleamine 2,3-Dioxigenase (IDO) Is Critical for Host Resistance against Trypanosoma Cruzi. *FASEB J* **2010**, *24* (2689–2701).
(72) Dean, D. A.; Gautham, G.; Siqueira-Neto, J. L.; McKerrow, J. H.; Dorrestein, P. C.; McCall, L.-I. Spatial Metabolomics Identifies Localized Chemical Changes in Heart Tissue during Chronic Cardiac Chagas Disease. *PLoS Negl. Trop. Dis* **2021**, *15* (10), 0009819.
(73) Hoffman, K.; Liu, Z.; Hossain, E.; Bottazzi, M. E.; Hotez, P. J.; Jones, K. M.; McCall, L.-I. Alterations to the Cardiac Metabolome Induced by Chronic Infection Relate to the Degree of Cardiac Pathology. *ACS Infect Dis* **2021**, *7* (6), 1638–1649.
(74) McCall, L.-I.; Morton, J. T.; Bernatchez, J. A.; Siqueira-Neto, J. L.; Knight, R.; Dorrestein, P. C.; McKerrow, J. H. Mass Spectrometry-Based Chemical Cartography of a Cardiac Parasitic Infection. *Anal. Chem* **2017**, *89* (19), 10414–10421.
(75) Ward, A. I.; Lewis, M. D.; Khan, A. A.; McCann, C. J.; Francisco, A. F.; Jayawardhana, S.; Taylor, M. C.; Kelly, J. M. Analysis of Trypanosoma Cruzi Persistence Foci at Single-Cell Resolution.
(76) McCall, L.-I.; Tripathi, A.; Vargas, F.; Knight, R.; Dorrestein, P. C.; Siqueira-Neto, J. L. Experimental Chagas Disease-Induced Perturbations of the Fecal Microbiome and Metabolome. *PLoS Negl. Trop. Dis* **2018**, *12* (3), 0006344.
(77) Hossain, E.; Khanam, S.; Dean, D. A.; Wu, C.; Lostracco-Johnson, S.; Thomas, D.; Kane, S. S.; Parab, A. R.; Flores, K.; Katemauswa, M. : : Mapping of Host-Parasite-Microbiome Interactions Reveals Metabolic Determinants of Tropism and Tolerance in Chagas Disease. *Sci Adv* **2020**, 6 2015.
(78) Picado, A.; Angheben, A.; Marchiol, A.; Alarcón de Noya, B.; Flevaud, L.; Pinazo, M. J.; Gállego, M.; Meymandi, S.; Moriana, S. Development of Diagnostics for Chagas Disease: Where Should We Put Our Limited Resources? *PLoS Negl Trop Dis* **2017**, *11* (1), e0005148. https://doi.org/10.1371/journal.pntd.0005148.
(79) Lewis, M. D.; Fortes Francisco, A.; Taylor, M. C.; Burrell-Saward, H.; McLatchie, A. P.; Miles, M. A.; Kelly, J. M. Bioluminescence Imaging of Chronic Trypanosoma Cruzi

Infections Reveals Tissue-Specific Parasite Dynamics and Heart Disease in the Absence of Locally Persistent Infection. *Cell. Microbiol* **2014**, *16* (9), 1285–1300.
(80) Lewis, M. D.; Francisco, A. F.; Taylor, M. C.; Kelly, J. M. A New Experimental Model for Assessing Drug Efficacy against Trypanosoma Cruzi Infection Based on Highly Sensitive in Vivo Imaging. *J. Biomol. Screen* **2015**, *20* (1), 36–43.
(81) Francisco, A. F.; Jayawardhana, S.; Lewis, M. D.; White, K. L.; Shackleford, D. M.; Chen, G.; Saunders, J.; Osuna-Cabello, M.; Read, K. D.; Charman, S. A.; Chatelain, E.; Kelly, J. M. Nitroheterocyclic Drugs Cure Experimental Trypanosoma Cruzi Infections More Effectively in the Chronic Stage than in the Acute Stage. *Sci. Rep* **2016**, *6*, 35351.
(82) Zingales, B.; Andrade, S. G.; Briones, M. R. S.; Campbell, D. A.; Chiari, E.; Fernandes, O.; Guhl, F.; Lages-Silva, E.; Macedo, A. M.; Machado, C. R.; Miles, M. A.; Romanha, A. J.; Sturm, N. R.; Tibayrenc, M.; Schijman, A. G.; Meeting, S. S. A New Consensus for Trypanosoma Cruzi Intraspecific Nomenclature. *Second Revision Meeting Recommends TcI to TcVI. Mem. Inst. Oswaldo Cruz* **2009**, *104* (7), 1051–1054.
(83) Zuluaga, A. F.; Salazar, B. E.; Rodriguez, C. A.; Zapata, A. X.; Agudelo, M.; Vesga, O. Neutropenia Induced in Outbred Mice by a Simplified Low-Dose Cyclophosphamide Regimen: Characterization and Applicability to Diverse Experimental Models of Infectious Diseases. *BMC Infect. Dis* **2006**, *6*, 55.
(84) Piron, M.; Fisa, R.; Casamitjana, N.; López-Chejade, P.; Puig, L.; Vergés, M.; Gascón, J.; Prat, J.; Portús, M.; Sauleda, S. Development of a Real-Time PCR Assay for Trypanosoma Cruzi Detection in Blood Samples. *Acta Trop* **2007**, *103* (3), 195–200.
(85) Cummings, K. L.; Tarleton, R. L. Rapid Quantitation of Trypanosoma Cruzi in Host Tissue by Real-Time PCR. *Molecular and Biochemical Parasitology* **2003**, *129* (1), 53–59. https://doi.org/10.1016/S0166-6851(03)00093-8.
(86) Tsujita, Y.; Muraski, J.; Shiraishi, I.; Kato, T.; Kajstura, J.; Anversa, P.; Sussman, M. A. Nuclear Targeting of Akt Antagonizes Aspects of Cardiomyocyte Hypertrophy. *Proc. Natl. Acad. Sci. U. S. A* **2006**, *103* (32), 11946–11951.
(87) Chen, R.; Zhao, L.; Bai, R.; Liu, Y.; Han, L.; Xu, Z.; Chen, F.; Autrup, H.; Long, D.; Chen, C. Silver Nanoparticles Induced Oxidative and Endoplasmic Reticulum Stresses in Mouse Tissues: Implications for the Development of Acute Toxicity after Intravenous Administration. *Toxicol. Res* **2016**, *5* (2), 602–608.
(88) Dunn, W. B.; Broadhurst, D.; Begley, P.; Zelena, E.; Francis-McIntyre, S.; Anderson, N.; Brown, M.; Knowles, J. D.; Halsall, A.; Haselden, J. N.; Nicholls, A. W.; Wilson, I. D.; Kell, D. B.; Goodacre, R.; Consortium, H. S. M. Procedures for Large-Scale Metabolic Profiling of Serum and Plasma Using Gas Chromatography and Liquid Chromatography Coupled to Mass Spectrometry. *Nat. Protoc* **2011**, *6* (7), 1060–1083.
(89) Kessner, D.; Chambers, M.; Burke, R.; Agus, D.; Mallick, P. ProteoWizard: Open Source Software for Rapid Proteomics Tools Development. *Bioinformatics* **2008**, *24* (21), 2534–2536.
(90) Pluskal, T.; Castillo, S.; Villar-Briones, A.; Oresic, M. MZmine 2: Modular Framework for Processing, Visualizing, and Analyzing Mass Spectrometry-Based Molecular Profile Data. *BMC Bioinformatics* **2010**, *11*, 395.
(91) Buck, J.; Shaykhutdinov, R.; Barkema, H. W.; Vogel, H. J. Metabolomic Profiling in Cattle Experimentally Infected with Mycobacterium Avium Subsp. *Paratuberculosis. PLoS One* **2014**, *9* (11), 111872.

(92) Anderson, M. J. A New Method for Non-Parametric Multivariate Analysis of Variance. *Austral Ecology* **2001**, *26* (1), 32–46. https://doi.org/10.1111/j.1442-9993.2001.01070.pp.x.
(93) Freeman, J. B.; Dale, R. Assessing Bimodality to Detect the Presence of a Dual Cognitive Process. *Behav Res* **2013**, *45* (1), 83–97. https://doi.org/10.3758/s13428-012-0225-x.
(94) Kass, R. E.; Raftery, A. E. Bayes Factors. *Journal of the American Statistical Association* **1995**, *90* (430), 773–795. https://doi.org/10.1080/01621459.1995.10476572.
(95) Wang, M.; Carver, J. J.; Phelan, V. V.; Sanchez, L. M.; Garg, N.; Peng, Y.; Nguyen, D. D.; Watrous, J.; Kapono, C. A.; Luzzatto-Knaan, T.; Porto, C.; Bouslimani, A.; Melnik, A. V.; Meehan, M. J.; Liu, W.-T.; Crüsemann, M.; Boudreau, P. D.; Esquenazi, E.; Sandoval-Calderón, M.; Kersten, R. D.; Pace, L. A.; Quinn, R. A.; Duncan, K. R.; Hsu, C.-C.; Floros, D. J.; Gavilan, R. G.; Kleigrewe, K.; Northen, T.; Dutton, R. J.; Parrot, D.; Carlson, E. E.; Aigle, B.; Michelsen, C. F.; Jelsbak, L.; Sohlenkamp, C.; Pevzner, P.; Edlund, A.; McLean, J.; Piel, J.; Murphy, B. T.; Gerwick, L.; Liaw, C.-C.; Yang, Y.-L.; Humpf, H.-U.; Maansson, M.; Keyzers, R. A.; Sims, A. C.; Johnson, A. R.; Sidebottom, A. M.; Sedio, B. E.; Klitgaard, A.; Larson, C. B.; P, C. A. B.; Torres-Mendoza, D.; Gonzalez, D. J.; Silva, D. B.; Marques, L. M.; Demarque, D. P.; Pociute, E.; O'Neill, E. C.; Briand, E.; Helfrich, E. J. N.; Granatosky, E. A.; Glukhov, E.; Ryffel, F.; Houson, H.; Mohimani, H.; Kharbush, J. J.; Zeng, Y.; Vorholt, J. A.; Kurita, K. L.; Charusanti, P.; McPhail, K. L.; Nielsen, K. F.; Vuong, L.; Elfeki, M.; Traxler, M. F.; Engene, N.; Koyama, N.; Vining, O. B.; Baric, R.; Silva, R. R.; Mascuch, S. J.; Tomasi, S.; Jenkins, S.; Macherla, V.; Hoffman, T.; Agarwal, V.; Williams, P. G.; Dai, J.; Neupane, R.; Gurr, J.; Rodríguez, A. M. C.; Lamsa, A.; Zhang, C.; Dorrestein, K.; Duggan, B. M.; Almaliti, J.; Allard, P.-M.; Phapale, P.; Nothias, L.-F.; Alexandrov, T.; Litaudon, M.; Wolfender, J.-L.; Kyle, J. E.; Metz, T. O.; Peryea, T.; Nguyen, D.-T.; VanLeer, D.; Shinn, P.; Jadhav, A.; Müller, R.; Waters, K. M.; Shi, W.; Liu, X.; Zhang, L.; Knight, R.; Jensen. Sharing and Community Curation of Mass Spectrometry Data with Global Natural Products Social Molecular Networking. *Nat. Biotechnol* **2016**, *34* (8), 828–837.
(96) Nothias, L.-F.; Petras, D.; Schmid, R.; Dührkop, K.; Rainer, J.; Sarvepalli, A.; Protsyuk, I.; Ernst, M.; Tsugawa, H.; Fleischauer, M.; Aicheler, F.; Aksenov, A. A.; Alka, O.; Allard, P.-M.; Barsch, A.; Cachet, X.; Caraballo-Rodriguez, A. M.; Silva, R. R.; Dang, T.; Garg, N.; Gauglitz, J. M.; Gurevich, A.; Isaac, G.; Jarmusch, A. K.; Kameník, Z.; Kang, K. B.; Kessler, N.; Koester, I.; Korf, A.; Le Gouellec, A.; Ludwig, M.; H, M.; C., M.; L.-I., M.; J., M.; W., S.; Mohimani, H.; Morsy, M.; Moyne, O.; Neumann, S.; Neuweger, H.; Nguyen, N. H.; Nothias-Esposito, M.; Paolini, J.; Phelan, V. V.; Pluskal, T.; Quinn, R. A.; Rogers, S.; Shrestha, B.; Tripathi, A.; Hooft, J. J. J.; Vargas, F.; Weldon, K. C.; Witting, M.; Yang, H.; Zhang, Z.; Zubeil, F.; Kohlbacher, O.; Böcker, S.; Alexandrov, T.; Bandeira, N.; Wang, M.; Dorrestein, P. C. Feature-Based Molecular Networking in the GNPS Analysis Environment. *Nat. Methods* **2020**, *17* (9), 905–908.
(97) Lesani, M.; Gosmanov, C.; Paun, A.; Lewis, M. D.; McCall, L.-I. Impact of Visceral Leishmaniasis on Local Organ Metabolism in Hamsters. *Metabolites* **2022**, *12* (9), 802. https://doi.org/10.3390/metabo12090802.
(98) Sumner, L. W.; Amberg, A.; Barrett, D.; Beale, M. H.; Beger, R.; Daykin, C. A.; Fan, T. W.-M.; Fiehn, O.; Goodacre, R.; Griffin, J. L.; Hankemeier, T.; Hardy, N.; Harnly, J.; Higashi, R.; Kopka, J.; Lane, A. N.; Lindon, J. C.; Marriott, P.; Nicholls, A. W.; Reily, M. D.; Thaden, J. J.; Viant, M. R. Proposed Minimum Reporting Standards for Chemical

Analysis Chemical Analysis Working Group (CAWG) Metabolomics Standards Initiative (MSI. *Metabolomics* **2007**, *3* (3), 211–221.
(99) Theodoridis, G.; Gika, H.; Raftery, D.; Goodacre, R.; Plumb, R. S.; Wilson, I. D. Ensuring Fact-Based Metabolite Identification in Liquid Chromatography-Mass Spectrometry-Based Metabolomics. *Anal. Chem* **2023**, *95* (8), 3909–3916.
(100) Jackson, Y.; Chatelain, E.; Mauris, A.; Holst, M.; Miao, Q.; Chappuis, F.; Ndao, M. Serological and Parasitological Response in Chronic Chagas Patients 3 Years after Nifurtimox Treatment. *BMC Infect Dis* **2013**, *13*, 85. https://doi.org/10.1186/1471-2334-13-85.
(101) Hartigan, J. A.; Hartigan, P. M. The Dip Test of Unimodality. *The Annals of Statistics* **1985**, *13* (1), 70–84. https://doi.org/10.1214/aos/1176346577.
(102) Lobo-Rojas, A.; Marchese, L.; Eufrasio, A. G.; Souza, G. T. D.; Catelli, M. F.; Faria, J. D. N.; Cordeiro, A. T. Exploring T. Cruzi IMPDH as a Promising Target through Chagas Box Screening and AVN-944 Inhibition. *Antimicrob Agents Chemother 70* (3), e01210-25. https://doi.org/10.1128/aac.01210-25.
(103) Lizardo, K.; Ayyappan, J. P.; Ganapathi, U.; Dutra, W. O.; Qiu, Y.; Weiss, L. M.; Nagajyothi, J. F. Diet Alters Serum Metabolomic Profiling in the Mouse Model of Chronic Chagas Cardiomyopathy. *Dis. Markers* **2019**, 4956016.
(104) Cutshaw, M. K.; Sciaudone, M.; Bowman, N. M. Risk Factors for Progression to Chronic Chagas Cardiomyopathy: A Systematic Review and Meta-Analysis. *The American Journal of Tropical Medicine and Hygiene* **2023**, *108* (4), 791–800. https://doi.org/10.4269/ajtmh.22-0630.
(105) Liu, Z.; Ulrich, R.; Kendricks, A.; Wheeler, K.; Leão, A. C.; Pollet, J.; Bottazzi, M. E.; Hotez, P.; Gusovsky, F.; Jones, K.; McCall, L.-I. Localized Cardiac Metabolic Trajectories and Post-Infectious Metabolic Sequelae in Experimental Chagas Disease. In Review January 20, 2023. https://doi.org/10.21203/rs.3.rs-2497474/v1.
(106) Jonge, N. F.; Mildau, K.; Meijer, D.; Louwen, J. J. R.; Bueschl, C.; Huber, F.; Hooft. *J. J. J. Good Practices and Recommendations for Using and Benchmarking Computational Metabolomics Metabolite Annotation Tools. Metabolomics* **2022**, *18* (12), 103.
(107) Gauglitz, J. M.; West, K. A.; Bittremieux, W.; Williams, C. L.; Weldon, K. C.; Panitchpakdi, M.; Ottavio, F.; Aceves, C. M.; Brown, E.; Sikora, N. C.; Jarmusch, A. K.; Martino, C.; Tripathi, A.; Meehan, M. J.; Dorrestein, K.; Shaffer, J. P.; Coras, R.; Vargas, F.; Goldasich, L. D.; Schwartz, T.; Bryant, M.; Humphrey, G.; Johnson, A. J.; Spengler, K.; Belda-Ferre, P.; Diaz, E.; McDonald, D.; Zhu, Q.; Elijah, E. O.; Wang, M.; Marotz, C.; Sprecher, K. E.; Vargas-Robles, D.; Withrow, D.; Ackermann, G.; Herrera, L.; Bradford, B. J.; Marques, L. M. M.; Amaral, J. G.; Silva, R. M.; Veras, F. P.; Cunha, T. M.; Oliveira, R. D. R.; Louzada-Junior, P.; Mills, R. H.; Piotrowski, P. K.; Servetas, S. L.; Silva, S. M.; Jones, C. M.; Lin, N. J.; Lippa, K. A.; Jackson, S. A.; Daouk, R. K.; Galasko, D.; Dulai, P. S.; Kalashnikova, T. I.; Wittenberg, C.; Terkeltaub, R.; Doty, M. M.; Kim, J. H.; Rhee, K. E.; Beauchamp-Walters, J.; Wright, K. P., Jr; Dominguez-Bello, M. G.; Manary, M.; Oliveira, M. F.; Boland, B. S.; Lopes, N. P.; Guma, M.; Swafford, A. D.; Dutton, R. J.; Knight, R.; Dorrestein, P. C. Enhancing Untargeted Metabolomics Using Metadata-Based Source Annotation. *Nat. Biotechnol* **2022**, *40* (12), 1774–1779.
(108) Bittremieux, W.; Wang, M.; Dorrestein, P. C. The Critical Role That Spectral Libraries Play in Capturing the Metabolomics Community Knowledge. *Metabolomics* **2022**, *18* (12), 1–16.

(109) Depner, C. M.; Cogswell, D. T.; Bisesi, P. J.; Markwald, R. R.; Cruickshank-Quinn, C.; Quinn, K.; Melanson, E. L.; Reisdorph, N.; Wright, K. P. Developing Preliminary Blood Metabolomics-Based Biomarkers of Insufficient Sleep in Humans. *Sleep* **2020**, *43* (7), zsz321. https://doi.org/10.1093/sleep/zsz321.
(110) Jia, H.; Shen, X.; Guan, Y.; Xu, M.; Tu, J.; Mo, M.; Xie, L.; Yuan, J.; Zhang, Z.; Cai, S.; Zhu, J.; Zhu, Z. Predicting the Pathological Response to Neoadjuvant Chemoradiation Using Untargeted Metabolomics in Locally Advanced Rectal Cancer. *Radiother. Oncol* **2018**, *128* (3), 548–556.
(111) Castro-Sesquen, Y. E.; Gilman, R. H.; Mejia, C.; Clark, D. E.; Choi, J.; Reimer-McAtee, M. J.; Castro, R.; Valencia-Ayala, E.; Flores, J.; Bowman, N.; Castillo-Neyra, R.; Torrico, F.; Liotta, L.; Bern, C.; Luchini, A.; The Chagas/HIV Working Group in Bolivia and Peru. Use of a Chagas Urine Nanoparticle Test (Chunap) to Correlate with Parasitemia Levels in T. Cruzi/HIV Co-Infected Patients. *PLoS Negl Trop Dis* **2016**, *10* (2), e0004407. https://doi.org/10.1371/journal.pntd.0004407.
(112) Castro-Sesquen, Y. E.; Gilman, R. H.; Galdos-Cardenas, G.; Ferrufino, L.; Sánchez, G.; Valencia Ayala, E.; Liotta, L.; Bern, C.; Luchini, A.; Bolivia, W. G.; Peru. Use of a Novel Chagas Urine Nanoparticle Test (Chunap) for Diagnosis of Congenital Chagas Disease. *PLoS Negl. Trop. Dis* **2014**, *8* (10), 3211.
(113) Corral, R. S.; Altcheh, J.; Alexandre, S. R.; Grinstein, S.; Freilij, H.; Katzin, A. M. Detection and Characterization of Antigens in Urine of Patients with Acute, Congenital, and Chronic Chagas' Disease. *J Clin Microbiol* **1996**, *34* (8), 1957–1962. https://doi.org/10.1128/jcm.34.8.1957-1962.1996.
(114) Tanowitz, H. B.; Kirchhoff, L. V.; Simon, D.; Morris, S. A.; Weiss, L. M.; Wittner, M. Chagas' Disease. *Clin. Microbiol. Rev* **1992**, *5* (4), 400–419.
(115) Freilij, H. L.; Corral, R. S.; Katzin, A. M.; Grinstein, S. Antigenuria in Infants with Acute and Congenital Chagas' Disease. *J. Clin. Microbiol* **1987**, *25* (1), 133–137.
(116) Castro-Sesquen, Y. E.; Gilman, R. H.; Yauri, V.; Cok, J.; Angulo, N.; Escalante, H.; Bern, C. Detection of Soluble Antigen and DNA of Trypanosoma Cruzi in Urine Is Independent of Renal Injury in the Guinea Pig Model. *PLoS One* **2013**, *8* (3), 58480.
(117) Lemos, J. R. D.; Rodrigues, W. F.; Miguel, C. B.; Parreira, R. C.; Miguel, R. B.; Paula Rogerio, A.; Oliveira, C. J. F.; Chica, J. E. L. Influence of Parasite Load on Renal Function in Mice Acutely Infected with Trypanosoma Cruzi. *PLoS One* **2013**, *8* (8), 71772.
(118) Junior, G. B. da S.; Silva Junior, G. B.; Antunes, V. V. H.; Motta, M.; Barros, E. J. G.; Francesco Daher, E. Chagas Disease-Associated Kidney Injury. *A Review. Nefrología Latinoamericana* **2017**, 22–26. https://doi.org/10.1016/j.nefrol.2016.12.001.
(119) Chen, J.-Y.; Zhou, J.-K.; Pan, W. Immunometabolism: Towards a Better Understanding the Mechanism of Parasitic Infection and Immunity. *Front. Immunol* **2021**, *12*, 661241.
(120) Golizeh, M.; Nam, J.; Chatelain, E.; Jackson, Y.; Ohlund, L. B.; Rasoolizadeh, A.; Camargo, F. V.; Mahrouche, L.; Furtos, A.; Sleno, L.; Ndao, M. New Metabolic Signature for Chagas Disease Reveals Sex Steroid Perturbation in Humans and Mice. *Heliyon* **2022**, *8* (12), 12380.
(121) Herreros-Cabello, A.; Bosch-Nicolau, P.; Pérez-Molina, J. A.; Salvador, F.; Monge-Maillo, B.; Rodriguez-Palomares, J. F.; Ribeiro, A. L. P.; Sánchez-Montalvá, A.; Sabino, E. C.; Norman, F. F.; Fresno, M.; Gironès, N.; Molina, I. Identification of Chagas Disease

Biomarkers Using Untargeted Metabolomics. *Sci Rep* **2024**, *14* (1), 18768. https://doi.org/10.1038/s41598-024-69205-w.
(122) Novoa-del-Toro, E. M.; Witting, M. Navigating Common Pitfalls in Metabolite Identification and Metabolomics Bioinformatics. *Metabolomics* **2024**, *20* (5), 103. https://doi.org/10.1007/s11306-024-02167-2.
(123) Wieder, C.; Frainay, C.; Poupin, N.; Rodríguez-Mier, P.; Vinson, F.; Cooke, J.; Lai, R. P.; Bundy, J. G.; Jourdan, F.; Ebbels, T. Pathway Analysis in Metabolomics: Recommendations for the Use of over-Representation Analysis. *PLoS Comput Biol* **2021**, *17* (9), e1009105. https://doi.org/10.1371/journal.pcbi.1009105.
(124) *Untargeted Metabolomics Strategies—Challenges and Emerging Directions | Journal of the American Society for Mass Spectrometry | ACS Publications*. https://pubs.acs.org/jamsef/article-abstract/27/12/1897/1777309/Untargeted-Metabolomics-Strategies-Challenges-and?redirectedFrom=fulltext (accessed 2026-07-29).
(125) Calderón-Santiago, M.; Priego-Capote, F.; Luque de Castro, M. D. Enhanced Detection and Identification in Metabolomics by Use of LC-MS/MS Untargeted Analysis in Combination with Gas-Phase Fractionation. *Anal Chem* **2014**, *86* (15), 7558–7565. https://doi.org/10.1021/ac501353n.
(126) Wurth, R.; Turgeon, C.; Stander, Z.; Oglesbee, D. An Evaluation of Untargeted Metabolomics Methods to Characterize Inborn Errors of Metabolism. *Molecular Genetics and Metabolism* **2024**, *141* (1), 108115. https://doi.org/10.1016/j.ymgme.2023.108115.
(127) Harris, M. B.; Lesani, M.; Liu, Z.; McCall, L.-I. Molecular Networking in Infectious Disease Models. *Methods Enzymol* **2022**, *663*, 341–375. https://doi.org/10.1016/bs.mie.2021.09.018.
(128) Fahy, E.; Subramaniam, S. RefMet: A Reference Nomenclature for Metabolomics. *Nat Methods* **2020**, *17* (12), 1173–1174. https://doi.org/10.1038/s41592-020-01009-y.
(129) Ravikrishnan, A.; Raman, K. Critical Assessment of Genome-Scale Metabolic Networks: The Need for a Unified Standard. *Brief Bioinform* **2015**, *16* (6), 1057–1068. https://doi.org/10.1093/bib/bbv003.
(130) Qi, X.; Ozsoyoglu, Z. M.; Ozsoyoglu, G. Matching Metabolites and Reactions in Different Metabolic Networks. *Methods* **2014**, *69* (3), 282–297. https://doi.org/10.1016/j.ymeth.2014.06.007.
(131) World Health Organization. *Global Tuberculosis Report 2025*; World Health Organization: Geneva, Switzerland, 2025.
(132) *Understanding Latent Tuberculosis: A Moving Target | The Journal of Immunology | Oxford Academic*. https://academic.oup.com/jimmunol/article-abstract/185/1/15/7977445?redirectedFrom=fulltext (accessed 2026-07-03).
(133) Muzzi, A.; Seminari, E.; Feletti, T.; Scudeller, L.; Marone, P.; Tinelli, C.; Minoli, L.; Marena, C.; Mangiarotti, P.; Strosselli, M. Post-Exposure Rate of Tuberculosis Infection among Health Care Workers Measured with Tuberculin Skin Test Conversion after Unprotected Exposure to Patients with Pulmonary Tuberculosis: 6-Year Experience in an Italian Teaching Hospital. *BMC Infect Dis* **2014**, *14*, 324. https://doi.org/10.1186/1471-2334-14-324.
(134) Reichler, M. R.; Khan, A.; Yuan, Y.; Chen, B.; McAuley, J.; Mangura, B.; Sterling, T. R. Duration of Exposure Among Close Contacts of Patients With Infectious Tuberculosis and Risk of Latent Tuberculosis Infection. *Clin Infect Dis* **2020**, *71* (7), 1627–1634. https://doi.org/10.1093/cid/ciz1044.

(135) Houben, R. M. G. J.; Dodd, P. J. The Global Burden of Latent Tuberculosis Infection: A Re-Estimation Using Mathematical Modelling. *PLoS Med* **2016**, *13* (10), e1002152. https://doi.org/10.1371/journal.pmed.1002152.
(136) Tobin, E. H.; Tristram, D. Tuberculosis Overview. In *StatPearls*; StatPearls Publishing: Treasure Island (FL), 2026.
(137) Narasimhan, P.; Wood, J.; MacIntyre, C. R.; Mathai, D. Risk Factors for Tuberculosis. *Pulm Med* **2013**, *2013*, 828939. https://doi.org/10.1155/2013/828939.
(138) Silva, D. R.; Muñoz-Torrico, M.; Duarte, R.; Galvão, T.; Bonini, E. H.; Arbex, F. F.; Arbex, M. A.; Augusto, V. M.; Rabahi, M. F.; Mello, F. C. de Q. Risk Factors for Tuberculosis: Diabetes, Smoking, Alcohol Use, and the Use of Other Drugs. *J Bras Pneumol* **2018**, *44* (2), 145–152. https://doi.org/10.1590/S1806-37562017000000443.
(139) Chung, E. S.; Kar, P.; Kamkaew, M.; Amir, A.; Aldridge, B. B. Single-Cell Imaging of the Mycobacterium Tuberculosis Cell Cycle Reveals Linear and Heterogenous Growth. *Nat Microbiol* **2024**, *9* (12), 3332–3344. https://doi.org/10.1038/s41564-024-01846-z.
(140) Verma, A.; Ghoshal, A.; Dwivedi, V. P.; Bhaskar, A. Tuberculosis: The Success Tale of Less Explored Dormant Mycobacterium Tuberculosis. *Front. Cell. Infect. Microbiol.* **2022**, *12*. https://doi.org/10.3389/fcimb.2022.1079569.
(141) *Mycobacterium tuberculosis Pathogenesis and Molecular Determinants of Virulence | Clinical Microbiology Reviews*. https://journals.asm.org/doi/full/10.1128/cmr.16.3.463-496.2003?casa_token=Ji0GRtjOgF4AAAAA%3AEYyJam61YDz74sT8IcOoOlVJSBqkuoGjqqbGY9fNGbOfJfcDnOK-Ljo8Sq2yxiyc9dQjS52MM-PJCg (accessed 2026-07-03).
(142) Podinovskaia, M.; Lee, W.; Caldwell, S.; Russell, D. G. Infection of Macrophages with Mycobacterium Tuberculosis Induces Global Modifications to Phagosomal Function. *Cell Microbiol* **2013**, *15* (6), 843–859. https://doi.org/10.1111/cmi.12092.
(143) Ndlovu, H.; Marakalala, M. J. Granulomas and Inflammation: Host-Directed Therapies for Tuberculosis. *Front Immunol* **2016**, *7*, 434. https://doi.org/10.3389/fimmu.2016.00434.
(144) CDC. *Clinical Overview of Tuberculosis Disease*. Tuberculosis (TB). https://www.cdc.gov/tb/hcp/clinical-overview/tuberculosis-disease.html (accessed 2026-07-03).
(145) Tiemersma, E. W.; Van Der Werf, M. J.; Borgdorff, M. W.; Williams, B. G.; Nagelkerke, N. J. D. Natural History of Tuberculosis: Duration and Fatality of Untreated Pulmonary Tuberculosis in HIV Negative Patients: A Systematic Review. *PLoS ONE* **2011**, *6* (4), e17601. https://doi.org/10.1371/journal.pone.0017601.
(146) *Global gains in tuberculosis response endangered by funding challenges*. https://www.who.int/news/item/12-11-2025-global-gains-in-tuberculosis-response-endangered-by-funding-challenges (accessed 2026-07-02).
(147) Nasiri, M. J.; Amiri, M.; Cheraghi, M.; Silva, D. R.; Sotgiu, G.; D'Ambrosio, L.; Centis, R.; Mileva-Lopez, M.; Hill, T. M.; Gidey, S.; Diaby, K.; Hittel, N.; Gandhi, H.; Dara, M. 15-Year Trends in Efficacy and Effectiveness of Treatment Outcomes in Drug-Resistant Pulmonary TB. *IJTLD Open* **2025**, *2* (4), 187–198. https://doi.org/10.5588/ijtldopen.24.0620.
(148) Pedersen, O. S.; Holmgaard, F. B.; Mikkelsen, M. K. D.; Lange, C.; Sotgiu, G.; Lillebaek, T.; Andersen, A. B.; Wejse, C. M.; Dahl, V. N. Global Treatment Outcomes of Extensively Drug-Resistant Tuberculosis in Adults: A Systematic Review and Meta-Analysis. *Journal of Infection* **2023**, *87* (3), 177–189. https://doi.org/10.1016/j.jinf.2023.06.014.

(149) CDC. *Treatment for Drug-Susceptible Tuberculosis Disease*. Tuberculosis (TB). https://www.cdc.gov/tb/hcp/treatment/tuberculosis-disease.html (accessed 2026-07-02).
(150) Shin, H.-J.; Kwon, Y.-S. Treatment of Drug Susceptible Pulmonary Tuberculosis. *Tuberc Respir Dis* **2015**, *78* (3), 161–167. https://doi.org/10.4046/trd.2015.78.3.161.
(151) CDC. *Treatment for Drug-Resistant Tuberculosis Disease*. Tuberculosis (TB). https://www.cdc.gov/tb/hcp/treatment/drug-resistant-tuberculosis-disease.html (accessed 2026-07-02).
(152) TOLA, H. H.; TOL, A.; SHOJAEIZADEH, D.; GARMAROUDI, G. Tuberculosis Treatment Non-Adherence and Lost to Follow Up among TB Patients with or without HIV in Developing Countries: A Systematic Review. *Iran J Public Health* **2015**, *44* (1), 1–11.
(153) TOLA, H. H.; TOL, A.; SHOJAEIZADEH, D.; GARMAROUDI, G. Tuberculosis Treatment Non-Adherence and Lost to Follow Up among TB Patients with or without HIV in Developing Countries: A Systematic Review. *Iran J Public Health* **2015**, *44* (1), 1–11.
(154) LaHood, A.; Rahman, R.; McKenna, L.; Frick, M.; Mitnick, C. D. Comparing Timelines and Evidence Available to Support New TB, HIV, and HCV Drug Approvals: The Same, Only Different. *PLOS ONE* **2022**, *17* (7), e0271102. https://doi.org/10.1371/journal.pone.0271102.
(155) Kufa, M.; Finger, V.; Kovar, O.; Soukup, O.; Torruellas, C.; Roh, J.; Korabecny, J. Revolutionizing Tuberculosis Treatment: Breakthroughs, Challenges, and Hope on the Horizon. *Acta Pharmaceutica Sinica B* **2025**, *15* (3), 1311–1332. https://doi.org/10.1016/j.apsb.2025.01.023.
(156) *The End TB Strategy*. https://www.who.int/teams/global-programme-on-tuberculosis-and-lung-health/the-end-tb-strategy (accessed 2026-07-09).
(157) Marley, G.; Zou, X.; Nie, J.; Cheng, W.; Xie, Y.; Liao, H.; Wang, Y.; Tao, Y.; Tucker, J. D.; Sylvia, S.; Chou, R.; Wu, D.; Ong, J.; Tang, W. Improving Cascade Outcomes for Active TB: A Global Systematic Review and Meta-Analysis of TB Interventions. *PLoS Med* **2023**, *20* (1), e1004091. https://doi.org/10.1371/journal.pmed.1004091.
(158) Liu, X.; Thompson, J.; Dong, H.; Sweeney, S.; Li, X.; Yuan, Y.; Wang, X.; He, W.; Thomas, B.; Xu, C.; Hu, D.; Vassall, A.; Huan, S.; Zhang, H.; Jiang, S.; Fielding, K.; Zhao, Y. Digital Adherence Technologies to Improve Tuberculosis Treatment Outcomes in China: A Cluster-Randomised Superiority Trial. *Lancet Glob Health* **2023**, *11* (5), e693–e703. https://doi.org/10.1016/S2214-109X(23)00068-2.
(159) Kedthongma, W.; Usaprom, S.; Phakdeekul, W. Community-Based Interventions to Improve Tuberculosis Treatment Outcomes: A Meta-Analysis. *MethodsX* **2026**, *16*, 103893. https://doi.org/10.1016/j.mex.2026.103893.
(160) Pradipta, I. S.; Houtsma, D.; van Boven, J. F. M.; Alffenaar, J.-W. C.; Hak, E. Interventions to Improve Medication Adherence in Tuberculosis Patients: A Systematic Review of Randomized Controlled Studies. *NPJ Prim Care Respir Med* **2020**, *30*, 21. https://doi.org/10.1038/s41533-020-0179-x.
(161) *Systematic screening for active tuberculosis: principles and recommendations*. https://iris.who.int/items/74677072-9082-43f2-9f88-990b4f8ea048 (accessed 2026-07-10).
(162) *Implementing tuberculosis diagnostics: policy framework*. https://www.who.int/publications/i/item/9789241508612 (accessed 2026-07-09).
(163) *WHO warns against the use of inaccurate blood tests for active tuberculosis*. https://www.who.int/news/item/20-07-2011-who-warns-against-the-use-of-inaccurate-blood-tests-for-active-tuberculosis (accessed 2026-07-10).

(164) *Commercial serodiagnostic tests for diagnosis of tuberculosis: policy statement*. https://www.who.int/publications/i/item/9789241502054 (accessed 2026-07-09).
(165) Steingart, K. R.; Flores, L. L.; Dendukuri, N.; Schiller, I.; Laal, S.; Ramsay, A.; Hopewell, P. C.; Pai, M. Commercial Serological Tests for the Diagnosis of Active Pulmonary and Extrapulmonary Tuberculosis: An Updated Systematic Review and Meta-Analysis. *PLoS Med* **2011**, *8* (8), e1001062. https://doi.org/10.1371/journal.pmed.1001062.
(166) Anderson, B. L.; Welch, R. J.; Litwin, C. M. Assessment of Three Commercially Available Serologic Assays for Detection of Antibodies to Mycobacterium Tuberculosis and Identification of Active Tuberculosis. *Clin Vaccine Immunol* **2008**, *15* (11), 1644–1649. https://doi.org/10.1128/CVI.00271-08.
(167) Waghmare, P. J.; Wankhade, G.; Anindita, M.; Wandile, K.; Badole, C.; Harinath, B. SEVA TB ELISA – Multi Antigen and Antibody Assays for Serodiagnosis of Suspected Cases of Pulmonary and Extra Pulmonary Tuberculosis in Tertiary Care Hospital –A Retrospective Study. *Asian Pacific Journal of Tropical Disease* **2012**, *2*, S827–S832. https://doi.org/10.1016/S2222-1808(12)60273-4.
(168) Kashyap, R. S.; Rajan, A. N.; Ramteke, S. S.; Agrawal, V. S.; Kelkar, S. S.; Purohit, H. J.; Taori, G. M.; Daginawala, H. F. Diagnosis of Tuberculosis in an Indian Population by an Indirect ELISA Protocol Based on Detection of Antigen 85 Complex: A Prospective Cohort Study. *BMC Infect Dis* **2007**, *7*, 74. https://doi.org/10.1186/1471-2334-7-74.
(169) Schubert, O. T.; Mouritsen, J.; Ludwig, C.; Röst, H. L.; Rosenberger, G.; Arthur, P. K.; Claassen, M.; Campbell, D. S.; Sun, Z.; Farrah, T.; Gengenbacher, M.; Maiolica, A.; Kaufmann, S. H. E.; Moritz, R. L.; Aebersold, R. The Mtb Proteome Library: A Resource of Assays to Quantify the Complete Proteome of Mycobacterium Tuberculosis. *Cell Host Microbe* **2013**, *13* (5), 602–612. https://doi.org/10.1016/j.chom.2013.04.008.
(170) Mehaffy, M. C.; Kruh-Garcia, N. A.; Dobos, K. M. Prospective on Mycobacterium Tuberculosis Proteomics. *J. Proteome Res.* **2012**, *11* (1), 17–25. https://doi.org/10.1021/pr2008658.
(171) Deng, J.; Bi, L.; Zhou, L.; Guo, S.; Fleming, J.; Jiang, H.; Zhou, Y.; Gu, J.; Zhong, Q.; Wang, Z.; Liu, Z.; Deng, R.; Gao, J.; Chen, T.; Li, W.; Wang, J.; Wang, X.; Li, H.; Ge, F.; Zhu, G.; Zhang, H.; Gu, J.; Wu, F.; Zhang, Z.; Wang, D.; Hang, H.; Li, Y.; Cheng, L.; He, X.; Tao, S.; Zhang, X.-E. Mycobacterium Tuberculosis Proteome Microarray for Global Studies of Protein Function and Immunogenicity. *Cell Reports* **2014**, *9* (6), 2317–2329. https://doi.org/10.1016/j.celrep.2014.11.023.
(172) Jagusztyn-Krynicka, E. K.; Roszczenko, P.; Grabowska, A. Impact of Proteomics on Anti-Mycobacterium Tuberculosis (MTB) Vaccine Development.
(173) Gunawardena, H. P.; Feltcher, M. E.; Wrobel, J. A.; Gu, S.; Braunstein, M.; Chen, X. Comparison of the Membrane Proteome of Virulent Mycobacterium Tuberculosis and the Attenuated Mycobacterium Bovis BCG Vaccine Strain by Label-Free Quantitative Proteomics. *J Proteome Res* **2013**, *12* (12), 5463–5474. https://doi.org/10.1021/pr400334k.
(174) Penn, B. H.; Netter, Z.; Johnson, J. R.; Von Dollen, J.; Jang, G. M.; Johnson, T.; Ohol, Y. M.; Maher, C.; Bell, S. L.; Geiger, K.; Golovkine, G.; Du, X.; Choi, A.; Parry, T.; Mohapatra, B. C.; Storck, M. D.; Band, H.; Chen, C.; Jäger, S.; Shales, M.; Portnoy, D. A.; Hernandez, R.; Coscoy, L.; Cox, J. S.; Krogan, N. J. An Mtb-Human Protein-Protein Interaction Map Identifies a Switch Between Host Anti-Viral and Anti-Bacterial

Responses. *Mol Cell* **2018**, *71* (4), 637-648.e5. https://doi.org/10.1016/j.molcel.2018.07.010.
(175) Zhai, W.; Wu, F.; Zhang, Y.; Fu, Y.; Liu, Z. The Immune Escape Mechanisms of Mycobacterium Tuberculosis. *Int J Mol Sci* **2019**, *20* (2), 340. https://doi.org/10.3390/ijms20020340.
(176) Zhou, Z.; Tian, J.; He, Y.; Xiong, H.; Wang, W. Proteomic Analysis of Plasma Unravels Dynamic Pathways and Potential Biomarkers Indicating Disease Stages Following Mtb Infection. *mSystems 10* (8), e00616-25. https://doi.org/10.1128/msystems.00616-25.
(177) Gopinath, V.; Raghunandanan, S.; Gomez, R. L.; Jose, L.; Surendran, A.; Ramachandran, R.; Pushparajan, A. R.; Mundayoor, S.; Jaleel, A.; Kumar, R. A. Profiling the Proteome of Mycobacterium Tuberculosis during Dormancy and Reactivation. *Mol Cell Proteomics* **2015**, *14* (8), 2160–2176. https://doi.org/10.1074/mcp.M115.051151.
(178) Nuti, D. E.; Crump, R. B.; Dwi Handayani, F.; Chantratita, N.; Peacock, S. J.; Bowen, R.; Felgner, P. L.; Davies, D. H.; Wu, T.; Lyons, C. R.; Brett, P. J.; Burtnick, M. N.; Kozel, T. R.; AuCoin, D. P. Identification of Circulating Bacterial Antigens by In Vivo Microbial Antigen Discovery. *mBio* **2011**, *2* (4), 10.1128/mbio.00136-11. https://doi.org/10.1128/mbio.00136-11.
(179) Chaves, S. J.; Schegg, K.; Kozel, T. R.; AuCoin, D. P. In Vivo Microbial Antigen Discovery (InMAD) to Identify Diagnostic Proteins and Polysaccharides That Are Circulating During Microbial Infections. In *Immunoproteomics: Methods and Protocols*; Fulton, K. M., Twine, S. M., Eds.; Humana Press: Totowa, NJ, 2013; pp 155–165. https://doi.org/10.1007/978-1-62703-589-7_9.
(180) Williams, A.; Orme, I. M. Animal Models of Tuberculosis: An Overview. *Microbiology Spectrum* **2016**, *4* (4), 10.1128/microbiolspec.tbtb2-0004–2015. https://doi.org/10.1128/microbiolspec.tbtb2-0004-2015.
(181) Flynn, J. L. Lessons from Experimental *Mycobacterium Tuberculosis* Infections. *Microbes and Infection* **2006**, *8* (4), 1179–1188. https://doi.org/10.1016/j.micinf.2005.10.033.
(182) Dharmadhikari, A. S.; Nardell, E. A. What Animal Models Teach Humans about Tuberculosis. *Am J Respir Cell Mol Biol* **2008**, *39* (5), 503–508. https://doi.org/10.1165/rcmb.2008-0154TR.
(183) Dorman, S. E.; Hatem, C. L.; Tyagi, S.; Aird, K.; Lopez-Molina, J.; Pitt, M. L. M.; Zook, B. C.; Dannenberg, A. M.; Bishai, W. R.; Manabe, Y. C. Susceptibility to Tuberculosis: Clues from Studies with Inbred and Outbred New Zealand White Rabbits. *Infect Immun* **2004**, *72* (3), 1700–1705. https://doi.org/10.1128/IAI.72.3.1700-1705.2004.
(184) Kato-Maeda, M.; Shanley, C. A.; Ackart, D.; Jarlsberg, L. G.; Shang, S.; Obregon-Henao, A.; Harton, M.; Basaraba, R. J.; Henao-Tamayo, M.; Barrozo, J. C.; Rose, J.; Kawamura, L. M.; Coscolla, M.; Fofanov, V. Y.; Koshinsky, H.; Gagneux, S.; Hopewell, P. C.; Ordway, D. J.; Orme, I. M. Beijing Sublineages of Mycobacterium Tuberculosis Differ in Pathogenicity in the Guinea Pig. *Clin Vaccine Immunol* **2012**, *19* (8), 1227–1237. https://doi.org/10.1128/CVI.00250-12.
(185) Shang, S.; Harton, M.; Tamayo, M. H.; Shanley, C.; Palanisamy, G. S.; Caraway, M.; Chan, E. D.; Basaraba, R. J.; Orme, I. M.; Ordway, D. J. Increased Foxp3 Expression in Guinea Pigs Infected with W-Beijing Strains of *M. Tuberculosis*. *Tuberculosis* **2011**, *91* (5), 378–385. https://doi.org/10.1016/j.tube.2011.06.001.
(186) Nuti, D. E.; Crump, R. B.; Dwi Handayani, F.; Chantratita, N.; Peacock, S. J.; Bowen, R.; Felgner, P. L.; Davies, D. H.; Wu, T.; Lyons, C. R.; Brett, P. J.; Burtnick, M. N.; Kozel, T.

R.; AuCoin, D. P. Identification of Circulating Bacterial Antigens by In Vivo Microbial Antigen Discovery. *mBio* **2011**, *2* (4), 10.1128/mbio.00136-11. https://doi.org/10.1128/mbio.00136-11.
(187) Liao, D.; Fan, Q.; Bao, L. The Role of Superoxide Dismutase in the Survival of Mycobacterium Tuberculosis in Macrophages. *Jpn J Infect Dis* **2013**, *66* (6), 480–488. https://doi.org/10.7883/yoken.66.480.
(188) Allen, S. S.; Evans, W.; Carlisle, J.; Hajizadeh, R.; Nadaf, M.; Shepherd, B. E.; Pride, D. T.; Johnson, J. E.; Drake, W. P. Superoxide Dismutase A Antigens Derived from Molecular Analysis of Sarcoidosis Granulomas Elicit Systemic Th-1 Immune Responses. *Respir Res* **2008**, *9* (1), 36. https://doi.org/10.1186/1465-9921-9-36.
(189) Chattopadhyay, D. K. Superoxide Dismutase: A Biomarker for Early Diagnosis of Tuberculosis. *JCDR* **2019**. https://doi.org/10.7860/JCDR/2019/35298.12968.
(190) Nagai, S.; Wiker, H. G.; Harboe, M.; Kinomoto, M. Isolation and Partial Characterization of Major Protein Antigens in the Culture Fluid of Mycobacterium Tuberculosis. *Infect Immun* **1991**, *59* (1), 372–382. https://doi.org/10.1128/iai.59.1.372-382.1991.
(191) Ramalingam, B.; Baulard, A. R.; Locht, C.; Narayanan, P. R.; Raja, A. Cloning, Expression, and Purification of the 27 kDa (MPT51, Rv3803c) Protein of Mycobacterium Tuberculosis. *Protein Expr Purif* **2004**, *36* (1), 53–60. https://doi.org/10.1016/j.pep.2004.01.016.
(192) Wilson, R. A.; Maughan, W. N.; Kremer, L.; Besra, G. S.; Fütterer, K. The Structure of Mycobacterium Tuberculosis MPT51 (FbpC1) Defines a New Family of Non-Catalytic Alpha/Beta Hydrolases. *J Mol Biol* **2004**, *335* (2), 519–530. https://doi.org/10.1016/j.jmb.2003.11.001.
(193) Aoshi, T.; Nagata, T.; Suzuki, M.; Uchijima, M.; Hashimoto, D.; Rafiei, A.; Suda, T.; Chida, K.; Koide, Y. Identification of an HLA-A*0201-Restricted T-Cell Epitope on the MPT51 Protein, a Major Secreted Protein Derived from Mycobacterium Tuberculosis, by MPT51 Overlapping Peptide Screening. *Infect Immun* **2008**, *76* (4), 1565–1571. https://doi.org/10.1128/IAI.01381-07.
(194) Dass, M.; Kaur, M.; Aittan, S.; Sharma, P.; Punia, S.; Muthumohan, R.; Anthwal, D.; Gupta, R. K.; Mahajan, G.; Kumari, P.; Sharma, N.; Taneja, R. S.; Sharma, L. K.; Shree, R.; Tyagi, J. S.; Lal, V.; Haldar, S. MPT51 and MPT64-Based Antigen Detection Assay for the Diagnosis of Extrapulmonary Tuberculosis from Urine Samples. *Diagnostic Microbiology and Infectious Disease* **2023**, *107* (1), 115973. https://doi.org/10.1016/j.diagmicrobio.2023.115973.
(195) Namugga, J. V.; Musubika, C.; Niwagaba, S.; Mayito, J.; Sande, O. J. Accuracy of Anti-Mycobacterial Protein 51 Antibodies as a Biomarker for Latent TB Infection in Asymptomatic HIV Positive Individuals: A Cross-Sectional Diagnostic Study. *BMC Res Notes* **2025**, *18*, 73. https://doi.org/10.1186/s13104-025-07134-1.
(196) Sharma, P.; Gupta, R. K.; Aittan, S.; Anthwal, D.; Dass, M.; Yadav, R.; Behera, A.; Dhiman, A.; Dhooria, S.; Sethi, S.; Singhal, R.; Arora, P.; Aggarwal, A. N.; Sharma, T. K.; Haldar, S. Development and Assessment of a Novel Magnetic Nanoparticle Antibody-Conjugate and Aptamer-Based Assay (MNp-Ab-Ap Assay) for the Rapid Diagnosis of Pleural Tuberculosis. *Nanotheranostics* **2025**, *9* (1), 20–30. https://doi.org/10.7150/ntno.95332.
(197) Dong, Y.; Zhou, L.; Zhang, C.; Li, K.; Liu, Z.; Chen, X.; Che, N. Detection of Antigen Ag85B Expression Is Useful for the Diagnosis of Tuberculosis, Especially for Those with

an Antituberculosis Treatment History. *Am J Clin Pathol* **2023**, *160* (1), 62–71. https://doi.org/10.1093/ajcp/aqad012.
(198) Mollenkopf, H. J.; Grode, L.; Mattow, J.; Stein, M.; Mann, P.; Knapp, B.; Ulmer, J.; Kaufmann, S. H. E. Application of Mycobacterial Proteomics to Vaccine Design: Improved Protection by Mycobacterium Bovis BCG Prime-Rv3407 DNA Boost Vaccination against Tuberculosis. *Infect Immun* **2004**, *72* (11), 6471–6479. https://doi.org/10.1128/IAI.72.11.6471-6479.2004.
(199) Phong, T. Q.; Ha, D. T. T.; Volker, U.; Hammer, E. Using a Label Free Quantitative Proteomics Approach to Identify Changes in Protein Abundance in Multidrug-Resistant Mycobacterium Tuberculosis. *Indian J Microbiol* **2015**, *55* (2), 219–230. https://doi.org/10.1007/s12088-015-0511-2.
(200) Dong, W.; Huang, J.; Li, Y.; Tan, Y.; Shen, Z.; Song, Y.; Wang, D.; Xiao, S.; Chen, H.; Fu, Z. F.; Peng, G. Crystal Structural Basis for Rv0315, an Immunostimulatory Antigen and Inactive Beta-1,3-Glucanase of Mycobacterium Tuberculosis. *Sci Rep* **2015**, *5*, 15073. https://doi.org/10.1038/srep15073.
(201) Målen, H.; Søfteland, T.; Wiker, H. G. Antigen Analysis of Mycobacterium Tuberculosis H37Rv Culture Filtrate Proteins. *Scandinavian Journal of Immunology* **2008**, *67* (3), 245–252. https://doi.org/10.1111/j.1365-3083.2007.02064.x.
(202) Andersen, P.; Askgaard, D.; Ljungqvist, L.; Bennedsen, J.; Heron, I. Proteins Released from Mycobacterium Tuberculosis during Growth. *Infect Immun* **1991**, *59* (6), 1905–1910. https://doi.org/10.1128/iai.59.6.1905-1910.1991.
(203) Kumar, G.; Shankar, H.; Sharma, D.; Sharma, P.; Bisht, D.; Katoch, V. M.; Joshi, B. Proteomics of Culture Filtrate of Prevalent *Mycobacterium Tuberculosis* Strains: 2D-PAGE Map and MALDI-TOF/MS Analysis. *SLAS Discovery* **2017**, *22* (9), 1142–1149. https://doi.org/10.1177/2472555217717639.
(204) He, X.-Y.; Zhuang, Y.-H.; Zhang, X.-G.; Li, G.-L. Comparative Proteome Analysis of Culture Supernatant Proteins of Mycobacterium Tuberculosis H37Rv and H37Ra. *Microbes Infect* **2003**, *5* (10), 851–856. https://doi.org/10.1016/s1286-4579(03)00179-5.
(205) Daradkeh, A. F.; Alawyia, B.; Ballas, H.; Spernovasilis, N.; Alon-Ellenbogen, D. Strategies for Tuberculosis Prevention in Healthcare Settings: A Narrative Review. *Trop Med Infect Dis* **2025**, *10* (11), 316. https://doi.org/10.3390/tropicalmed10110316.
(206) Yang, H.; Ruan, X.; Li, W.; Xiong, J.; Zheng, Y. Global, Regional, and National Burden of Tuberculosis and Attributable Risk Factors for 204 Countries and Territories, 1990–2021: A Systematic Analysis for the Global Burden of Diseases 2021 Study. *BMC Public Health* **2024**, *24*, 3111. https://doi.org/10.1186/s12889-024-20664-w.
(207) Zumla, A.; Sahu, S.; Ditiu, L.; Singh, U.; Park, Y.-J.; Yeboah-Manu, D.; Osei-Wusu, S.; Asogun, D.; Nyasulu, P.; Tembo, J.; Kapata, N.; Alyaqoubi, F.; Maani, A. A.; Blumberg, L.; Zumla, A.; Ahmed, R.; Go, U.; Hui, D. S.; Goletti, D.; Petersen, E. Inequities Underlie the Alarming Resurgence of Tuberculosis as the World's Top Cause of Death from an Infectious Disease - Breaking the Silence and Addressing the Underlying Root Causes. *IJID Reg* **2025**, *14* (Suppl 2), 100587. https://doi.org/10.1016/j.ijregi.2025.100587.
(208) Gualano, G.; Musso, M.; Mencarini, P.; Mosti, S.; Cerva, C.; Vittozzi, P.; Mazzarelli, A.; Cannas, A.; Navarra, A.; Ianniello, S.; Faccendini, P.; Palmieri, F. Safety and Effectiveness of BPaL-Based Regimens to Treat Multidrug-Resistant TB: First Experience of an Italian Tuberculosis Referral Hospital. *Antibiotics (Basel)* **2024**, *14* (1), 7. https://doi.org/10.3390/antibiotics14010007.

(209) Oelofse, S.; Esmail, A.; Diacon, A. H.; Conradie, F.; Olayanju, O.; Ngubane, N.; Howell, P.; Everitt, D.; Crook, A. M.; Mendel, C. M.; Wills, G. H.; Olugbosi, M.; del Parigi, A.; Sun, E.; Calatroni, A.; Spigelman, M.; Dheda, K. Pretomanid with Bedaquiline and Linezolid for Drug-Resistant TB: A Comparison of Prospective Cohorts. *Int J Tuberc Lung Dis* **2021**, *25* (6), 453–460. https://doi.org/10.5588/ijtld.21.0035.
(210) *DailyMed - PRETOMANID tablet*. https://dailymed.nlm.nih.gov/dailymed/drugInfo.cfm?setid=f1906fc9-cb3c-4e13-8a4a-da76100c1bf3 (accessed 2026-07-02).
(211) Myrzaliev, B.; Ahmatov, M.; Duishekeeva, A.; Kulzhabaeva, A.; Kadyrov, A.; Toktogonova, A.; Abdulaeva, G.; Wares, D. F.; Mirtskhulava, V.; Mbenga, M.; Slyzkyi, A.; Foraida, S.; Diachenko, M.; Juneja, S.; Turdumambetova, G.; Musaeva, A.; Gebhard, A. Experiences in the Introduction of Bedaquiline Pretomanid Linezolid for Drug-Resistant Tuberculosis in Kyrgyzstan. *J Clin Tuberc Other Mycobact Dis* **2024**, *36*, 100472. https://doi.org/10.1016/j.jctube.2024.100472.
(212) Medicine (US), I. of. Research on the Global Control of TB: Understanding the Role of Drugs, Vaccines, and Funding. In *Addressing the Threat of Drug-Resistant Tuberculosis: A Realistic Assessment of the Challenge: Workshop Summary*; National Academies Press (US), 2009.
(213) Maxmen, A. Drug Development: A Combined Effort. *Nature* **2013**, *502* (7470), S4–S6. https://doi.org/10.1038/502S4a.
(214) Lienhardt, C.; Vernon, A. A.; Cavaleri, M.; Nambiar, S.; Nahid, P. Development of New TB Regimens: Harmonizing Trial Design, Product Registration Requirements, and Public Health Guidance. *PLoS Med* **2019**, *16* (9), e1002915. https://doi.org/10.1371/journal.pmed.1002915.
(215) Purohit, M. R.; Sharma, M.; Rosales-Klintz, S.; Lundborg, C. S. 'Multiple-Test' Approach to the Laboratory Diagnosis of Tuberculosis -Perception of Medical Doctors from Ujjain, India. *BMC Infect Dis* **2015**, *15*, 322. https://doi.org/10.1186/s12879-015-1037-2.
(216) Olbrich, L.; Franckling-Smith, Z.; Larsson, L.; Sabi, I.; Ntinginya, N. E.; Khosa, C.; Banze, D.; Nliwasa, M.; Corbett, E. L.; Semphere, R.; Verghese, V. P.; Michael, J. S.; Ninan, M. M.; Saathoff, E.; McHugh, T. D.; Razid, A.; Graham, S. M.; Song, R.; Nabeta, P.; Trollip, A.; Nicol, M. P.; Hoelscher, M.; Geldmacher, C.; Heinrich, N.; Zar, H. J.; RaPaed-AIDA-TB consortium. Sequential and Parallel Testing for Microbiological Confirmation of Tuberculosis Disease in Children in Five Low-Income and Middle-Income Countries: A Secondary Analysis of the RaPaed-TB Study. *Lancet Infect Dis* **2025**, *25* (2), 188–197. https://doi.org/10.1016/S1473-3099(24)00494-8.
(217) World Health Organization. *WHO Consolidated Guidelines on Tubaerculosis. Module 3: Diagnosis*; Geneva, 2025.
(218) *2.2 Diagnostic testing*. https://www.who.int/teams/global-programme-on-tuberculosis-and-lung-health/tb-reports/global-tuberculosis-report-2024/tb-diagnosis-and-treatment/2-2-diagnostic-testing (accessed 2026-07-09).
(219) Pathmanathan, I.; Date, A.; Coggin, W. L.; Nkengasong, J.; Piatek, A. S.; Alexander, H. Rolling out Xpert MTB/RIF® for Tuberculosis Detection in HIV-Positive Populations: An Opportunity for Systems Strengthening. *African Journal of Laboratory Medicine* **2017**, *6* (2), 9. https://doi.org/10.4102/ajlm.v6i2.460.
(220) Hermans, S.; Caldwell, J.; Kaplan, R.; Cobelens, F.; Wood, R. The Impact of the Roll-out of Rapid Molecular Diagnostic Testing for Tuberculosis on Empirical Treatment in Cape

Town, South Africa. *Bull World Health Organ* **2017**, *95* (8), 554–563. https://doi.org/10.2471/BLT.16.185314.
(221) Muyoyeta, M.; Moyo, M.; Kasese, N.; Ndhlovu, M.; Milimo, D.; Mwanza, W.; Kapata, N.; Schaap, A.; Faussett, P. G.; Ayles, H. Implementation Research to Inform the Use of Xpert MTB/RIF in Primary Health Care Facilities in High TB and HIV Settings in Resource Constrained Settings. *PLOS ONE* **2015**, *10* (6), e0126376. https://doi.org/10.1371/journal.pone.0126376.
(222) Cox, H. S.; Mbhele, S.; Mohess, N.; Whitelaw, A.; Muller, O.; Zemanay, W.; Little, F.; Azevedo, V.; Simpson, J.; Boehme, C. C.; Nicol, M. P. Impact of Xpert MTB/RIF for TB Diagnosis in a Primary Care Clinic with High TB and HIV Prevalence in South Africa: A Pragmatic Randomised Trial. *PLOS Medicine* **2014**, *11* (11), e1001760. https://doi.org/10.1371/journal.pmed.1001760.
(223) Mupfumi, L.; Makamure, B.; Chirehwa, M.; Sagonda, T.; Zinyowera, S.; Mason, P.; Metcalfe, J. Z.; Mutetwa, R. Impact of Xpert MTB/RIF on Antiretroviral Therapy-Associated Tuberculosis and Mortality: A Pragmatic Randomized Controlled Trial. *Open Forum Infect Dis* **2014**, *1* (1), ofu038. https://doi.org/10.1093/ofid/ofu038.
(224) Theron, G.; Zijenah, L.; Chanda, D.; Clowes, P.; Rachow, A.; Lesosky, M.; Bara, W.; Mungofa, S.; Pai, M.; Hoelscher, M.; Dowdy, D.; Pym, A.; Mwaba, P.; Mason, P.; Peter, J.; Dheda, K. Feasibility, Accuracy, and Clinical Effect of Point-of-Care Xpert MTB/RIF Testing for Tuberculosis in Primary-Care Settings in Africa: A Multicentre, Randomised, Controlled Trial. *The Lancet* **2014**, *383* (9915), 424–435. https://doi.org/10.1016/S0140-6736(13)62073-5.
(225) Han, K. H.; Li, Y.-C.; Parveen, R.; Venkataraman, S.; Lin, C.-W. Technologies for Monoclonal Antibody Discovery and Development. *Int J Mol Sci* **2025**, *26* (21), 10470. https://doi.org/10.3390/ijms262110470.
(226) Smith, S. A.; Crowe, J. E. Use of Human Hybridoma Technology To Isolate Human Monoclonal Antibodies. *Microbiology Spectrum* **2015**, *3* (1), 10.1128/microbiolspec.aid-0027–2014. https://doi.org/10.1128/microbiolspec.aid-0027-2014.
(227) Battineni, J. K.; Mamidisetti, Y. D.; Kuchukuntla, M.; Amaravadi, D.; Ravula, S. R.; Jadi, R. K. Mass Spectrometry Based Multi-Omics Integration: Analytical Methods and Biological Applications. *Rapid Commun Mass Spectrom* **2026**, *40* (15), e70097. https://doi.org/10.1002/rcm.70097.
(228) Kim, D. Y.; Lee, J.; Choi, J.; Shin, H.; Lee, J. S.; Kim, E. J. Spatial Multi-Omics in Precision Medicine: Integrating Biological Insights through Multidisciplinary Collaboration. *Semin Cancer Biol* **2026**, *119*, 24–37. https://doi.org/10.1016/j.semcancer.2025.12.009.
(229) Khan, M. I.; Liu, L.; Sani, A.; Sun, X.; Ying, B.; Chen, H. Chip Electrophoresis Titration Biosensors: Recent Developments for Biomedical Targets. *Biosens Bioelectron* **2026**, *306*, 118665. https://doi.org/10.1016/j.bios.2026.118665.
(230) Peng, Y.; Rabin, C.; Walgama, C. T.; Pollok, N. E.; Smith, L.; Richards, I.; Crooks, R. M. Silver Nanocubes as Electrochemical Labels for Bioassays. *ACS Sens* **2021**, *6* (3), 1111–1119. https://doi.org/10.1021/acssensors.0c02377.
(231) Uritboonthai, W.; Hoang, L.; Aisporna, A.; Giera, M.; Siuzdak, G. The Dark Metabolome/Lipidome and In-Source Fragmentation. *Anal Sci Adv* **2025**, *6* (1), e70012. https://doi.org/10.1002/ansa.70012.

(232) da Silva, R. R.; Dorrestein, P. C.; Quinn, R. A. Illuminating the Dark Matter in Metabolomics. *Proc Natl Acad Sci U S A* **2015**, *112* (41), 12549–12550. https://doi.org/10.1073/pnas.1516878112.
(233) Giera, M.; Aisporna, A.; Uritboonthai, W.; Siuzdak, G. The Hidden Impact of In-Source Fragmentation in Metabolic and Chemical Mass Spectrometry Data Interpretation. *Nat Metab* **2024**, *6* (9), 1647–1648. https://doi.org/10.1038/s42255-024-01076-x.
(234) Djoumbou-Feunang, Y.; Fiamoncini, J.; Gil-de-la-Fuente, A.; Greiner, R.; Manach, C.; Wishart, D. S. BioTransformer: A Comprehensive Computational Tool for Small Molecule Metabolism Prediction and Metabolite Identification. *J Cheminform* **2019**, *11* (1), 2. https://doi.org/10.1186/s13321-018-0324-5.
(235) Cardon, T.; Fournier, I.; Salzet, M. Shedding Light on the Ghost Proteome. *Trends in Biochemical Sciences* **2021**, *46* (3), 239–250. https://doi.org/10.1016/j.tibs.2020.10.003.
(236) Cardon, T.; Fournier, I.; Salzet, M. SARS-Cov-2 Interactome with Human Ghost Proteome: A Neglected World Encompassing a Wealth of Biological Data. *Microorganisms* **2020**, *8* (12), 2036. https://doi.org/10.3390/microorganisms8122036.
(237) Dean, D. A.; Klechka, L.; Hossain, E.; Parab, A. R.; Eaton, K.; Hinsdale, M.; McCall, L.-I. Spatial Metabolomics Reveals Localized Impact of Influenza Virus Infection on the Lung Tissue Metabolome.
(238) Myers, O. D.; Sumner, S. J.; Li, S.; Barnes, S.; Du, X. One Step Forward for Reducing False Positive and False Negative Compound Identifications from Mass Spectrometry Metabolomics Data: New Algorithms for Constructing Extracted Ion Chromatograms and Detecting Chromatographic Peaks. *Anal. Chem* **2017**, *89* (17), 8696–8703.

6 Appendix A

Q Exactive Plus (Thermo Scientific) instrument parameters (untargeted data acquisition).

Run time	0 to 12.5 min
Polarity	Positive
Default charge state	1
Full MS	
Resolution	70,000
AGC target	1e6
Maximum IT	246 ms
Scan range	70 to 1050 *m/z*
dd-MS2	
Resolution	17,500
AGC target	2e5
Maximum IT	54 ms
Loop count	5
TopN	5
Isolation window	1.0 *m/z*
(N)ce/stepped (N)CE	NCE: 20, 40, 60
dd Settings - as in [237]	
Tune Data - as in [237]	

7 Appendix B

MZmine (version 2.53) Parameters

Type	Parameter	Value
Feature detection	MS1 Mass Detection	Centroid
	MS1 noise level	4e5
	MS2 noise level	1e3
Chromatogram builder	Masses	
	Time span	0.01 min
	Min height	1.2e6
	m/z tolerance	10 ppm
Chromatogram deconvolution [238]	Local minimum	
	Chromatographic Threshold	20%
	Search Minimum in Retention Time Range (minutes)	1
	Minimum Relative Height	40%
	Minimum Absolute Height	1.0e0
	Minimum Ratio of Peak Top/Edge	1.20
	Peak Duration Range	0.04 - 5.00
	m/z MS2	0.01
	RT MS2 (minutes)	0.1
Isotopic peaks grouper	*m/z* tolerance	10 ppm
	Retention Time Tolerance (minutes)	0.1
	Charge	3
	Lowest *m/z*	
	Monotonic shape	Checked

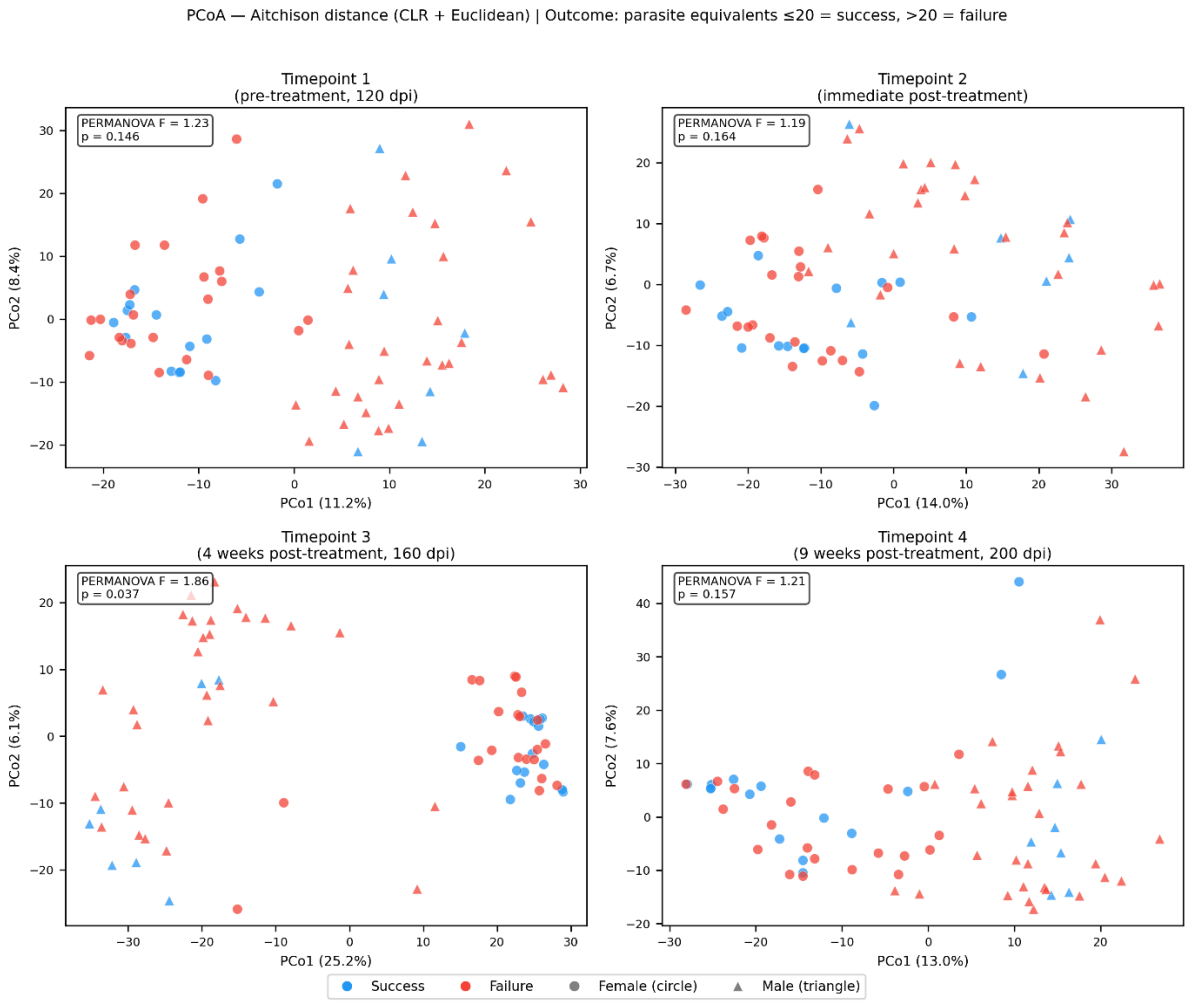
Alignment	Join aligner	10 ppm
	Retention Time Tolerance (minutes)	0.1
	Weight *m/z*	1
	Weight RT	1
Feature list	Keep only with MS2 scan (discovery cohort only)	
	Cut off first 20s (discovery cohort only)	
	Cut off last 30s	
	Minimum peaks in a row (discovery cohort and treatment effect analysis only)	10
	Reset ID	

8 Appendix C

GNPS Parameters.

Feature-Based Molecular Network	
Precursor Ion Mass Tolerance	0.02 Da
Fragment Ion Mass Tolerance	0.02 Da
Minimum Matched Fragment Ions	4
Maximum Connected Component Size (Beta)	100
Maximum shift between precursors	500
Min Pairs Cosine	0.7
Network TopK	10
Library Search Minimum Matched Peaks	4
Search analogs	Do Search
Top results to report per query	1
Score Threshold	0.7
Maximum analog difference	100.0 Da
Minimum Peak Intensity	0.0
Filter Precursor Window	Filter
Filter peaks in 50 Da Window	Filter
Filter Library	Filter Library
Normalization per file	Row Sum Normalization (Per file Sum to 1,000,000)
Aggregation Method for peak abundances per group	Mean
Run Dereplicator	Run

9 Appendix D



PCoA of serum metabolomic profiles using Aitchison distance.

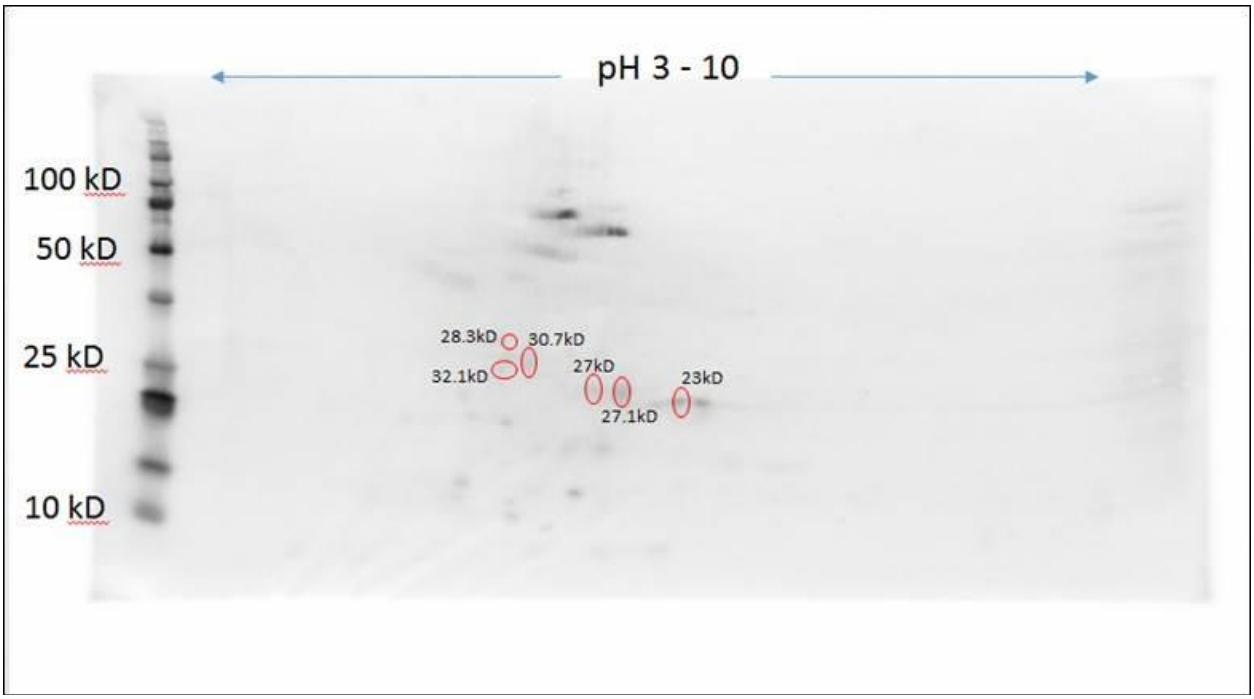
Principal coordinate analysis (PCoA) of Aitchison distance (centered log-ratio transformation followed by Euclidean distance) calculated for the benznidazole treatment group across four timepoints. Each point represents one mouse serum sample, colored by treatment outcome (blue = success, ≤20 parasite equivalents; red = failure, >20 parasite equivalents), shaped by sex (circle = female, triangle = male). The 20 parasite equivalent cutoff was defined as the mean plus three standard deviations of DMEM uninfected control values. PERMANOVA results are annotated per panel (999 permutations). The parallel distribution with central gap observed under Bray–Curtis dissimilarity (Figure 2-1) does not persist under Aitchison distance, consistent with the gap being a geometric artifact of the distance metric rather than a true structural feature of the data. This finding corroborates the statistical tests of bimodality reported in the main text (Hartigan's dip test $p = 0.316$; bimodality coefficient = 0.44; $\Delta BIC = 3.87$).

10 Appendix E

Features from Bz group demonstrating BH-Significance but unannotated.

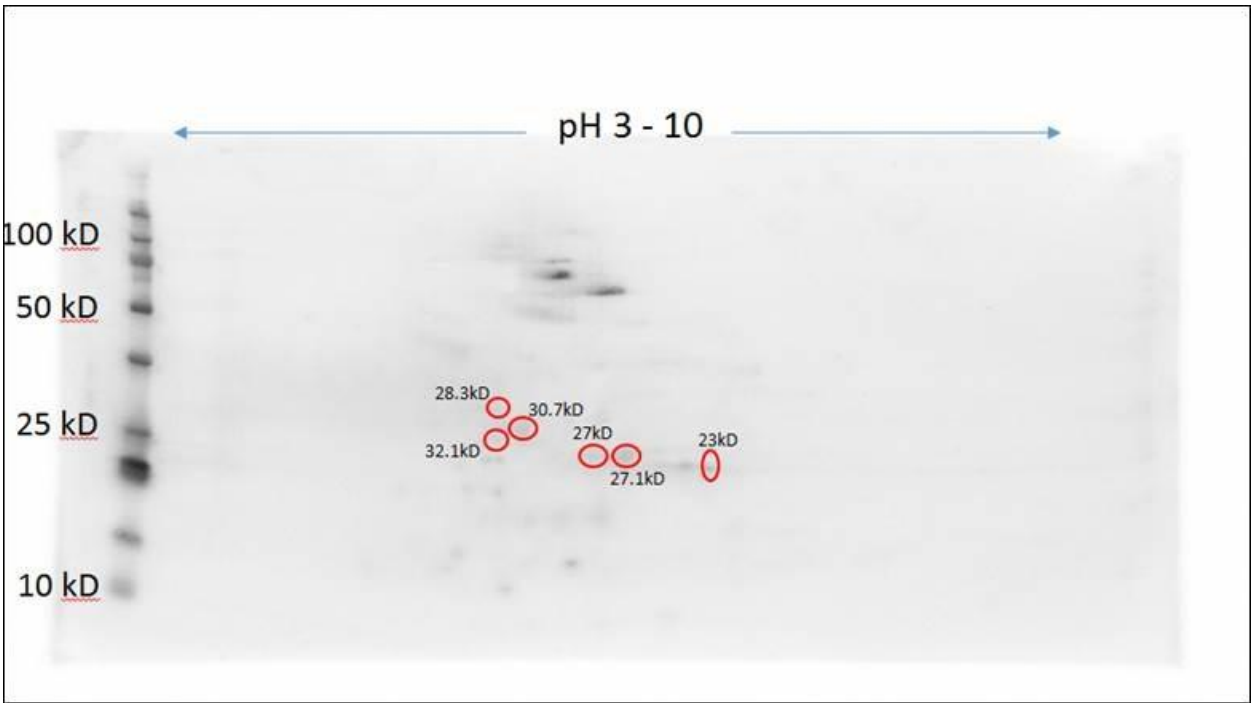
m/z	RT (min)	BH-Sig Timepoint(s)	Direction Consistency (of 4 TPs)	Direction of Association
357.2400	3.69	TP2, TP3	2	Higher in failure
144.0800	1.39	TP2	4	Higher in success
146.0600	1.39	TP2	4	Higher in success
118.0700	1.39	TP2	4	Higher in success
159.0900	1.39	TP2	4	Higher in success
225.1500	6.46	TP2	4	Higher in success
200.2000	6.45	TP3	4	Higher in failure
214.1800	4.89	TP3	4	Higher in failure
221.0900	1.38	TP2	4	Higher in success
242.2100	5.73	TP3	4	Higher in failure
274.1800	4.86	TP1	4	Higher in success
300.2000	5.16	TP2	4	Higher in success
664.4200	7.51	TP2	3	Higher in failure
130.0700	1.38	TP2	2	Higher in success
283.2600	7.35	TP3	2	Higher in success
297.1600	3.21	TP3	2	Higher in failure
379.2500	3.75	TP3	2	Higher in failure
401.2600	3.81	TP3	2	Higher in failure
423.2700	3.87	TP3	2	Higher in failure
689.5600	9.23	TP1	2	Higher in success
704.4500	7.51	TP2	2	Higher in failure
324.2900	7.38	TP1	0	Mixed
73.0700	2.44	TP1	2	Higher in success
120.0700	0.37	TP2	2	Higher in success
149.1200	2.43	TP1	2	Higher in success
171.1000	2.43	TP1	2	Higher in success
241.1500	0.50	TP3	2	Higher in failure
291.0700	0.54	TP1	2	Higher in success
398.3300	6.26	TP1	2	Higher in failure
624.3900	7.17	TP2	0	Mixed

11 Appendix F



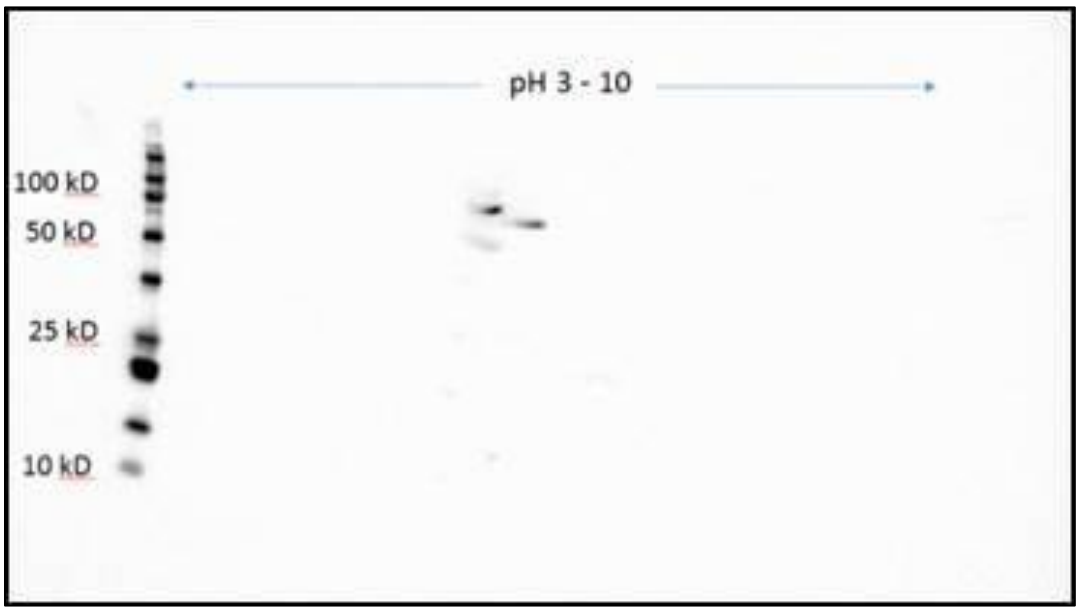
Six *Mtb* biomarker candidates identified by probing CFPs with urine-immunized InMAD rabbit serum. *Mtb* culture filtrate proteins separated by isoelectric point across the x-axis and molecular mass across the y-axis, transferred to PVDF, and probed with pooled *Mtb*-infected urine-immunized rabbit serum (1:30 dilution). 2° = Mouse anti-rabbit-HRP. Identified protein spots circled in red and labeled by molecular weight corresponding to potential biomarker listed in Table 3.1.

12 Appendix G



Six *Mtb* biomarker candidates identified by probing CFPs with serum-immunized InMAD rabbit serum. *Mtb* culture filtrate proteins separated by isoelectric point across the x-axis and molecular mass across the y-axis, transferred to PVDF, and probed with pooled *Mtb*-infected serum-immunized rabbit serum(1:30 dilution). 2° = Mouse anti-rabbit-HRP. Identified protein spots circled in red and labeled by molecular weight corresponding to potential biomarker listed in Table 3.1.

13 Appendix H



A 2-dimensional western blot using naïve rabbit serum toprobe Mtb culture filtrate proteins from protein gel. Pre-immune sera is minimally reactive to Mtb CFPs.